

2006

**CONCENTRATION AND MOLECULAR WEIGHT DISTRIBUTION OF
POLYGLUTAMIC ACID PRODUCED BY BACILLUS LICHENIFORMIS
IN A CONTINUOUS STIRRED TANK BIOREACTOR**

Sunil V. Patel
Western University

Follow this and additional works at: <https://ir.lib.uwo.ca/digitizedtheses>

Recommended Citation

Patel, Sunil V., "CONCENTRATION AND MOLECULAR WEIGHT DISTRIBUTION OF POLYGLUTAMIC ACID PRODUCED BY BACILLUS LICHENIFORMIS IN A CONTINUOUS STIRRED TANK BIOREACTOR" (2006). *Digitized Theses*. 4883.
<https://ir.lib.uwo.ca/digitizedtheses/4883>

This Thesis is brought to you for free and open access by the Digitized Special Collections at Scholarship@Western. It has been accepted for inclusion in Digitized Theses by an authorized administrator of Scholarship@Western. For more information, please contact wlsadmin@uwo.ca.

**CONCENTRATION AND MOLECULAR WEIGHT
DISTRIBUTION OF POLYGLUTAMIC ACID
PRODUCED BY *BACILLUS LICHENIFORMIS* IN A
CONTINUOUS STIRRED TANK BIOREACTOR**

Spine title: Polyglutamic Acid Produced by *B. licheniformis* in a CSTR

Thesis format: Monograph

by

Sunil V. Patel

Graduate Program in Engineering Science
Department of Chemical and Biochemical Engineering

A thesis submitted in partial fulfillment
of the requirements for the degree of
Master of Engineering Science

Faculty of Graduate Studies
The University of Western Ontario
London, Ontario, Canada

© Sunil V. Patel 2006

THE UNIVERSITY OF WESTERN ONTARIO

FACULTY OF GRADUATE STUDIES

CERTIFICATE OF EXAMINATION

Supervisor

Dr. Argyrios Margaritis

Examiners

Dr. Dimitre Karamanev

Dr. Amarjeet Bassi

Dr. Ernest Yanful

The thesis by

Sunil Vijay Patel

entitled:

**Concentration and Molecular Weight Distribution of Polyglutamic Acid
Produced by *Bacillus licheniformis* in a Continuous Stirred Tank
Bioreactor**

is accepted in partial fulfillment of the
requirements for the degree of

Master of Engineering Science

Date _____

Chair of the Thesis Examination Board

ABSTRACT

The production of the biopolymer polyglutamic acid, using *Bacillus licheniformis* within a continuous stirred tank bioreactor was studied. This study into the continuous production of polyglutamic acid is the first to be reported. The effect of varying the dilution rate on the biomass concentration, the polyglutamic acid concentration and the substrates concentration were measured and the data were analyzed and correlated. The biomass productivity peaked at 0.16 g/L/h, and the poly glutamic acid productivity reached 1.2 g/L/h. The poly glutamic acid yield from the total carbon sources reached 0.33 g/g.

The specific growth as a function of the total substrate concentration was fitted using the Richard – Margaritis empirical model. The maximum specific growth rate was 0.13 h^{-1} , the saturation constant was 59.1 g/L and the relative coefficient was 4.3.

KEY WORDS

Bacillus licheniformis, polyglutamic acid, continuous bioreactor, biopolymer, molecular weight distribution, aerobic fermentation.

ACKNOWLEDGEMENTS

I wish to thank my thesis supervisor, Dr. Argyrios Margaritis, for his enthusiastic support and guidance throughout the course of my research. Many thanks to Dr. Margaritis for reviewing my thesis and for his suggestions during the writing of this thesis. Without his help, this work would not have been possible. Also, I would like to thank Dr. Gerry Rowe for his guidance in the set up and operation of the bioreactor system. I would like to thank Dr. Andrew Richard for his suggestions and input into my work. I also want express my appreciation for Soheil Afara and Mike Gaylard for their expertise and guidance in the operation of many of the analytical devices. I would also like to thank the other members of my research group for their advice and cooperation.

This work was supported by the Natural Sciences and Engineering Research Council of Canada (NSERC) through a Discovery Grant No. OGD4388 awarded to Dr. Margaritis.

TABLE OF CONTENTS

CERTIFICATE OF EXAMINATION	ii
ABSTRACT.....	iii
ACKNOWLEDGEMENTS.....	iv
TABLE OF CONTENTS.....	v
LIST OF TABLES.....	vii
LIST OF FIGURES.....	ix
LIST OF APPENDICES.....	xii
LIST OF NOMENCLATURE.....	xiii
1. INTRODUCTION.....	1
1.1 Commercial Significance of Polyglutamic Acid.....	1
1.2 Research Objectives.....	1
1.3 Thesis Layout and Scope.....	2
2. LITERATURE REVIEW.....	4
2.1 Introduction.....	4
2.2 Polyglutamic Acid.....	4
2.3 PGA Producing Bacteria.....	8
2.4 Bacillus licheniformis ATCC 9945a.....	8
2.5 Growth Kinetics.....	12
2.5.1 Batch Growth.....	12
2.5.2 Continuous Stirred Tank Reactor (CSTR).....	16
2.5.3 Richard – Margaritis Empirical Model.....	20
2.5.4 Growth Model for Multiple Substrate Growth.....	22
2.6 Number and Weight Average Molecular Weight Calculations.....	23
2.7 Volumetric Mass Transfer Coefficient, Oxygen Uptake Rate and Specific Oxygen Uptake Rate.....	24
2.8 High Performance Liquid Chromatography.....	26
2.9 Gel Permeation Chromatography.....	28
3. EXPERIMENTAL METHODS.....	31
3.1 Bacillus licheniformis Growth.....	31
3.1.1 Microorganism.....	31
3.1.2 Medium Composition.....	31
3.1.3 Bioreactor System.....	32
3.1.4 Batch reactor system operation.....	35

3.1.5	Continuous Stirred Tank Reactor System Operation.....	36
3.1.6	Oxygen Uptake Rate, Specific Oxygen Uptake Rate and the Volumetric Mass Transfer Coefficient.....	37
3.1.7	Contamination Evaluation	37
3.2	Analytical Methods	37
3.2.1	Biomass Concentration	37
3.2.2	Citric Acid and Glutamic Acid Concentration.....	38
3.2.3	Glycerol Concentration.....	38
3.2.4	Polyglutamic Acid Concentration.....	39
3.2.5	Polyglutamic Acid Molecular Weight Characteristics	39
3.2.6	Broth Viscosity	40
4.	RESULTS AND DISCUSSION	42
4.1	Batch Fermentation	42
4.1.1	Biomass, Substrates and Polyglutamic Acid	42
4.1.2	Viscosity, Oxygen Uptake Rate, Specific Oxygen Uptake Rate and Volumetric Mass Transfer Coefficient	49
4.1.3	Molecular Weight Characteristics of the Biopolymer	56
4.2	Continuous Fermentation of <i>Bacillus licheniformis</i>	60
4.2.1	Washout Data and the Maximum Specific Growth Rate.....	60
4.2.2	Transient Time and Steady State Equilibrium.....	63
4.2.3	Repeatability of the Continuous Fermentation of <i>B. licheniformis</i>	64
4.2.4	Biomass, Substrates and Polyglutamic Acid Concentration.....	66
4.2.5	Biomass and Polyglutamic Acid Productivity	73
4.2.6	Biomass and Polyglutamic Acid Yield	76
4.2.7	Molecular Weight Characteristics.....	83
4.2.8	Richard – Margaritis Empirical Model	88
5.	CONCLUSIONS AND RECOMMENDATIONS.....	91
5.1	Conclusions.....	91
5.2	Recommendations	92
6.	REFERENCES.....	94
	APPENDIX	100
	CURRICULUM VITAE.....	137

LIST OF TABLES

<i>Table 2-1 The effect of substrates on the PGA concentration, productivity and yield from selected works</i>	11
<i>Table 3-1 Medium E, used for growth and production in the fermentation of B. licheniformis</i>	31
<i>Table A-1 Biomass Concentration, Natural Log of the Biomass, Specific Growth Rate and PGA Concentration as a function of Fermentation Time for the Batch Fermentation of B. licheniformis</i>	101
<i>Table A-2 Citric Acid, Glutamic Acid and Glycerol Concentration as a function of Fermentation Time for the Batch Fermentation of B. licheniformis</i>	102
<i>Table A-3 Biomass Yield from Citric Acid, Glutamic Acid, Glycerol and Total Substrates as a function of Fermentation time for the Batch Fermentation of B. licheniformis</i>	103
<i>Table A-4 PGA yield from Biomass and Substrates as a function of Fermentation Time for the Batch fermentation of B. licheniformis</i>	104
<i>Table A-5 Oxygen Uptake Rate, Specific Oxygen Uptake Rate, Volumetric Mass Transfer Coefficient and Viscosity as a function of Fermentation Time for the Batch Fermentation of B. licheniformis</i>	105
<i>Table A-6 Biomass and PGA Productivity as a function of Fermentation Time for the Batch Fermentation of B. licheniformis</i>	106
<i>Table A-7 Number and Weight Average Molecular Weight and Polydispersity as a function of Fermentation Time for the Batch Fermentation of B. licheniformis</i>	107
<i>Table B-1 Biomass, Substrate and Product Concentration as a function of Fermentation Time for $D = 0.023 \text{ h}^{-1}$</i>	109
<i>Table B-2 Biomass, Substrate and Product Concentration as a function of Fermentation Time for $D = 0.035 \text{ h}^{-1}$</i>	110
<i>Table B-3 Biomass, Substrate and Product Concentration as a function of Fermentation Time for $D = 0.051 \text{ h}^{-1}$</i>	111
<i>Table B-4 Biomass, Substrate and Product Concentration as a function of Fermentation Time for $D = 0.063 \text{ h}^{-1}$</i>	112
<i>Table B-5 Biomass, Substrate and Product Concentration as a function of Fermentation Time for $D = 0.082a \text{ h}^{-1}$</i>	113
<i>Table B-6 Biomass, Substrate and Product Concentration as a function of Fermentation Time for $D = 0.082b \text{ h}^{-1}$</i>	114
<i>Table B-7 Biomass, Substrate and Product Concentration as a function of Fermentation Time for $D = 0.097 \text{ h}^{-1}$</i>	115
<i>Table B-8 Biomass Concentration as a Function of Fermentation Time for $D = 0.063 \text{ h}^{-1}$ and $D = 0.082b \text{ h}^{-1}$</i>	116

<i>Table B-9 Biomass Concentration as a Function of Fermentation Time for $D = 0.082\text{ h}^{-1}$ and $D = 0.051\text{ h}^{-1}$</i>	<i>117</i>
<i>Table C-1 Biomass, Substrate and Product Concentrations as a function of Dilution Rate for the Continuous Fermentation of <i>B. licheniformis</i></i>	<i>119</i>
<i>Table C-2 Biomass and PGA Productivity and Substrate Consumption Rate as a function of Dilution Rate for the Continuous Fermentation of <i>B. licheniformis</i></i>	<i>120</i>
<i>Table C-3 Biomass Yield from Substrates as a function of Dilution Rate for the Continuous Fermentation of <i>B. licheniformis</i>.....</i>	<i>121</i>
<i>Table C-4 PGA yield from Biomass and Substrates as a function of Dilution Rate for the Continuous Fermentation of <i>B. licheniformis</i>.....</i>	<i>122</i>
<i>Table C-5 Number and Weight Average Molecular Weight and Polydispersity as a function of Dilution Rate for the Continuous Fermentation of <i>B. licheniformis</i></i>	<i>123</i>
<i>Table D-1 Biomass Concentration and the Natural Log of the biomass concentration as a function of Washout Time for Washout Experiment #1</i>	<i>125</i>
<i>Table D-2 Biomass Concentration and the Natural Log of the biomass concentration as a function of Washout Time for Washout Experiment #2</i>	<i>125</i>
<i>Table D-3 Slope of $\ln(X)$ vs Washout Time, Dilution Rate and the Calculated Maximum Specific Growth Rate for the Washout Experiments.....</i>	<i>126</i>

LIST OF FIGURES

<i>Figure 2-1 γ-Polyglutamic acid</i>	5
<i>Figure 2-2 Typical Biomass Concentration as a function of Fermentation Time for Batch Fermentation (Blanch and Clark, 1996)</i>	13
<i>Figure 2-3: Biomass Concentration as a function of Time for the Continuous System ...</i>	17
<i>Figure 2-4 Specific Growth Rate as a function of Substrate Concentration using the Richard- Margaritis Empirical Model</i>	21
<i>Figure 2-5 Sample Plot of the Dynamic Gas off/Gas on method for determination of k_{La}, OUR and Q_{O_2}</i>	25
<i>Figure 2-6 Sample Chromatogram, the Absorbance (AU) as a function of Retention Time</i>	27
<i>Figure 2-7 Typical GPC Calibration Curve, log Molecular Weight as a function of Elution Time (Wu, 2004)</i>	30
<i>Figure 3-1 Bioreactor system for the continuous fermentation of B. licheniformis</i>	33
<i>Figure 3-2 Bioreactor Dimensions</i>	34
<i>Figure 3-3 Calibration Curve for the GPC determination of Molecular Weight of PGA. The Log Molecular Weight as a function of Elution Volume</i>	41
<i>Figure 4-1 Biomass Concentration as a function of Fermentation Time for the Batch Fermentation of B. licheniformis ATCC 9945a (Table A-1)</i>	43
<i>Figure 4-2 Specific Growth Rate of B. licheniformis as a function of Fermentation Time (Table A-1)</i>	44
<i>Figure 4-3 Natural Log of the Biomass Concentration as a function of Fermentation Time for the Batch Fermentation of B. licheniformis (Table A-1)</i>	45
<i>Figure 4-4: Polyglutamic Acid Concentration as a function of Fermentation Time from the Batch Fermentation of B. licheniformis ATCC 9945a (Table A-1)</i>	47
<i>Figure 4-5 Citric Acid (●), Glutamic Acid (○) and Glycerol (■) Concentrations as a function of Fermentation Time for the Batch Fermentation of B. licheniformis ATCC 9945a (Table A-2)</i>	48
<i>Figure 4-6 Broth Viscosity (○) and the Combined (PGA+Biomass) Concentration (●) as a function of Batch fermentation time (Table A-1 and Table A-5)</i>	50
<i>Figure 4-7 Oxygen Uptake Rate as a function of Fermentation Time for the Batch Fermentation of B. licheniformis ATCC 9945a (Table A-5)</i>	52
<i>Figure 4-8 Specific Oxygen Uptake Rate as a function of Fermentation Time for B. licheniformis ATCC 9945a (Table A-5)</i>	54
<i>Figure 4-9 Volumetric Mass Transfer Coefficient of Oxygen as a function of Fermentation Time for B. licheniformis ATCC 9945a (Table A-5)</i>	55

<i>Figure 4-10 The Number Average Molecular Weight (Mn) of PGA as a function of Fermentation Time for the Batch Fermentation of B. licheniformis ATCC 9945a (Table A-7)</i>	<i>57</i>
<i>Figure 4-11 The Weight Average Molecular Weight (Mw) of PGA as a function of Fermentation Time for the Batch Fermentation of B. licheniformis ATCC 9945a (Table A-7)</i>	<i>58</i>
<i>Figure 4-12 The Polydispersity (Mw/Mn) of PGA as a function of Fermentation Time for the Batch Fermentation of B. licheniformis ATCC 9945a (Table A-7)</i>	<i>59</i>
<i>Figure 4-13 Biomass Concentration as a function of Washout Time for washout experiment 1 (●) and washout experiment 2 (○) (Table D-1 and Table D-2)</i>	<i>61</i>
<i>Figure 4-14 Natural Log of the Biomass Concentration from washout experiment #1 (●) and #2 (○) as a function of Washout Time for the washout experiments (Table D-1 and Table D-2).....</i>	<i>62</i>
<i>Figure 4-15 Biomass Concentration as a function of Real Fermentation Time for $D = 0.063 \text{ h}^{-1}$ and $D = 0.082 \text{ h}^{-1}$ (Table B-8).....</i>	<i>65</i>
<i>Figure 4-16 The Biomass Concentration as a function of Dilution Rate for the Continuous Fermentation of B. licheniformis ATCC 9945a (Table C-1).....</i>	<i>68</i>
<i>Figure 4-17 The Polyglutamic Acid Concentration as a function of Dilution Rate for the Continuous Fermentation of B. licheniformis ATCC 9945a (Table C-1).....</i>	<i>69</i>
<i>Figure 4-18 The Citric Acid Concentration as a function of Dilution Rate for the Continuous Fermentation of B. licheniformis ATCC 9945a (Table C-1).....</i>	<i>70</i>
<i>Figure 4-19 The Glutamic Acid Concentration as a function of Dilution Rate for the Continuous Fermentation of B. licheniformis ATCC 9945a (Table C-1).....</i>	<i>71</i>
<i>Figure 4-20 The Glycerol Concentration as a function of Dilution Rate for the Continuous Fermentation of B. licheniformis ATCC 9945a (Table C-1).....</i>	<i>72</i>
<i>Figure 4-21 Biomass Productivity as a function of Dilution Rate for the Continuous Fermentation of B. licheniformis ATCC 9945a (Table C-2)</i>	<i>74</i>
<i>Figure 4-22 Polyglutamic Acid Productivity as a function of Dilution Rate for the Continuous Fermentation of B. licheniformis ATCC 9945a (Table C-2).....</i>	<i>75</i>
<i>Figure 4-23 Biomass Yield from Citric Acid (●) and Glutamic Acid (○) as a function of Dilution Rate for the Continuous Fermentation of B. licheniformis ATCC 9945a (Table C-3)</i>	<i>77</i>
<i>Figure 4-24 Biomass Yield from Glycerol (●) and Total Carbon Sources (○) as a function of Dilution Rate for the Continuous Fermentation of B. licheniformis ATCC 9945a (Table C-3)</i>	<i>78</i>
<i>Figure 4-25 Polyglutamic Acid yield from Biomass as a function of Dilution Rate for the Continuous Fermentation of B. licheniformis ATCC 9945a (Table C-4).....</i>	<i>80</i>
<i>Figure 4-26 Polyglutamic Acid Yield from Citric Acid (●) and Glutamic Acid (○) as a function of Dilution Rate for the Continuous Fermentation of B. licheniformis ATCC 9945a (Table C-4).....</i>	<i>81</i>

<i>Figure 4-27 Polyglutamic Acid Yield from Glycerol (●) and Total Carbon Sources (○) as a function of Dilution Rate for the Continuous Fermentation of B. licheniformis ATCC 9945a (Table C-4).....</i>	<i>82</i>
<i>Figure 4-28 Number Average Molecular Weight of PGA as a function of Dilution Rate for the Continuous Fermentation of B. licheniformis ATCC 9945a (Table C-5)</i>	<i>85</i>
<i>Figure 4-29 Weight Average Molecular Weight as a function of Dilution Rate for the Continuous Fermentation of B. licheniformis ATCC 9945a (Table C-5).....</i>	<i>86</i>
<i>Figure 4-30 Polydispersity as a function of Dilution Rate for the Continuous Fermentation of B. licheniformis ATCC 9945a (Table C-5)</i>	<i>87</i>
<i>Figure 4-31 The Specific Growth Rate as a function of the Citric Acid Concentration for the Continuous Fermentation of B. licheniformis ATCC 9945a (Table C-1)</i>	<i>89</i>
<i>Figure 4-32 The Specific Growth Rate as a function of Total Carbon Source Concentration for the Continuous Fermentation of B. licheniformis ATCC 9945a (Table C-1)</i>	<i>90</i>
<i>Figure E-1 GPC Calibration Curve for the PGA Polymer using Standards with Mn of 1×10^6 Da, 1×10^5 Da and 5×10^4 Da.....</i>	<i>128</i>
<i>Figure E-2 GPC Chromatogram for the PGA Standard with a Mn of 1×10^5.....</i>	<i>129</i>
<i>Figure E-3 Sample GPC Chromatogram from Late Batch Run.....</i>	<i>130</i>
<i>Figure E-4 GPC Chromatogram from $D = 0.051$</i>	<i>131</i>
<i>Figure E-5 Citric Acid Standard HPLC Chromatogram.....</i>	<i>132</i>
<i>Figure E-6 Glutamic Acid Standard HPLC Chromatogram.....</i>	<i>133</i>
<i>Figure E-7 HPLC Chromatogram of Medium.....</i>	<i>134</i>
<i>Figure E-8 HPLC Chromatogram for $D = 0.063 \text{ h}^{-1}$</i>	<i>135</i>
<i>Figure E-9 HPLC Chromatogram for $D = 0.051 \text{ h}^{-1}$</i>	<i>136</i>

LIST OF APPENDICES

<i>APPENDIX A Batch Fermentation Data</i>	<i>100</i>
<i>APPENDIX B Continuous and Transient Data as a Function of Real Fermentation Time</i>	<i>108</i>
<i>APPENDIX C Steady State Continuous Bioreactor Data as a Function of Dilution Rate</i>	<i>118</i>
<i>APPENDIX D Washout Experiment Data</i>	<i>124</i>
<i>APPENDIX E SAMPLE GPC AND HPLC CHROMATOGRAMS.....</i>	<i>127</i>

LIST OF NOMENCLATURE

C_{O_2}	Oxygen Concentration, mg/L
$C_{O_2}^*$	Equilibrium Oxygen Concentration, mg/L
D	Dilution Rate, h^{-1}
D_{max}	Maximum Dilution Rate, h^{-1}
F	Feed Rate, L/h
F_{in}	Inlet Flow Rate, L/h
F_{out}	Outlet Flow Rate, L/h
K_S	Substrate Saturation Constant, g/L
k_{La}	Volumetric Mass Transfer Coefficient, h^{-1}
M_n	Number Average Molecular Weight, Da
M_v	Viscosity Average Molecular Weight, Da
M_w	Weight Average Molecular Weight, Da
M_w/M_n	Polydispersity, Da/Da
N	Number of Molecules
P	Polyglutamic Acid concentration, g/L
P_X	Biomass Productivity (g/L/h)
P_P	Polyglutamic Acid Productivity (g/L/h)
Q_{O_2}	Specific Oxygen Uptake Rate, mmol O_2 per gram dry weight per hour
Q_{O_2X} (or OUR)	Oxygen Uptake Rate, mmol O_2 per litre per hour
r	Relative Coefficient
S	Substrate Concentration, g/L

S_0	Initial Substrate Concentration, g/L
S_1	Citric Acid Concentration, g/L
S_2	Glutamic Acid Concentration, g/L
S_3	Glycerol Concentration, g/L
S_{tot}	Total Carbon Source Concentration, g/L
t	Time, h
t_i	Initial Time, h
t_0	Initial Washout Time, h
V	Bioreactor Volume, L
V_0	Void Volume within a GPC column, mL
V_t	Total permeation volume in a GPC column, mL
VVM	Air Flow Rate, L air/L liquid volume per minute
X	Biomass Concentration, g/L
X_i	Initial Biomass Concentration, g/L
X_0	Initial Washout Biomass Concentration, g/L
$Y_{P/S}$	Polyglutamic Acid yield from substrate, g/g
$Y_{P/X}$	Polyglutamic Acid yield from biomass, g/g
$Y_{X/S}$	Biomass Yield from substrate, g/g
μ	Specific Growth Rate, h^{-1}
μ_{max}	Maximum Specific Growth Rate, h^{-1}

1. INTRODUCTION

1.1 *Commercial Significance of Polyglutamic Acid*

Polyglutamic acid is a water soluble biopolymer which can be produced through microbial fermentation of several *Bacillus* species. There are several promising and exciting applications of polyglutamic acid, most importantly as a drug carrier for the anti-cancer drug paclitaxel. By conjugating paclitaxel to the polyglutamic acid polymer, several benefits are achieved. The conjugate is more water soluble, has a higher anti-tumor activity and has less side effects than paclitaxel alone (Holmes et al., 1995; Li et al., 2000; Richard and Margaritis, 2003; Shih and Van, 2001). A specific molecular weight of polyglutamic acid (30,000 – 50,000 Da) is required for this particular application.

1.2 *Research Objectives*

Although the production of polyglutamic acid has been studied in depth for several decades (Birrner et al., 1994; Cheng et al., 1989; Cromwick and Gross, 1995; Cromwick et al., 1996; Goto and Kunioka, 1992; Hara et al., 1982; Ito et al., 1996; Kubota et al., 1993; Ogawa et al., 1997; Richard and Margaritis, 2001; Thorne et al., 1954; Troy, 1973), to the author's knowledge, there has been no investigation into the continuous production of polyglutamic acid in a continuous stirred tank bioreactor (CSTR). The use of a CSTR will allow for a more accurate determination of the kinetic constants used in the modeling of growth for this system. Additionally, it has been traditionally thought that a CSTR will increase both the yield and productivity of the

polymer, which will be determined in this study. It was hoped that during the course of the continuous experiments, the desired molecular weight (30 – 50 kDa) would be produced.

In addition to the investigations into the continuous production of polyglutamic acid, the rheology and oxygen transfer characteristics of the batch system will be investigated. At present, there has been no determination of the specific oxygen uptake rate, the oxygen uptake rate or the volumetric mass transfer coefficient for this particular strain.

1.3 Thesis Layout and Scope

This thesis has been organized in the monograph form. Chapter 2 is a detailed review of all relevant literature. It contains information on the production of polyglutamic acid, the characteristics and applications of polyglutamic acid and a general review of the available bacteria, with a more in depth look at *B. licheniformis* ATCC 9945a. The growth models for both the batch and continuous systems as well as the Richard – Margaritis empirical model were examined. Finally, information on both high performance liquid chromatography and gel permeation chromatography were included.

The material and methods are included in chapter 3, and details the analytical methods, as well as the experimental procedures used in this investigation.

The results and discussion section gives a detailed account of the experimental findings. Included were the biomass, product and substrate concentrations at various fermentation times in the batch fermentation of *B. licheniformis* as well as the molecular weight, viscosity and oxygen transfer characteristics.

In the continuous system, the biomass, product and substrate concentrations were found at various dilution rates. The productivity and yield of the biomass and product were found as a function of dilution rate. The molecular weight distribution was determined as a function of dilution rate. The maximum specific growth rate was found using both washout experiments and the Richard – Margaritis empirical model.

The thesis is concluded with the conclusions and recommendations section. This section includes a summary of the experimental findings and recommendations for future work.

2. LITERATURE REVIEW

2.1 Introduction

The production of polyglutamic acid by microbial fermentation has been investigated for the past 60 years. Several *Bacillus* species have been isolated, and produce polyglutamic acid at various culture conditions. In most cases, polyglutamic acid has been produced in controlled batch fermentations and shake flask experiments. In one case, polyglutamic acid was produced in fed-batch conditions. To the author's knowledge, no investigation into the continuous production of polyglutamic acid has been attempted or reported.

2.2 Polyglutamic Acid

Polyglutamic acid (PGA) is a naturally occurring pseudo-poly (amino acid), originally discovered by Ivánovics and co-workers in 1937, as a capsule of *Bacillus anthracis* (Shih and Van, 2001). PGA was released from *B. anthracis* after autoclaving or upon aging and autolysis of the cells. PGA has long been known to be a main constituent of the mucilage of "natto" (a traditional Japanese food) which is produced by *Bacillus natto* Sawamura (Shih and Van, 2001).

Several *Bacillus* species have been shown to produce polyglutamic acid during fermentation, including *B. anthracis*, *B. licheniformis* ATCC 9945a, *B. subtilis* IFO 3335, *B. subtilis* TAM-4, *B. licheniformis* A35, *B. subtilis* F02-1 and *B. subtilis* (natto) (Cheng et al., 1989; Goto and Kunioka, 1992; Hara et al., 1982; Ito et al., 1996; Kubota et al., 1993; Ogawa et al., 1997; Thorne et al., 1954; Troy, 1973).

γ -Polyglutamic acid is structurally different from proteins, in that the glutamic acid monomers are attached through the γ -amide linkage (as opposed to the α -amide linkage found in proteins). Since there is this fundamental difference in structure, it is believed that the γ -PGA is synthesized independently from ribosomes (Shih and Van, 2001). Polyglutamic acid is produced as a mixture of both L and R glutamic acid monomers. The ratio of L to R monomers depends on the strain of bacteria used and medium composition.

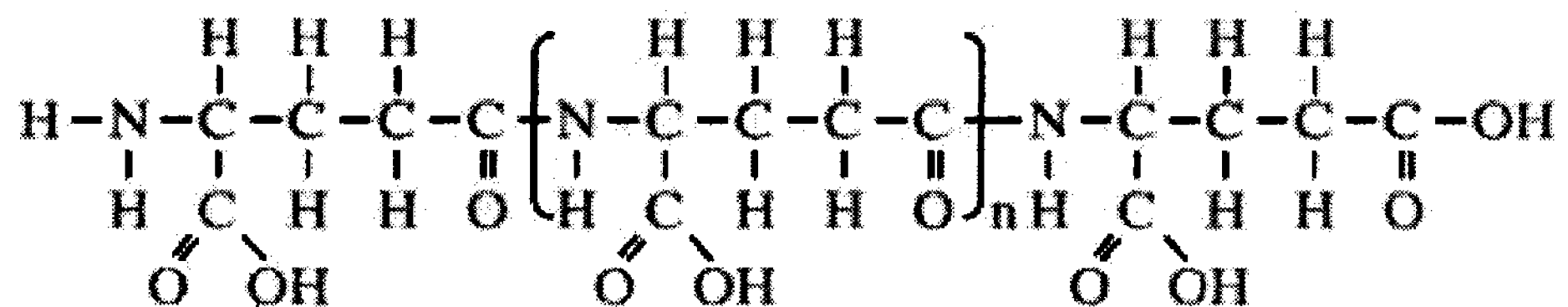


Figure 2-1 γ -Polyglutamic acid

The location and identification of the genes related to PGA synthesis has been investigated by several researchers (Ashiuchi et al., 1998; Ashiuchi et al., 1999; Hara and Ueda, 1982; Nagai et al., 1997; Onodera et al., 1994; Vietri et al., 1995). Depending on the species producing PGA, the genes have been shown to be in different locations. In *B. subtilis* (natto) the PGA synthesis genes are located in the genomic DNA (Nagai et al., 1997), while in *B. anthracis*, the genes lie on a large plasmid (Vietri et al., 1995). The genes responsible for the synthesis of PGA were identified by Ashiuchi and co-workers (1998, 1999). Three genes are responsible for the synthesis, and this system has been referred to as pgsBCA.

The purification of PGA from culture broth is straightforward, as the polymer is produced outside of the cells. The purification requires three steps, centrifugation of the culture broth to remove cells, precipitation of the PGA from the cell free medium using methanol or ethanol, and the removal of low molecular weight impurities through ultra filtration (Goto and Kunioka, 1992). PGA from fermentation typically has a molecular weight between 100,000 – 8,000,000 Da, and a polydispersity between 2 – 5 (Shih and Van, 2001).

PGA is completely biodegradable, water soluble, edible and non-toxic to humans, and has been suggested for use in a wide range of applications. Especially important applications include the use of PGA in medicine as a drug carrier, and a biological adhesive.

Recently, research has shown that PGA is an ideal candidate for the controlled release of the anticancer drug Paclitaxel. Paclitaxel (Taxol ®) is a natural anti-microtubule agent extracted from the needles and bark of the Pacific Yew tree (*Taxis brevifolia*). Taxol has potent anti-tumor activity against both breast and ovarian tumors (Holmes et al., 1995). Unfortunately, paclitaxel is quite insoluble in water, preventing proper treatment of the tumors. By conjugating paclitaxel to PGA through covalent bonding, the drug compound becomes more stable and more water soluble (Li et al., 2000; Richard and Margaritis, 2003). The conjugate (TXL-PGA) exhibits a much higher anti-tumor activity, and complete regression of the tumors has been observed in both ovarian and breast cancer in animal models. In addition, this anti-tumor activity can be seen with only one intravenous injection of the paclitaxel-PGA conjugate. The uptake of the conjugate is up to five times greater than an equal dose of paclitaxel alone (Shih and

Van, 2001). Once in the cells, the PGA polymer is digested, and a more potent dose of paclitaxel is released directly to the cancer cell. PGA can also act as a drug depot for sustained controlled release, which enables a longer exposure to tumor cells (Li et al., 1999). The TXL-PGA conjugate is also quite stable in the plasma (less than 0.1% is released in 144h), reducing the release of paclitaxel to the non-tumor locations, thus reducing side effects to the patient (Li et al., 1999). Recent studies have investigated the use of PGA nano particles in targeting liver cancer cells (Liang et al., 2005).

As a biological adhesive, PGA has shown promise. Biological adhesives are important for the control of massive bleeding, and wound closure in surgery. Unlike many of the currently used biological adhesives (such as cyanoacrylate, urethane prepolymers and gelatin resorcinol-formaldehyde), the PGA – gelatin biological adhesive has lower cytotoxicity, a more rapid degradation rate and a much lower toxicity of degradation products to the patient. The PGA – gelatin adhesive has shown much higher adhesion than similar low toxic biological adhesives, such as fibrin glue. Also, a new potential biological adhesive made from porcine collagen and PGA has been developed as a superior alternate to fibrin in sealing air leakages from the lungs (Shih and Van, 2001).

In addition to the medical applications listed above, PGA has been used as a biopolymer flocculant, as a heavy metal and radionuclide binder, as a biodegradable polymer, and in food applications.

2.3 PGA Producing Bacteria

Polyglutamic acid is produced by several *Bacillus* species. Nutrient requirements varied according to the *Bacillus* strain used. There are two general categories of PGA producing strains. The first group, which includes *B. anthracis* (Thorne et al., 1953), *B. licheniformis* ATCC 9945a (Birrer et al., 1994; Cromwick and Gross, 1995; Cromwick et al., 1996; Thorne et al., 1954), *B. subtilis* IFO 3335 (Goto and Kunioka, 1992; Kunioka and Goto, 1994; Richard and Margaritis, 2001; Richard and Margaritis 2003), and *B. subtilis* F-2-01 (Kubota et al., 1993), requires the addition of L-glutamic acid to the medium to stimulate PGA production. The second group comprising *B. subtilis* TAM-4 (Ito et al., 1996), and *B. licheniformis* A35 (Cheng et al., 1989), is able to produce PGA independent of L-glutamic acid.

In the case of L-glutamic acid dependent bacteria, other carbon sources are often required, most often being glycerol, citric acid, fructose or glucose. L-glutamic acid independent bacteria most often used sugars (glucose and maltose) as the primary carbon source.

2.4 *Bacillus licheniformis* ATCC 9945a

Bacillus licheniformis ATCC 9945a was used in this thesis. *B. licheniformis* is a Gram positive rod, most commonly found in soil. *B. licheniformis* ATCC 9945a fermentation has been extensively investigated within controlled batch fermentations, shake flask fermentations and fed batch fermentations (Birrer et al., 1994; Bovarnick, 1942; Cromwick and Gross, 1995; Cromwick et al., 1996; Hwan Do et al., 2001; Ko and Gross, 1998; Leonard et al., 1958; Thorne et al., 1954; Troy, 1973; Yoon et al., 2000).

Leonard and co-workers (1958) were the first to examine PGA production through the optimization of the culture medium. The following medium (designated medium C) was first used to produce PGA to concentrations of up to 15 g/L after 3-4 days: glycerol, 80 g/L; citric acid, 12 g/L; L-glutamic acid, 20 g/L; NH_4Cl , 7 g/L; $\text{MgSO}_4 \cdot 7\text{H}_2\text{O}$, 0.5 g/L; $\text{FeCl}_3 \cdot 6\text{H}_2\text{O}$, 0.04 g/L; K_2HPO_4 , 0.5 g/L and tap water. Studies by Leonard et al. (1958) showed that only tap water and a specified lot of FeCl_3 would produce the PGA polymer. Further investigations revealed that the tap water used had a significant amount of Ca^{+2} present. Additionally the lot of FeCl_3 was found to be contaminated with a small amount of Mn^{+2} . Medium C was then optimized to include distilled water (instead of tap water), $\text{MnSO}_4 \cdot \text{H}_2\text{O}$ (0.000026 – 0.42 g/L) and $\text{CaCl}_2 \cdot 2\text{H}_2\text{O}$ (0.15 g/L) (Leonard et al., 1958).

The mechanism involved with PGA production by *B. licheniformis* is poorly understood. According to past works (Cromwick and Gross, 1995; Goto and Kunioka, 1992) citric acid and glutamic acid are involved in the TCA cycle. It is not clear how glycerol increases PGA production, but it has been shown that glycerol is required for production of PGA to high concentrations (Shih and Van, 2001).

Further investigations into the actual role of Mn^{+2} were performed by Cromwick and Gross (1995). They investigated the effect of varying the MnSO_4 concentration from 0 – 0.104 g/L. By increasing the concentration of MnSO_4 cell viability was greatly increased. At low concentrations of MnSO_4 cell viability was significantly reduced after 50 hours, while at high concentrations, cell viability was maintained throughout the 144 hour fermentation. Sporulation was not observed during the fermentation, and therefore did not explain the prolonged cell viability. In addition to prolonged cell viability,

greater carbon source utilization and higher PGA concentrations were observed with increasing MnSO_4 concentration (Cromwick and Gross, 1995). Magnesium sulfate has been shown to affect the L to D ratio of glutamic acid monomers within the PGA polymer. By increasing the MgSO_4 concentration from 0 to 615 μM , the L-glutamate content is reduced from 59% to 10% (Cromwick and Gross, 1995).

The effects of pH and aeration were investigated by Cromwick and co-workers (1996). The effect of pH (5.5, 6.5, 7.4, 8.25) on PGA concentration, using medium E, was studied. The maximum PGA concentration was found at a pH of 6.5 (14.2 g/L), the concentration of PGA at a pH of 5.5, 7.4, and 8.25 was 9.9 g/L, 6.9 g/L and 4.2 g/L respectively (Cromwick et al., 1996). By increasing the aeration rate from 0.5 vvm to 2 vvm at pH 6.5, the PGA concentration was increased to 23 g/L. The cell dry weight showed the same trend, having the highest concentration at pH 6.5 and aeration of 2 vvm.

Table 2-1 contains a summary of some of these past works. It includes the major substrate concentrations, the PGA concentration produced, the PGA productivity and the PGA yield from total carbon sources.

Nutrients	PGA Concentration (g/L)	PGA Productivity (g/L/h)	PGA Yield (g/g total Carbon Sources)	References
Glutamic Acid (20 g/L) Glycerol (80 g/L) Citric Acid (12 g/L)	23	0.34	0.214	Cromwick et al. (1996)
Glutamic Acid (20 g/L) Glycerol (80 g/L) Citric Acid (12 g/L)	6	0.06	0.054	Ko and Gross (1998) ^a
Glucose (40 g/L) Glutamic Acid (20 g/L) Citric Acid (12 g/L) Glycerol (40g/L)	20	0.21	0.152	Ko and Gross (1998)
Glutamic Acid (20 g/L) Glycerol (80 g/L) Citric Acid (12 g/L)	35	0.83	0.207	Yoon et al. (2000) ^b
Glutamic Acid (20 g/L) Glycerol (80 g/L) Citric Acid (12 g/L)	19	0.173	0.275	Cromwick and Gross (1995)
Glutamic Acid (20 g/L) Glycerol (80 g/L) Citric Acid (12 g/L)	20	-	0.223	Hwan Do et al. (2001)

^a Results from shake flask experiments

^b Results from fed-batch experiments

Table 2-1 The effect of substrates on the PGA concentration, productivity and yield from selected works

2.5 Growth Kinetics

2.5.1 Batch Growth

Batch growth occurs in a closed bioreactor, containing nutrient medium. The bioreactor is inoculated and no fresh medium is added to the system. The microorganisms begin and continue to grow until the limiting substrate is exhausted, or an inhibitor accumulates.

As seen in Figure 2-2, batch growth contains five main phases, lag (1), exponential growth (2), decline (3) stationary (4), and death (5). The lag phase refers to the initial period, after inoculation of the batch system. There is little change in the number of cells, and is associated with a time of adaptation of the microorganisms to their environment. During the exponential growth phase, the microorganisms divide rapidly producing an exponential increase in cell population. During this time, the limiting substrate is plentiful, and no inhibition occurs. The decline phase is characterized in a reduction in the growth rate of the microbes. The stationary phase begins when nutrients are depleted to the point of interfering with cell growth. During the stationary phase, there is no change in cell concentration as the number of cells being produced is equal to those dying. During the death phase, the limiting substrate has been depleted to the point that cells cannot reproduce fast enough to replace dying cells, and the overall cell concentration is greatly reduced (Blanch and Clark, 1996).

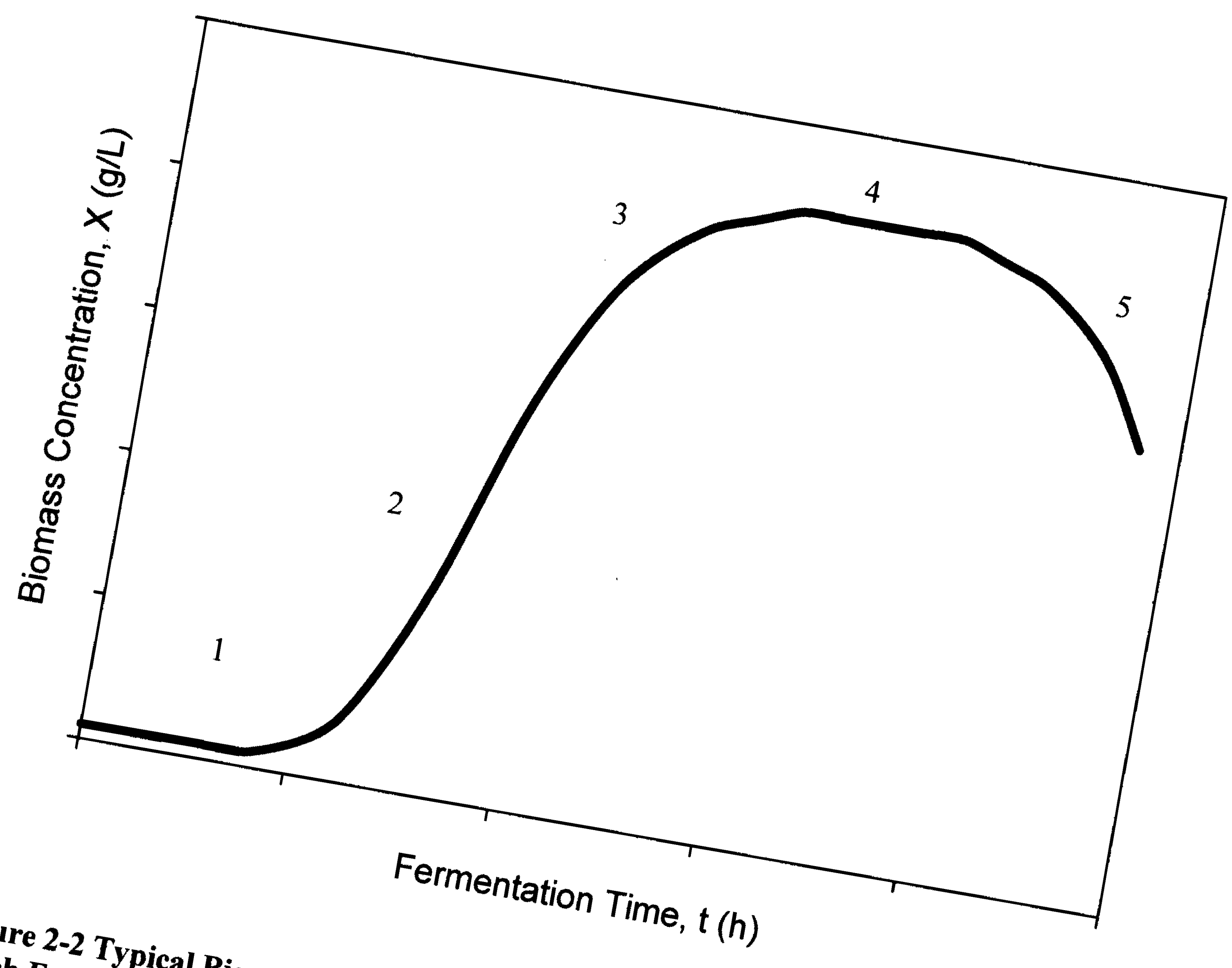


Figure 2-2 Typical Biomass Concentration as a function of Fermentation Time for Batch Fermentation (Blanch and Clark, 1996)

Modeling of cell growth within a batch system, assuming a homogeneous population and a balanced growth, requires an expression for the change in cell concentration with respect to time. For unicellular microorganisms that reproduce through binary fission, the following expression is most often used.

$$\frac{dX}{dt} = \mu X \quad (2.1)$$

Where, X is the biomass concentration (g/L), t is the time (h) and μ is the specific growth rate (h^{-1}). The specific growth rate is dependent on many different factors, including medium composition, temperature, pH, and in the case of aerobic growth, dissolved oxygen concentration (Blanch and Clark, 1996).

In many systems, the specific growth rate can be modeled using the Monod equation:

$$\frac{dX}{dt} = \mu X = \frac{(\mu_{\max} S)}{(K_s + S)} X \quad (2.2)$$

Where; S is the concentration of the limiting substrate (g/L), K_s is the substrate saturation constant (g/L) and μ_{\max} is the maximum specific growth rate (h^{-1}). The saturation constant, or the half velocity constant is the concentration of substrate at which the specific growth rate is equal to half the maximum specific growth rate (Arbige et al., 1993).

At very high concentrations of the limiting substrate (i.e. $S \gg K_s$), equation 2.2 is reduced to the first order equation:

$$\frac{dX}{dt} = \mu_{\max} X \quad (2.3)$$

Integrating this equation yields,

$$\ln(X/X_i) = \mu_{\max}(t - t_i) \quad (2.4)$$

Applying this equation to the exponential cell growth (i.e. the exponential growth phase), the maximum specific growth rate can be determined for batch fermentations. At low substrate concentrations, equation 2.2 is reduced to the second order equation:

$$\frac{dX}{dt} = \frac{\mu_{\max} S}{K_s} X \quad (2.5)$$

In this case, the cell growth rate depends on both the cell concentration and the substrate concentration.

The change of substrate concentration with time can be expressed using the following equation:

$$\frac{dS}{dt} = \frac{-\mu X}{Y_{X/S}} \quad (2.6)$$

Where $Y_{X/S}$ is the cell growth yield (g cells produced/ g of substrate consumed).

The estimation of the kinetic constants (μ_{\max} and K_s) using batch culture experiments has several limitations. First, the specific growth rate only reaches the maximum specific growth rate for very short periods, if at all. This situation occurs at very high substrate concentrations, which are often difficult to achieve. Often, data from the beginning of the exponential growth phase are used. At this point, substrate concentration may be high, but may not be high compared to the saturation constant. This results in only an estimation of the maximum specific growth rate (Blanch and Clark, 1996).

In addition, the absence of balanced growth makes the use of the Monod equation questionable. Since environmental conditions are constantly changing with time, the

cells are constantly modifying their growth rate depending on the state of their metabolic processes (Kovarova-Kovar and Egli, 1998).

2.5.2 Continuous Stirred Tank Reactor (CSTR)

Continuous growth is a steady state process, achieved in a CSTR. A vessel is first filled with nutrient medium, and inoculated with microbes. An input stream is continually fed to the bioreactor, while a withdrawal stream removes culture broth from the bioreactor, such that a constant volume is achieved. At steady state, the biomass, substrate and product concentrations are all constant.

A continuous system generally has three operating regions (as seen in Figure 2-3), the first is the initial batch region (1), used to increase biomass concentration. The second region is the transient unsteady-state region (2), where the fresh medium is first introduced into the system and is characterized by changing biomass concentration with time. The third is the steady state continuous operation region (3), where constant biomass concentration is achieved.

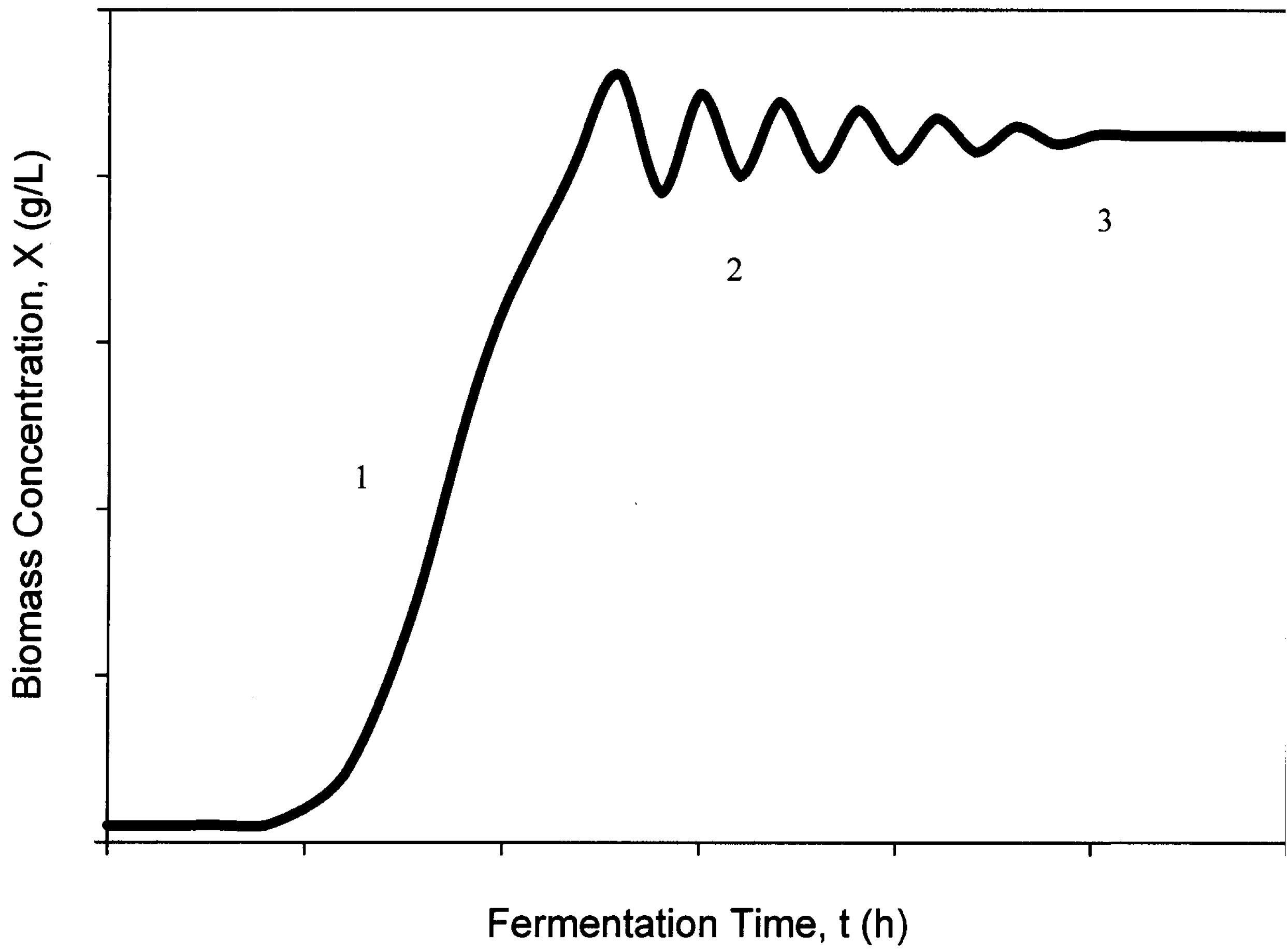


Figure 2-3: Biomass Concentration as a function of Time for the Continuous System

Within a continuous system, the change of cell concentration with time is expressed by the following mass balance.

$$\frac{dX}{dt} = F_{in}X_0 - F_{out}X + V\mu X \quad (2.7)$$

Where, F_{in} is the inlet flow rate (L/h), X_0 is the inlet cell concentration (g/L), F_{out} is the outlet flow rate (L/h), X is the cell concentration within the bioreactor, V is the reactor volume (L) and μ is the specific growth rate (h^{-1}). Assuming the inlet and outlet flow rates are equal (to maintain a consistent volume), and the inlet cell concentration is zero, equation 2.7 is reduced to:

$$\frac{dX}{dt} = -FX + V\mu X \quad (2.8)$$

At steady state, the change in cell concentration with time is zero, and equation 2.8 becomes:

$$FX = V\mu X \quad (2.9)$$

The dilution rate is a term often employed within a continuous system. Dilution rate is determined by equation 2.10.

$$D = \frac{F}{V} \quad (2.10)$$

Substituting equation 2.10 into 2.9 gives the following equation.

$$DX = \mu X \quad (2.11)$$

$$D = \mu = \frac{\mu_{max}S}{K_S + S} \quad (2.12)$$

The relationship expressed in equation 2.12 is an important one. It shows that control of the specific growth rate can be achieved through the manipulation of two hydrodynamic properties, namely the reactor volume and flow rate.

To determine the highest dilution rate that can be used for the system, equation 2.12 is used, and the inlet substrate concentration (of the fresh medium) is used as the substrate concentration, as seen in equation 2.13.

$$D_{\max} = \frac{\mu_{\max} S_0}{K_S + S_0} \quad (2.13)$$

Where D_{\max} is the maximum achievable dilution rate and S_0 is the inlet substrate concentration. It can be seen that as the saturation constant (K_S) is increased, the maximum achievable dilution rate is decreased, while at very high substrate concentrations, the maximum dilution rate becomes equivalent to the maximum specific growth rate.

An important feature of the continuous system is that the dilution rate must be maintained at a level lower than the maximum dilution rate. If the dilution rate is higher than the maximum dilution rate, the cells will be withdrawn from the system more quickly than they can be replaced, resulting in a washout situation. Washout of cells is an unsteady state system and is described by the following equation:

$$\frac{dX}{dt} = (\mu_{\max} - D)X \quad (2.14)$$

By integrating equation 2.14, the following equation is produced:

$$\ln(X) = \ln(X_0) - (D - \mu_{\max})(t - t_0) \quad (2.15)$$

Where X_0 is the cell concentration at the beginning of the washout experiment and t_0 is the time at the beginning of the washout experiment.

By setting a higher dilution rate than the expected maximum specific growth rate, and plotting equation 2.15, the maximum specific growth rate can be calculated. The slope of the plot will be $-(D - \mu_{\max})$.

2.5.3 Richard – Margaritis Empirical Model

According to studies performed by Richard and Margaritis (2004), a modification to the Monod equation is required for the modeling of a fermentation in which a biopolymer is produced. From past studies, it had been noted that the specific growth rate of the microorganisms approached zero, even when significant amounts of the limiting substrate were present (Richard and Margaritis, 2004). Plotting the specific growth rate as a function of the limiting substrate concentration yielded an “S” type curve (Figure 2-4).

Richard and Margaritis modified the Monod equation to allow for a sigmoidal fit of specific growth rate as a function of the substrate concentration. The following is the modified equation.

$$\mu = \frac{\mu_{\max} S^r}{(K_s^r + S^r)} \quad (2.16)$$

The constant “r” is the relative coefficient. The relative coefficient represents how growth related the biopolymer production is. The closer “r” is to 1, the more growth related the biopolymer production, while larger values of “r” indicate non-growth related biopolymer production (Richard and Margaritis, 2004).

The Richard – Margaritis model is similar to that proposed by Moser:

$$\mu = \mu_{\max} \frac{S^\lambda}{K_s + S^\lambda}$$

This modified Monod equation can be applied to both the batch and continuous operations, to give a more accurate description of the biopolymer production.

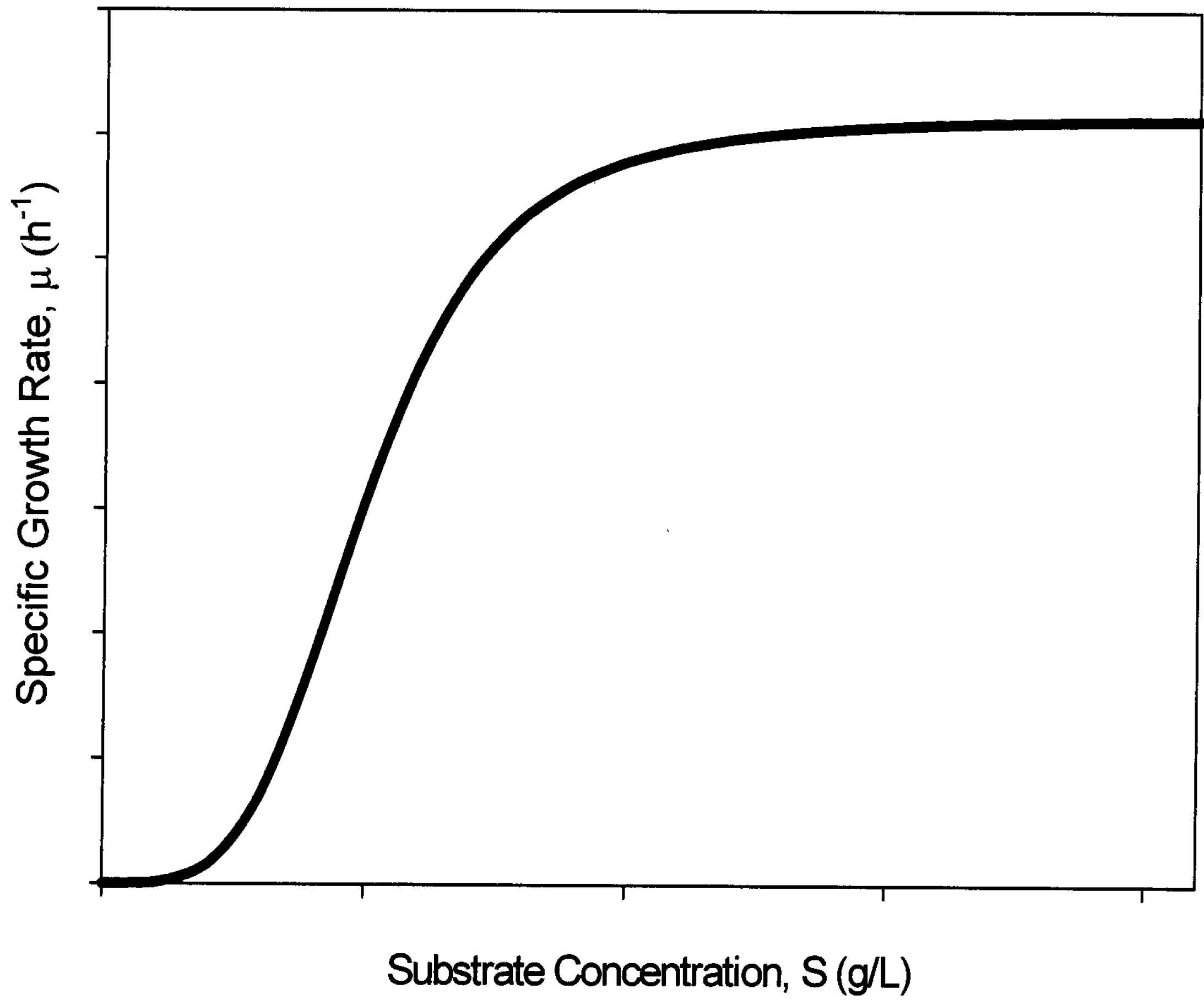


Figure 2-4 Specific Growth Rate as a function of Substrate Concentration using the Richard- Margaritis Empirical Model

2.5.4 Growth Model for Multiple Substrate Growth

Since the system that is being investigated in this thesis contains several major substrates (glycerol, glutamic acid and citric acid) a growth model involving all three substrates should be examined. Two common models used are the additive kinetic model and the multiplicative kinetic model. The additive kinetic model is as follows:

$$\mu = \frac{\mu_{\max 1} S_1}{K_1 + S_1} + \frac{\mu_{\max 2} S_2}{K_2 + S_2} + \dots + \frac{\mu_{\max n} S_n}{K_n + S_n}$$

Where $\mu_{\max n}$ is the maximum specific growth rate found with substrate “n”, S_n is the “n” substrate concentration and K_n is the saturation constant of substrate “n”. The multiplicative kinetic model is:

$$\mu = \mu_{\max} \left(\frac{S_1}{K_1 + S_1} \times \frac{S_2}{K_2 + S_2} \times \dots \times \frac{S_n}{K_n + S_n} \right)$$

Where μ_{\max} is the maximum specific growth rate of the entire system, S_n is the “n” substrate concentration and K_n is the saturation constant of substrate “n” (Blanch and Clark, 1996). Although these models may give an accurate description of the microbial growth on multiple substrates, Kovarova-Kovar and Egli (1998) have found that in reality these models are difficult to apply. The large number of parameters needed for an accurate determination of this model leads to difficulty in applying the model. To reduce the difficulty in applying the above mentioned models, two solutions may be used. The first is to use only the limiting substrate concentration (when one is identified) in the growth models described in sections 2.5.1 -2.5.3. The second solution is to use the total carbon source concentration in the models described in sections 2.5.1 -2.5.3 (Kovarova-Kovar and Egli, 1998).

2.6 Number and Weight Average Molecular Weight Calculations

There are several commonly used terms used to describe the size (or molecular weight) of a polymer. Two of the more common are the Number Average Molecular Weight (M_n) and the Weight Average Molecular Weight (M_w). A third term, polydispersity (M_w/M_n) can be use as well.

The number average molecular weight (M_n) represents the total weight of the molecules in a mixture (M_i), divided by the number of molecules present (N_i). Number average molecular weight represents the arithmetic mean. The following equation can be used:

$$M_n = \frac{\sum_{i=0}^{\infty} N_i M_i}{\sum_{j=0}^{\infty} N_j} \quad (2.17)$$

The weight average molecular weight (M_w) is calculated using equation 2.18.

$$M_w = \frac{\sum_{i=0}^{\infty} N_i M_i^2}{\sum_{j=0}^{\infty} N_j M_j} \quad (2.18)$$

The polydispersity of the polymer is given by equation 2.19, and is the ratio of weight average molecular weight and the number average molecular weight. The polydispersity represents how widely distributed the polymer is.

$$PolyDispersity = \frac{M_w}{M_n} \quad (2.19)$$

2.7 Volumetric Mass Transfer Coefficient, Oxygen Uptake Rate and Specific Oxygen Uptake Rate

The volumetric mass transfer coefficient ($k_L a$), the oxygen uptake rate (OUR or $Q_{O_2} X$) and the specific oxygen uptake rate (Q_{O_2}) are important design parameters in an aerated bioreactor. The change of oxygen concentration with time (dC_{O_2}/dt) is related to these terms through equation 2.20, which is the oxygen mass balance for the system.

$$\frac{dC_{O_2}}{dt} = k_L a (C_{O_2}^* - C_{O_2}) - Q_{O_2} X \quad (2.20)$$

Where $C_{O_2}^*$ is equal to the concentration of oxygen in equilibrium with the partial pressure of oxygen in the atmosphere, and C_{O_2} is the concentration of the dissolved oxygen in the fermentation broth. The oxygen uptake rate (OUR) is equivalent to the specific oxygen uptake rate (Q_{O_2}) times the biomass concentration (X).

At equilibrium (i.e. when $dC_{O_2}/dt = 0$) equation 2.20 is reduced to equation 2.21.

$$k_L a (C_{O_2}^* - C_{O_2}) = Q_{O_2} X \quad (2.21)$$

In this case, the amount of oxygen consumed by the microbes ($Q_{O_2} X$) is equivalent to that transferred to them ($k_L a (C_{O_2}^* - C_{O_2})$).

To determine $k_L a$, OUR and Q_{O_2} the dynamic gas off/ gas on method suggested by Bandyopadhyay and Humphrey (1967) can be used. Figure 2-5 gives a typical plot of this method.

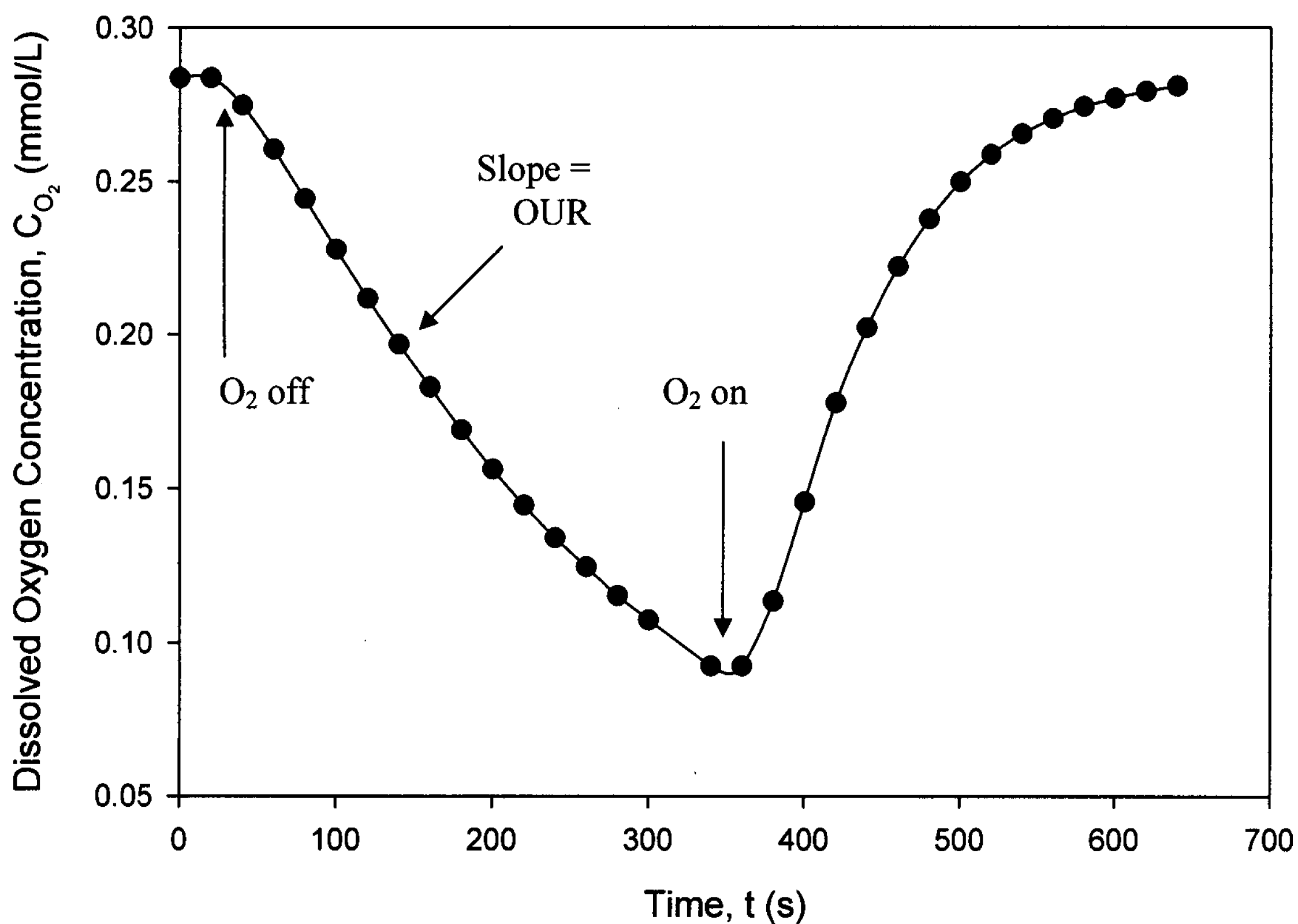


Figure 2-5 Sample Plot of the Dynamic Gas off/Gas on method for determination of k_{La} , OUR and Q_{O_2}

In this method, during the fermentation, the oxygen flow is stopped (gas off), at which point the change in dissolved oxygen concentration with time is attributed solely to the OUR (and thus Q_{O_2}), and is equivalent to the slope of the plot during this time. The oxygen flow is then turned on (gas on), and the k_{La} value can be found from the slope of the following equation:

$$C_{O_2} = \frac{-1}{k_L a} \left(\frac{dC_{O_2}}{dt} + Q_{O_2} X \right) + C_{O_2}^* \quad (2.22)$$

2.8 High Performance Liquid Chromatography

High performance liquid chromatography (or HPLC) is an effective tool in the identification and quantification of different compounds in solution. A high performance liquid chromatography system is composed of an HPLC column, a mobile phase and a detector capable of identifying the compound of interest.

Chromatography is a broad classification of techniques used for separating the components of a mixture using a stationary phase and a mobile phase. In the case of HPLC, the mobile phase is a liquid and the stationary phase is a solid. The components in the mixture are separated based on their adsorption affinities for the stationary phase.

The HPLC columns are either normal phase or reverse phase. In normal phase, the columns are usually packed with silica gel and work in the mode of conventional chromatography. Normal phase systems are generally used to identify and separate lipids and fats, and the mobile phase is typically an organic solvent (or non-polar solvents). During normal phase HPLC, non-polar compounds elute first, as they do not interact with the polar packing as much as polar compounds. In reverse phase systems, the columns are typically packed with chemically bonded octadecylsilyl coated silica and are very non-polar and have a polar mobile phase (typically aqueous solutions with methanol). Unlike normal phase HPLC, polar compounds are eluted first.

The HPLC system is very effective in separating the compounds in the mixture. The elution time of a peak identifies the compound, while the area under the peak (or the height of the peak in some cases) will give the concentration of the compound in solution. A calibration curve can be generated relating the peak area to the concentration in solution, and can be employed to determine unknown concentrations from a sample.

Figure 2-6 is a sample chromatogram of a mixture containing three different compounds, eluting at 5.1 minutes, 7.6 minutes and 8.65 minutes.

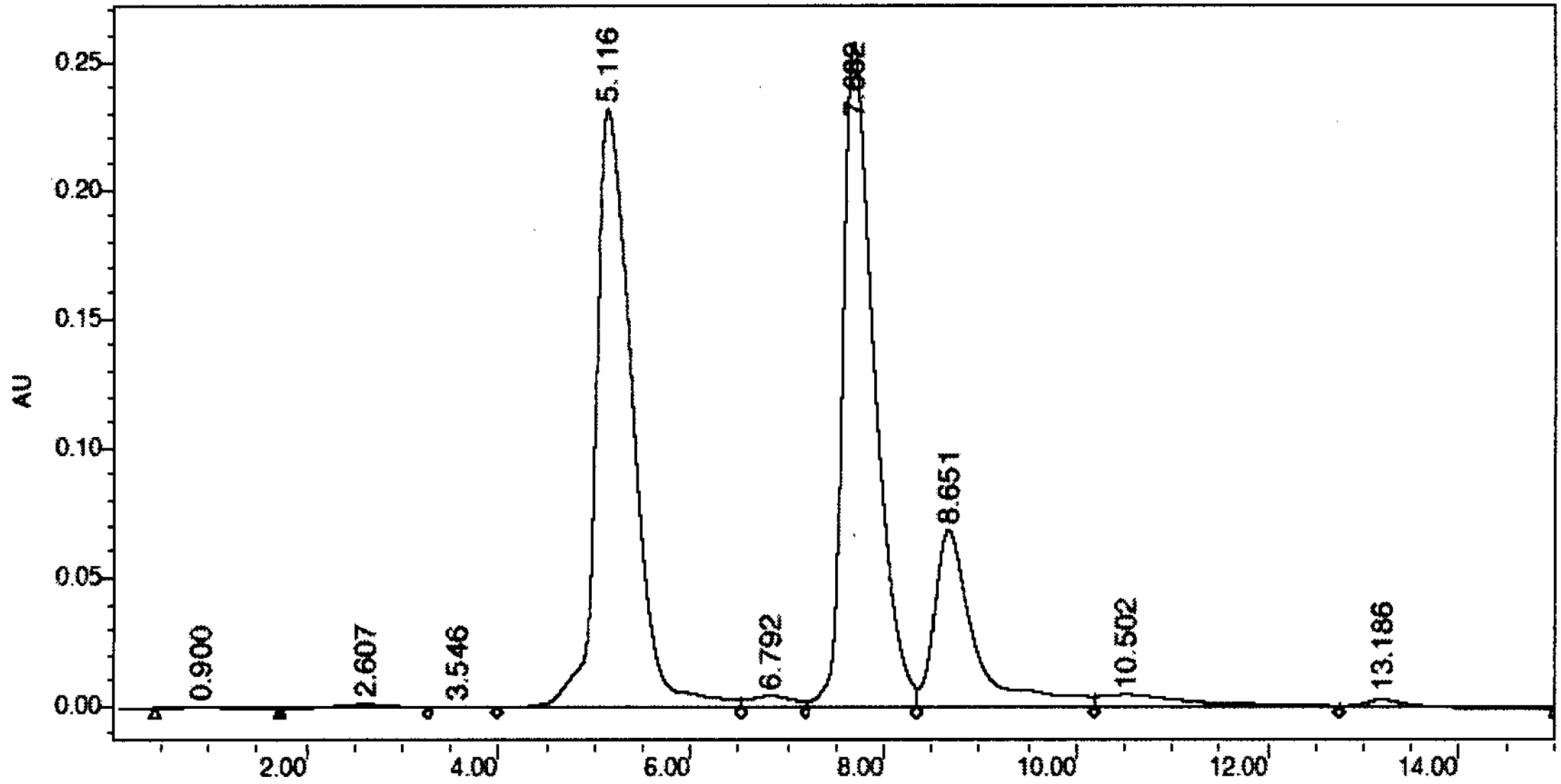


Figure 2-6 Sample Chromatogram, the Absorbance (AU) as a function of Retention Time

2.9 Gel Permeation Chromatography

Gel permeation chromatography (GPC), also called size exclusion chromatography (SEC), is an effective tool in the analysis of the molecular weight characteristics of polymers.

A GPC system consists of a GPC column, a solvent for the carrying of the polymer, and a detector to detect the polymer. A GPC column is typically packed with small (5 – 10 μm) silica or polymer particles, consisting of a series of uniform pores, into which the polymer and solvent can diffuse. While in the pores, the molecules are trapped and removed from the flow of mobile phase. Molecules larger than the pores are not retained, and are eluted first. The molecules which are significantly smaller than the pores penetrate throughout the pore maze and are entrapped for the greatest time. Intermediate sized molecules are retained in packing for various times, depending on the diameter of the molecules. Fractionation occurs, which is related to molecular weight, and allows for the analysis of the average molecular weight and the dispersity of molecular weights within the polymer sample (Skoog and Leary, 1992).

The mobile phase is selected primarily based on several parameters. It must dissolve the polymer completely, it must be low enough in viscosity for the GPC system to operate in normal pressure ranges and there must be no interaction between the mobile phase and the polymer.

The elution volume (or elution time) of the polymer is a function of the molecular weight, and typically forms a logarithmic relationship. The void volume, or total exclusion volume (V_0) is the total interstitial volume in the chromatographic system, and is the point before which no polymer can elute. The total permeation volume (V_t)

represents the sum of the interstitial volume and the total pore volume. This is the volume at which point the smallest molecules will elute. Polymers outside the effective range will not be selectively eluted. The larger polymer will elute at V_0 and the smaller particles will elute at V_t (Wu, 2004).

Calibration curves can be created using two methods, the first is using several narrowly distributed standards of the same polymer, the second is using broad (or polydisperse) samples with known molecular weight characteristics (most often M_n and either M_w or M_v).

When calibrating a system with narrowly distributed standards, a plot similar to the one found in Figure 2-7 will be generated, and molecular weight characteristics can be determined using this plot. For broadly disperse standards, computer software can be employed to develop a similar plot.

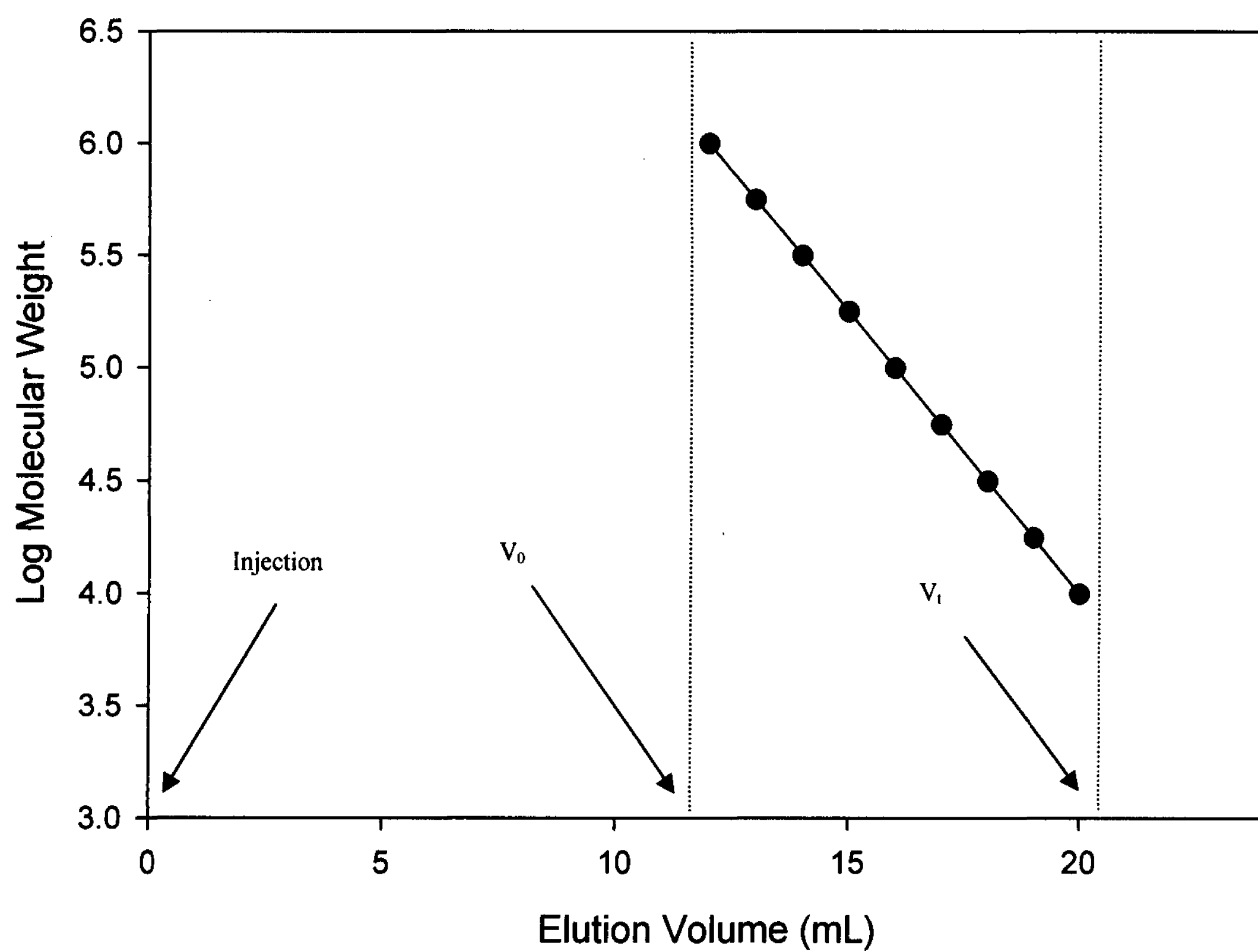


Figure 2-7 Typical GPC Calibration Curve, log Molecular Weight as a function of Elution Time (Wu, 2004)

3. EXPERIMENTAL METHODS

3.1 *Bacillus licheniformis* Growth

3.1.1 Microorganism

Bacillus licheniformis ATCC 9945a, obtained from the American Type Culture Collection (Manassus, VA), was used in this study. The culture was first re-hydrated from freeze dried cultures using ATCC medium 21 consisting of 0.5 g/L K_2HPO_4 , 0.5 g/L Ferric Ammonium Citrate, 0.5 g/L $MgSO_4$, 20 g/L Glycerol, 2 g/L Citric Acid and 4 g/L L-Glutamic Acid at a pH of 7.4. The re-hydrated culture was grown aerobically in shake flasks at 37°C for 24 hours. The culture broth was then used to inoculate agar slants prepared with ATCC medium 21, and the strain was maintained on agar slants at 4°C.

3.1.2 Medium Composition

The medium used in the experiments was designated “medium E” and suggested by Cromwick et al. (1995). The medium composition is shown in Table 3-1.

Component	g/L	Component	g/L
Glycerol	80	K_2HPO_4	0.5
L-Glutamic Acid	20	$FeCl_3 \cdot 6H_2O$	0.04
Citric Acid	12	$CaCl_2 \cdot 2H_2O$	0.15
NH_4Cl	7	$MnSO_4 \cdot H_2O$	0.104
$MgSO_4 \cdot 7H_2O$	0.5		

Table 3-1 Medium E, used for growth and production in the fermentation of *B. licheniformis*

3.1.3 Bioreactor System

A two liter jacketed bioreactor was used for batch and continuous experiments. The bioreactor was agitated using a six blade pitched blade impeller (Fischer Scientific, Nepean ON), and air was added continuously using a sparger. The pH was monitored using a pH electrode (Mettler-Toledo, Columbus, OH) and controlled using a pH controller (Cole-Palmer, Chicago, IL). Dissolved oxygen was measured with a D.O. galvanic probe (Cole Palmer, Chicago, IL) and a dissolved oxygen analyzer model (New Brunswick Scientific Co., Edison, NJ). The temperature of the bioreactor was maintained at 37°C by a warm water circulation bath. The foam in the system was controlled by the manual addition of antifoam.

The bioreactor was equipped with ports for the addition of acid, base, antifoam, fresh medium and air. It was also equipped with ports for sample withdrawal, withdrawal of reaction mixture (during continuous runs), and gas exhaust. Air was added to the bioreactor after passing through a glass fiber filter, and was kept at 2 VVM.

During the continuous experiments, fresh medium was fed to the bioreactor through a variable speed Masterflex peristaltic pump at a constant flow rate. The reaction mixture was also withdrawn using a Masterflex peristaltic pump. The working volume for the continuous experiments was 925 mL, while for the batch experiments, the volume was 1050 mL. A picture of the bioreactor system used can be found in Figure 3-1 and the bioreactor dimensions can be found in Figure 3-2.

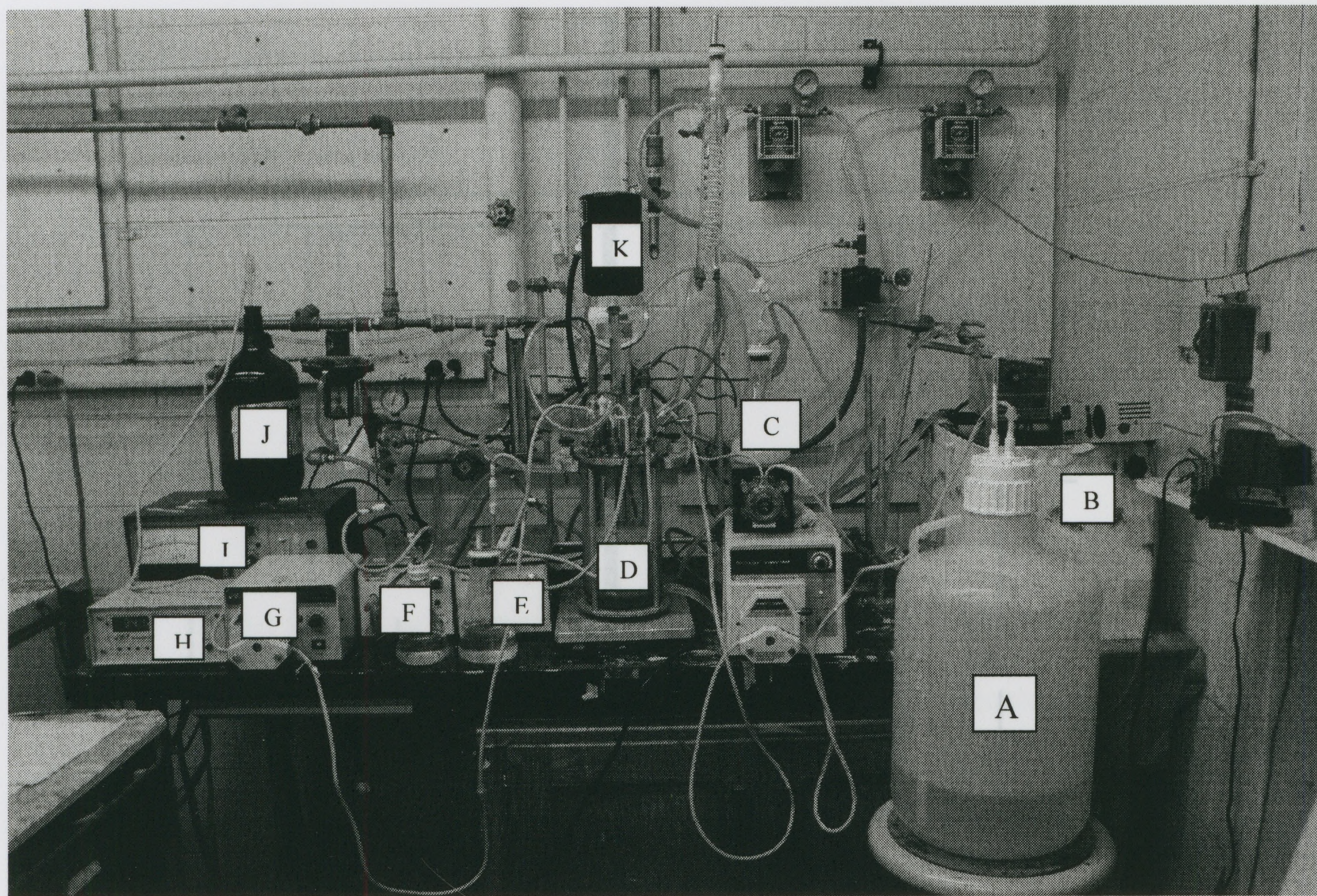


Figure 3-1 Bioreactor system for the continuous fermentation of *B. licheniformis*

- A Fresh Medium Reservoir
- B Warm Water Bath
- C Antifoam
- D Bioreactor
- E Base
- F Acid
- G Outlet Pump
- H DO Meter
- I pH Controller (from Reactor Bottom) = 1.8 cm
- J Use Medium Reservoir
- K Impeller Motor

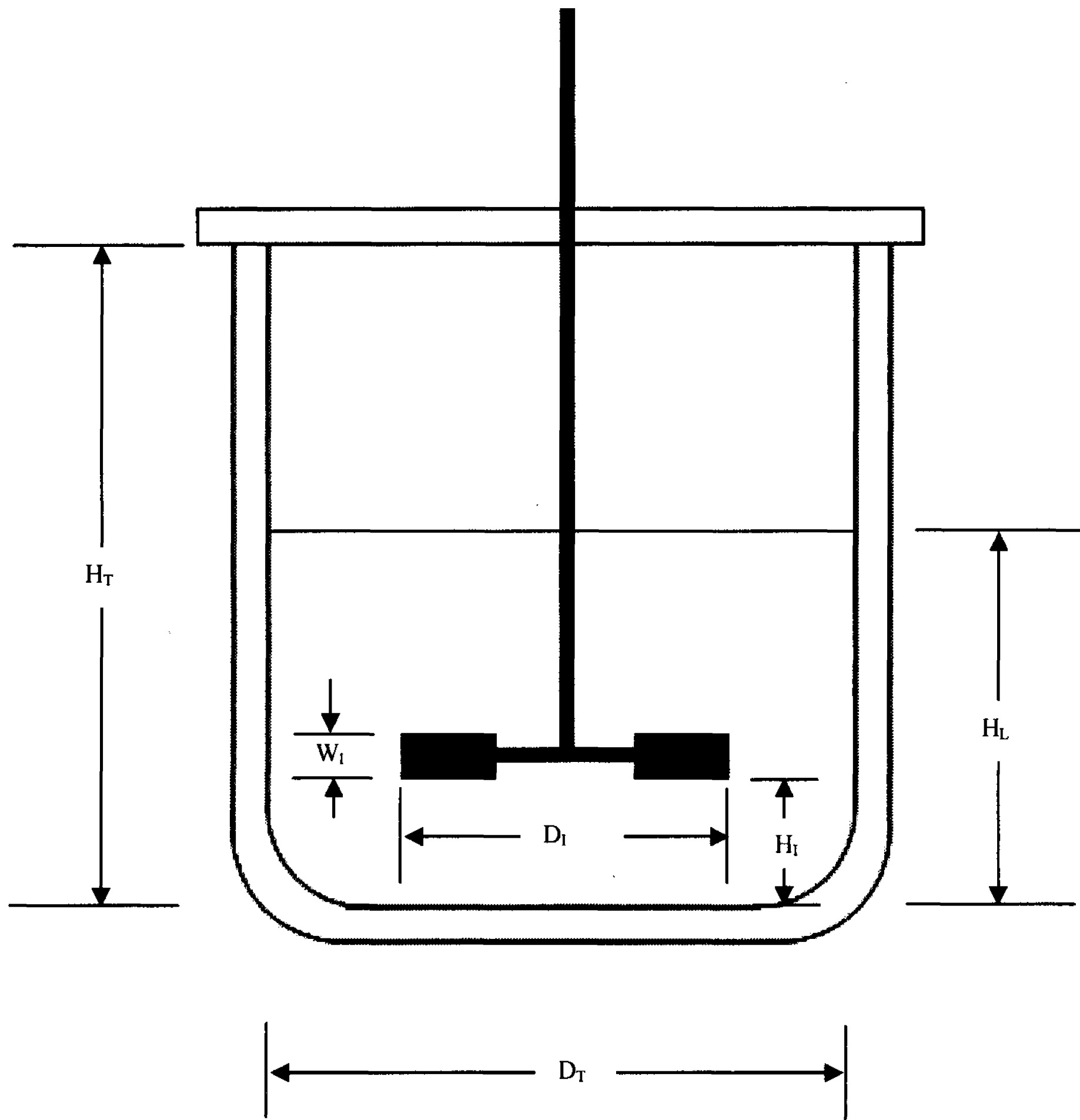


Figure 3-2 Bioreactor Dimensions

H_T = Reactor Height = 22.8 cm

H_L = Liquid Height = 11.6 cm

D_T = Reactor Diameter = 11.5 cm

W_I = Impeller Width = 1.6 cm

H_I = Impeller Height (from Reactor Bottom) = 1.8 cm

D_I = Impeller Diameter = 5.8 cm

3.1.4 Batch reactor system operation

The medium for the batch experiments was prepared in a 2 L beaker with 1 L of medium E, and was added to the bioreactor. The acid (250 mL of 1M HCl) and base (250 mL of 1M NaOH) were placed in separate 500 mL flasks, and attached to their respective ports using autoclavable Masterflex tubing. The antifoam (100 mL) was placed in a 250 mL flask and also attached to a port with autoclavable Masterflex tubing. The calibrated pH and dissolved oxygen probes were both inserted into their respective ports. Both the air inlet filter and air exhaust filter were attached to the bioreactor with autoclavable tubing. The tubing was clamped closed, and the bioreactor system was autoclaved for 30 minutes at 121°C.

The inoculum was prepared in a 250 mL flask, containing 50 mL of medium E. The medium was autoclaved for 15 minutes at 121°C. After cooling, it was inoculated with two to three loops of *B. licheniformis* from stored agar slants. The shake flask was then incubated at 37°C and 150 RPM for three days.

After the bioreactor was cooled to 37°C, the dissolved oxygen probe was calibrated according to the operating instructions. The inoculum was then added to the bioreactor system, and the fermentation began.

Samples were taken every 2 – 12 hours, as necessary, and used to determine biomass concentration, substrate concentration, PGA concentration and molecular weight characteristics. The batch experiments lasted approximately 100 hours.

3.1.5 Continuous Stirred Tank Reactor System Operation

For the continuous operation, the same equipment as the batch experiments was used, with some modification. The continuous culture required the addition of fresh medium, the withdrawal of reaction mixture, and the maintenance of a constant bioreactor volume.

The fresh medium was prepared beforehand in a 20 L polyethylene container connected to the feed medium port of the bioreactor by autoclavable Masterflex tubing. The fresh medium was fed at a constant flow rate by a variable speed Masterflex peristaltic pump. The removal of reaction mixture was carried out with a separate variable speed Masterflex peristaltic pump.

The reaction volume was maintained at a constant level, using level control. The withdrawal tube was located on the surface at the required level. The withdrawal pump was set at a higher volumetric flow rate than the feed pump, such that the level in the bioreactor did not increase above the specified level. If the reaction mixture was withdrawn too quickly, the liquid level would decrease below the end of the outlet tube, thus stopping the removal of liquid until the desired level was achieved again.

Continuous experiments began in a batch phase, until cells reached exponential growth. The batch phase of the continuous experiments lasted approximately 24 – 48 hours. After exponential phase was reached, the continuous operation was initiated. The feed pump and withdrawal pumps were turned on, and continuous operation was achieved. Samples were taken at the beginning of each continuous phase, and samples were taken every 2 – 6 hours to determine when steady state was achieved. Steady state

occurred when there was a consistent biomass concentrations for a significant amount of time.

3.1.6 Oxygen Uptake Rate, Specific Oxygen Uptake Rate and the Volumetric Mass Transfer Coefficient

The oxygen uptake rate was determined using the dynamic air off/ air on method described by Bandyopadhyay and Humphrey (1967) and discussed in Chapter 2. The dissolved oxygen electrode was attached to a New Brunswick Analyzer and a computer equipped with the Lab View software (National Instruments Corporation, Austin, TX).

3.1.7 Contamination Evaluation

The evaluation of the sterilized medium and inoculum for contamination was achieved through light microscopy, Gram staining and growing the inoculum and medium on agar plates.

3.2 Analytical Methods

3.2.1 Biomass Concentration

The biomass concentration was determined in all experiments by the dry weight method. Periodically, 5 mL samples of fermentation broth were withdrawn from the bioreactor from the sample port. The samples were diluted up to five times and filtered through a 0.45 μm cellulose nitrate filter under vacuum. The filters were then dried at 110°C until constant weight was achieved. Dry weight biomass concentration was then determined by dividing the change in dry filter weight (before and after filtration) by the sample volume.

3.2.2 Citric Acid and Glutamic Acid Concentration

After sample filtration through a 0.45 μ m cellulose nitrate filter, citric acid and glutamic acid concentrations were determined using high performance liquid chromatography (HPLC). A Waters Breeze HPLC system was used, equipped with a binary low flow pump, an autosampler and a UV detector (Waters Corporation,, Milford, MA). This system was used with a Hydrosil C₁₈ reverse phase 5 μ m, 250 mm x 4.6 mm column. The mobile phase was a 90:10 mixture of 0.2M phosphoric acid and methanol and had a flow rate of 0.5 mL/min. The UV detector was set to record at a wavelength of 210 nm, as suggested by Waters Corporation.

Citric Acid eluted at 7.5 minutes, while the glutamic acid eluted at 5 minutes. A calibration plot was generated using standards with known concentrations of either citric acid or glutamic acid. Sample concentrations were determined by comparing the areas of unknown samples to those in the calibrated plots.

Citric Acid concentration was verified using an enzymatic analysis kit (Boehringer Mannheim, Indianapolis, IN). A similar kit was used to verify the L-glutamic acid concentration.

3.2.3 Glycerol Concentration

Glycerol concentration was determined using an enzymatic analysis kit (Boehringer Mannheim, Indianapolis, IN). Glycerol concentration was determined after filtration of the sample through a 0.45 μ m cellulose nitrate filter under vacuum.

3.2.4 Polyglutamic Acid Concentration

Polyglutamic acid concentration was determined using both gel permeation chromatography (GPC) and acid hydrolysis. Gel permeation chromatography was performed using a Waters Breeze system, equipped with a low flow binary pump, an auto sampler and a UV detector with an Ultrahydrogel Linear GPC column (Waters Corporation, Milford, MA). The mobile phase was 0.3 M Na₂SO₄ with 0.05% (w/v) sodium azide. The flow rate was 1 mL/min and the UV detector was set at 271 nm. The PGA concentration was found by comparing the area of the unknown sample with a standard with known concentration, the PGA concentration was determined.

Acid hydrolysis using 5 M HCl was conducted at 100°C for 10 – 24 hours, which results in complete degradation of PGA to glutamic acid (Goto and Kunioka, 1992). The new glutamic acid concentration was then determined using the HPLC system described above, and the difference in concentrations from pre-hydrolysis and post-hydrolysis, gave the concentration of PGA in the sample.

3.2.5 Polyglutamic Acid Molecular Weight Characteristics

The number average molecular weight, weight average molecular weight and the polydispersity were determined using the GPC system described above. Standards with known molecular weight characteristics were used to calibrate the Breeze software. The standards included samples with molecular weights of 10⁶ Da, 10⁵ Da and 53x10³ Da. The molecular weight characteristics of the unknown samples were determined by

comparing the elution volume and peak area with those of the standards. The calibration curve used to determine the molecular weight characteristics is given in Figure 3-3.

3.2.6 Broth Viscosity

The viscosity of the sample broth was determined using a Brookfield Viscometer with digital read out. The viscosity (in centipoises) was found at different shear rates, and recorded.

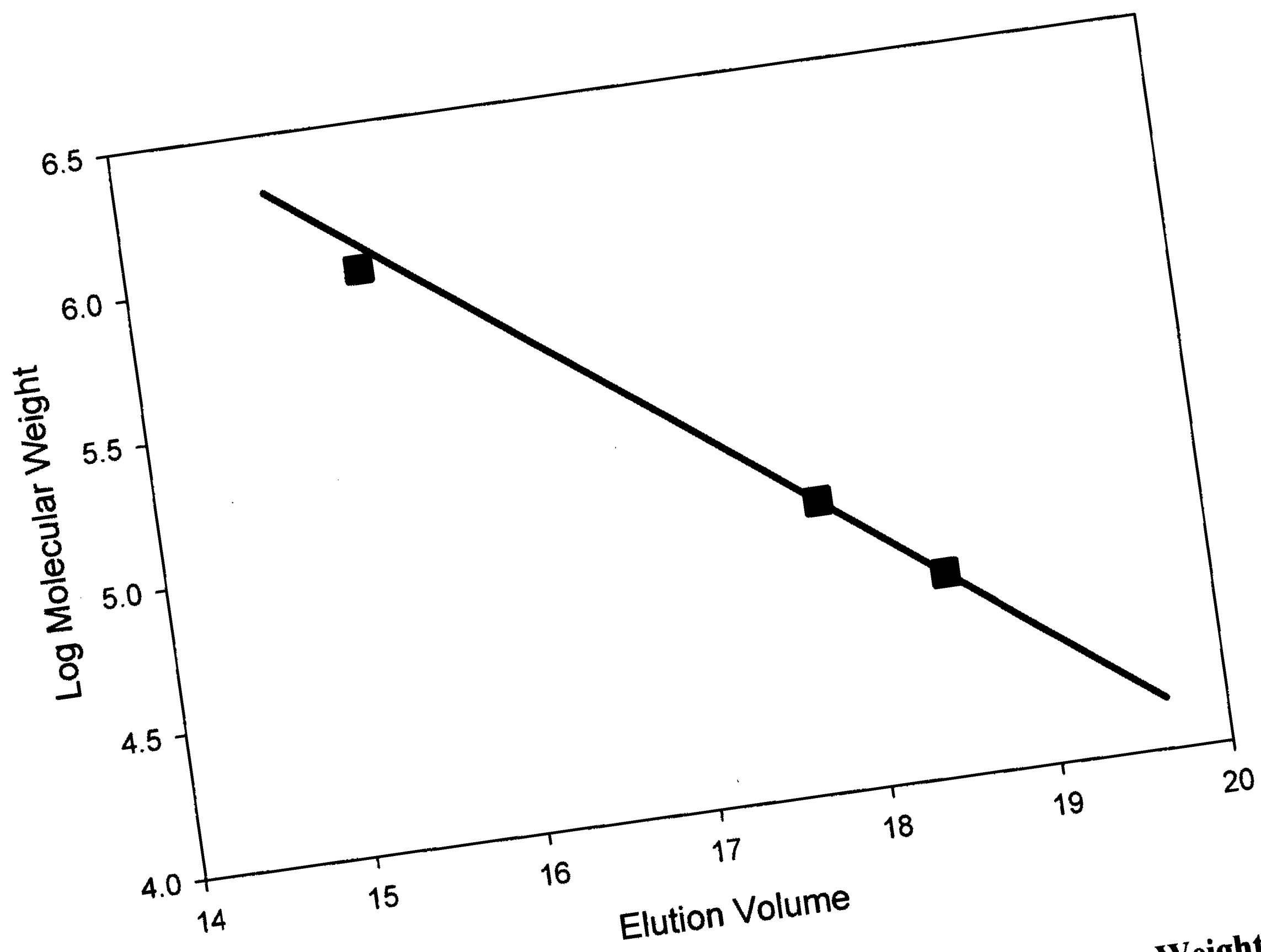


Figure 3-3 Calibration Curve for the GPC determination of Molecular Weight of PGA. The Log Molecular Weight as a function of Elution Volume

4. RESULTS AND DISCUSSION

4.1 Batch Fermentation

4.1.1 Biomass, Substrates and Polyglutamic Acid

The batch fermentation was initiated with 50 mL of inoculum, containing approximately 1 g/L of *B. licheniformis*. As seen in Figure 4-1, the lag phase of this batch fermentation lasted approximately 8 hours, during which time, only a slight increase in biomass concentration was observed (from 0.05 g/L to 0.26 g/L). The exponential growth phase lasted from 8 hours to 58 hours, during which the biomass concentration increased from 0.26 g/L to 4.22 g/L. The stationary phase then proceeded to 96 hours with little change in the biomass concentration (it varied between 4.08 g/L to 4.40 g/L). A stationary phase biomass concentration above 4 g/L is consistent with that reported in the literature (Cromwick et al., 1996; Hwan Do et al., 2001).

The biomass productivity (Table A-6) varied considerably during the batch fermentation, peaking in the exponential phase. During the exponential phase (between 8– 58 hours), the average biomass productivity was 0.092 g/L/h.

The specific growth rate of the bacteria as a function of fermentation time was plotted in Figure 4-2. It can be seen that the highest growth rates occurred during the early phases of the batch fermentation. The maximum specific growth rate achieved in this batch fermentation was 0.113 h^{-1} .

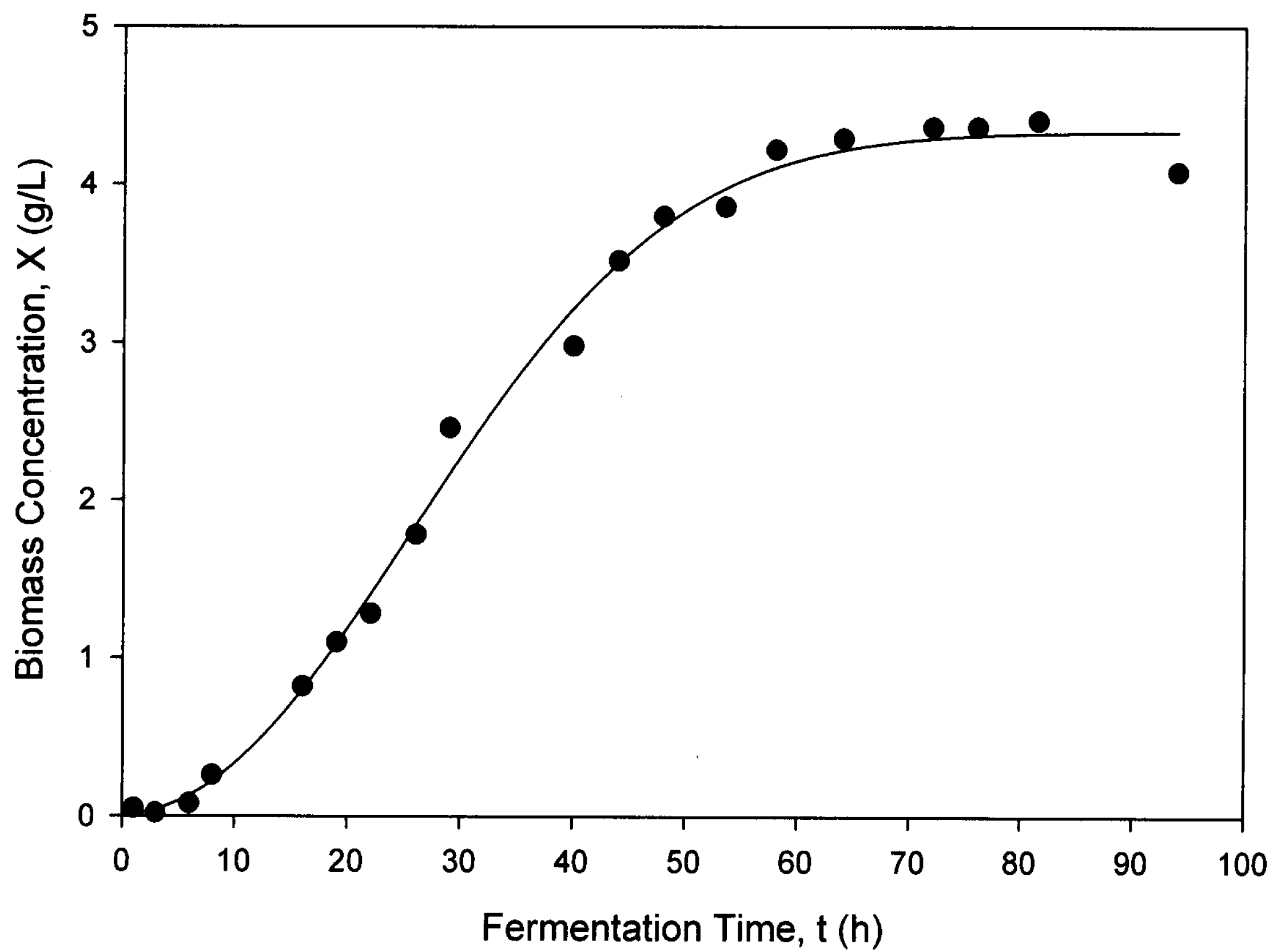


Figure 4-1 Biomass Concentration as a function of Fermentation Time for the Batch Fermentation of *B. licheniformis* ATCC 9945a (Table A-1)

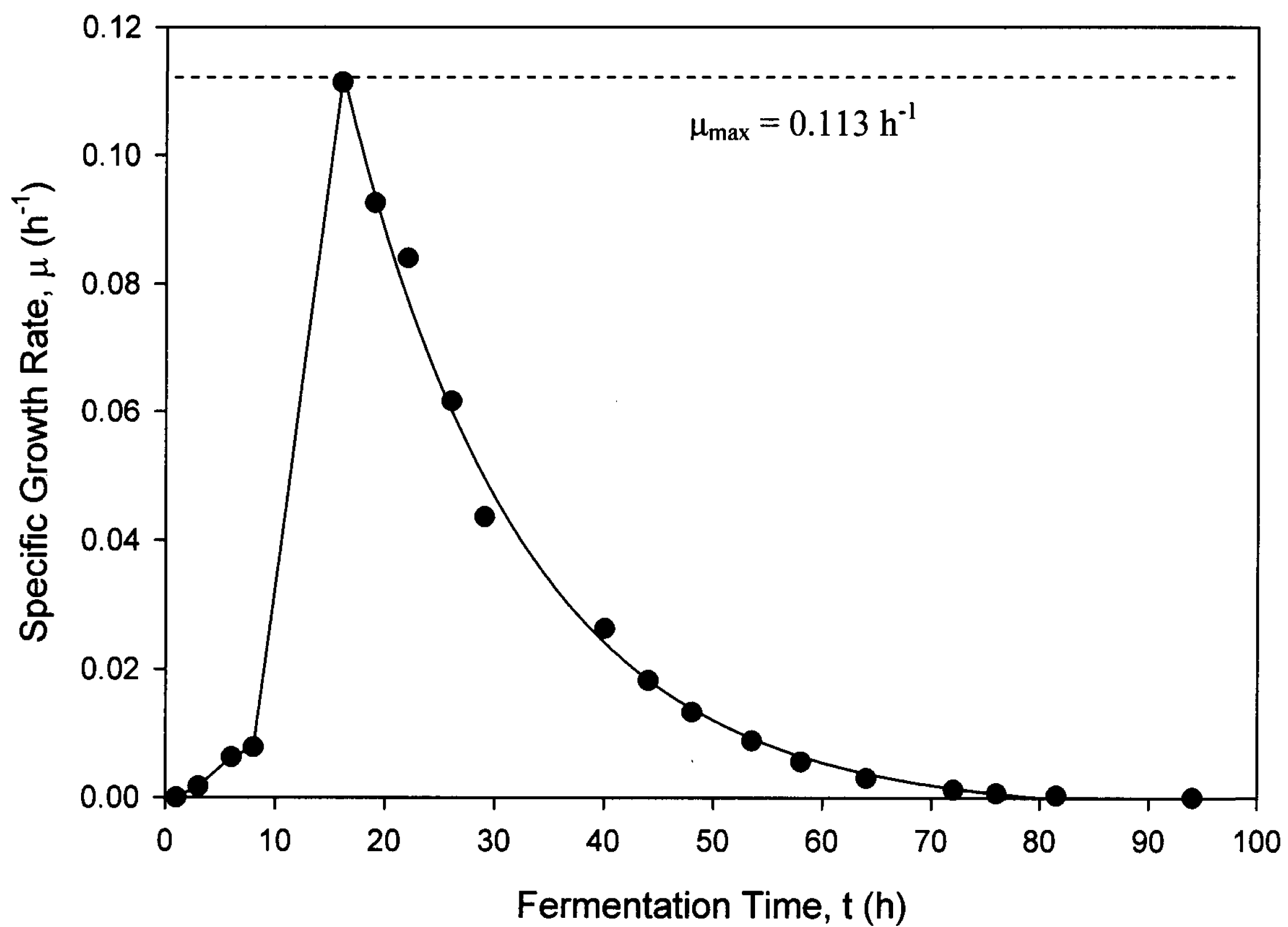


Figure 4-2 Specific Growth Rate of *B. licheniformis* as a function of Fermentation Time (Table A-1)

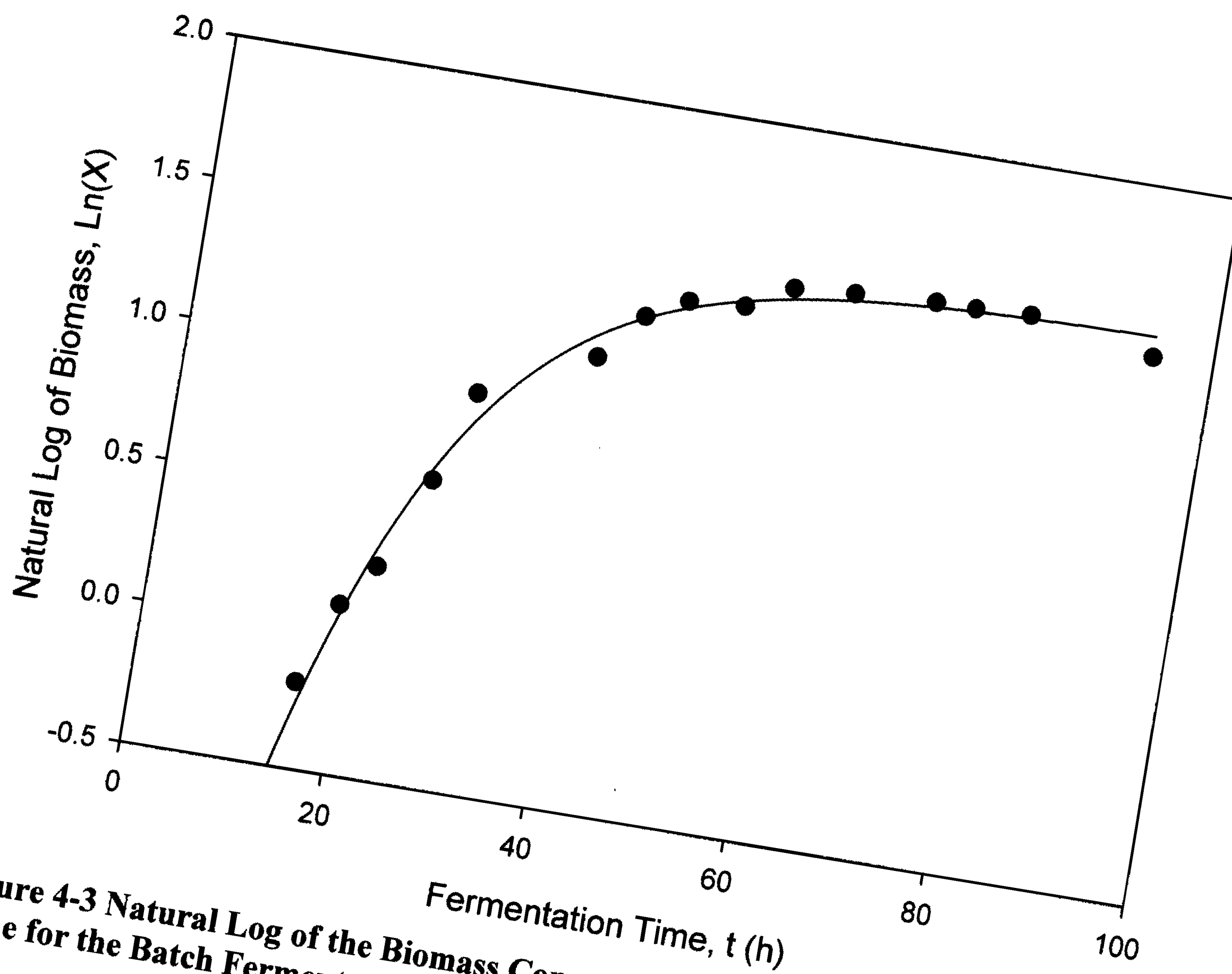


Figure 4-3 Natural Log of the Biomass Concentration as a function of Fermentation Time for the Batch Fermentation of *B. licheniformis* (Table A-1)

As seen in Figure 4-4 the polyglutamic acid concentration increased to a maximum concentration of 24.1 g/L at 94 hours. This concentration is in the typical range reported in previous works (Birrer et al., 1994; Bovarnick, 1942; Cromwick and Gross, 1995; Cromwick et al., 1996; Hwan Do et al., 2001; Ko and Gross, 1998). Interestingly, the Polyglutamic acid did not experience the same length lag phase as the biomass. This may suggest that *B. licheniformis* begins to produce PGA before rapid cell division occurs. During the exponential growth phase, the PGA productivity reached an average value of 0.23 g/L/h (Table A-6).

The citric acid, glutamic acid and glycerol concentrations were all significantly reduced during the batch fermentation (Figure 4-5). The citric acid was reduced to 3.7 g/L (from an initial concentration of 12 g/L) after 94 hours, the glutamic acid concentration was reduced to 9.6 g/L (from an initial concentration of 20 g/L) and the glycerol concentration was reduced to 15.4 g/L (from an initial concentration of 80 g/L). The citric acid and glutamic acid concentrations were consistent with those typically found with this strain. The glycerol concentration was reduced more than that found typically during batch fermentations (Shih and Van, 2001).

The total biomass yield from citric acid was 0.53 g/g, from glutamic acid 4.3 g/g and from glycerol 0.068 g/g. The biomass yield from the total carbon sources was 0.053 g/g. The PGA yield from the total carbon sources was 0.29 g/g and the PGA yield from the biomass was 5.5 g/g (Table A-4). Typical PGA yield from total carbon sources for controlled batch fermentations were 0.214 g/g (Cromwick et al, 1996) to 0.275 g/g (Hwan Do et al., 2001)

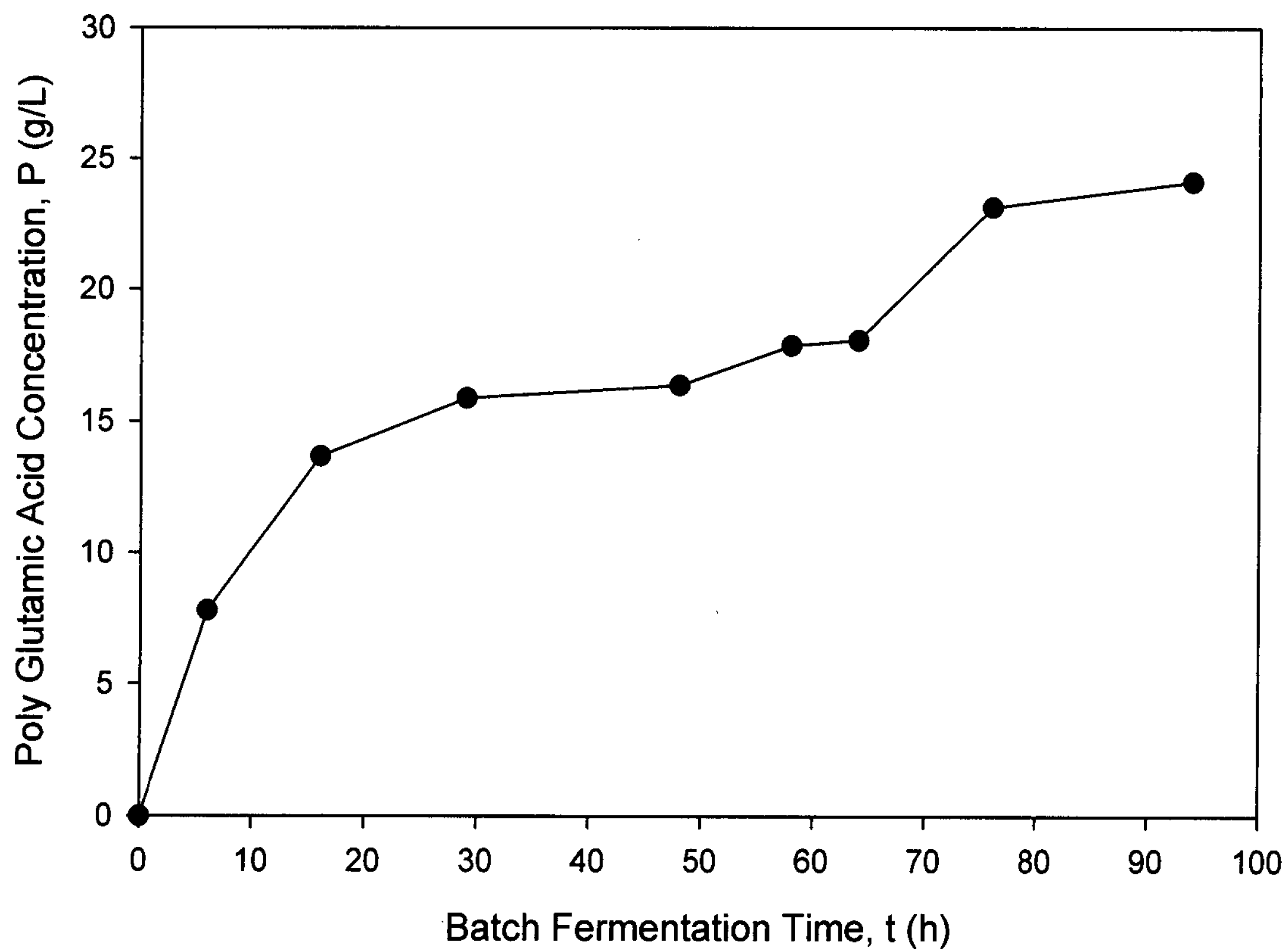


Figure 4-4: Polyglutamic Acid Concentration as a function of Fermentation Time from the Batch Fermentation of *B. licheniformis* ATCC 9945a (Table A-1)

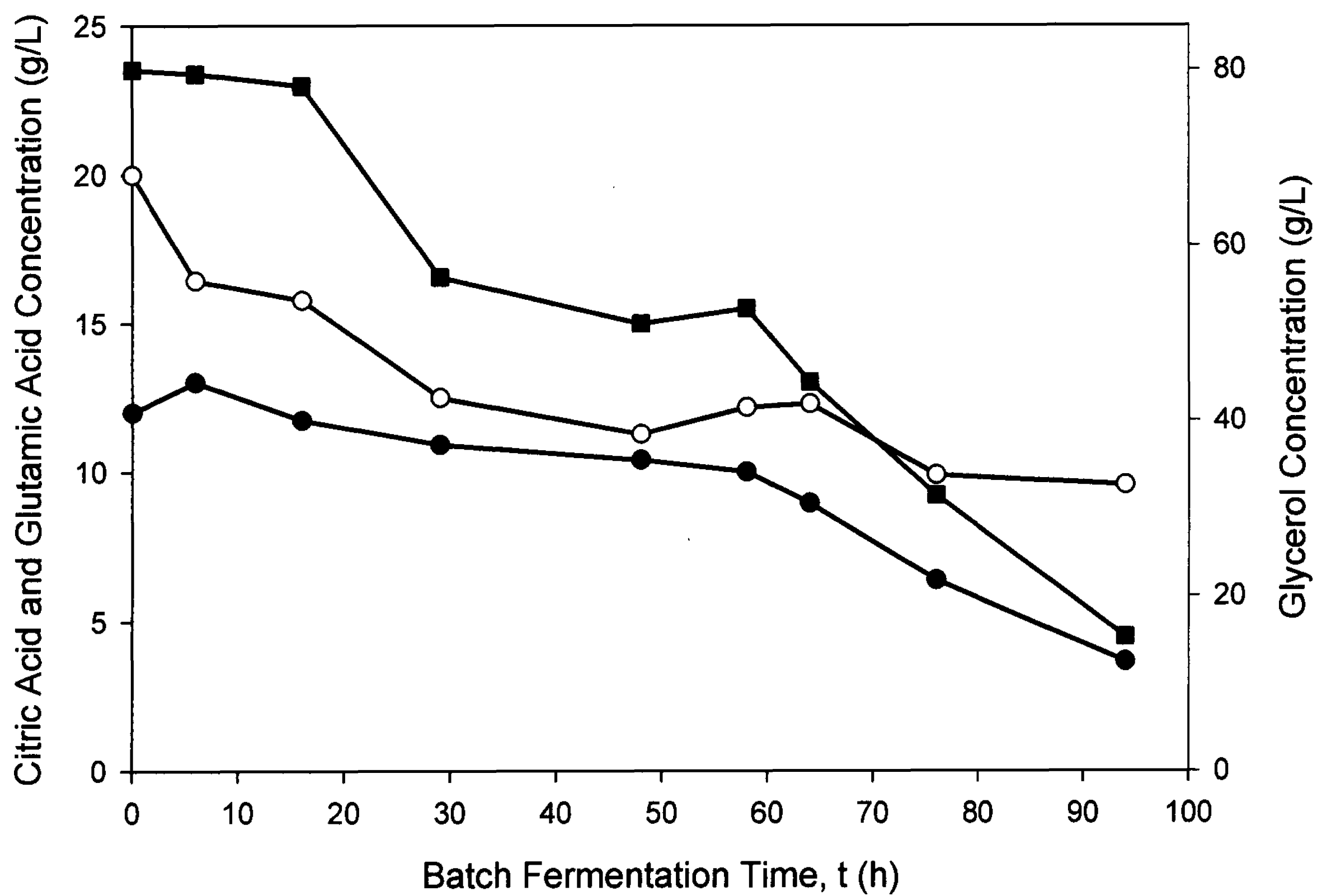


Figure 4-5 Citric Acid (●), Glutamic Acid (○) and Glycerol (■) Concentrations as a function of Fermentation Time for the Batch Fermentation of *B. licheniformis* ATCC 9945a (Table A-2)

4.1.2 Viscosity, Oxygen Uptake Rate, Specific Oxygen Uptake Rate and Volumetric Mass Transfer Coefficient

The viscosity of the culture broth was determined at various times during the batch fermentation and along with the combined PGA concentration plus biomass concentration is shown in Figure 4-6. According to previous works (Richard and Margaritis, 2003) during the production of a biopolymer, the viscosity of the culture broth is most closely related to the combined biomass and biopolymer concentration. This trend can be seen in the production of PGA. The viscosity was highest as PGA and biomass accumulated in the culture broth, and reached a value of 0.42 Pa.s.

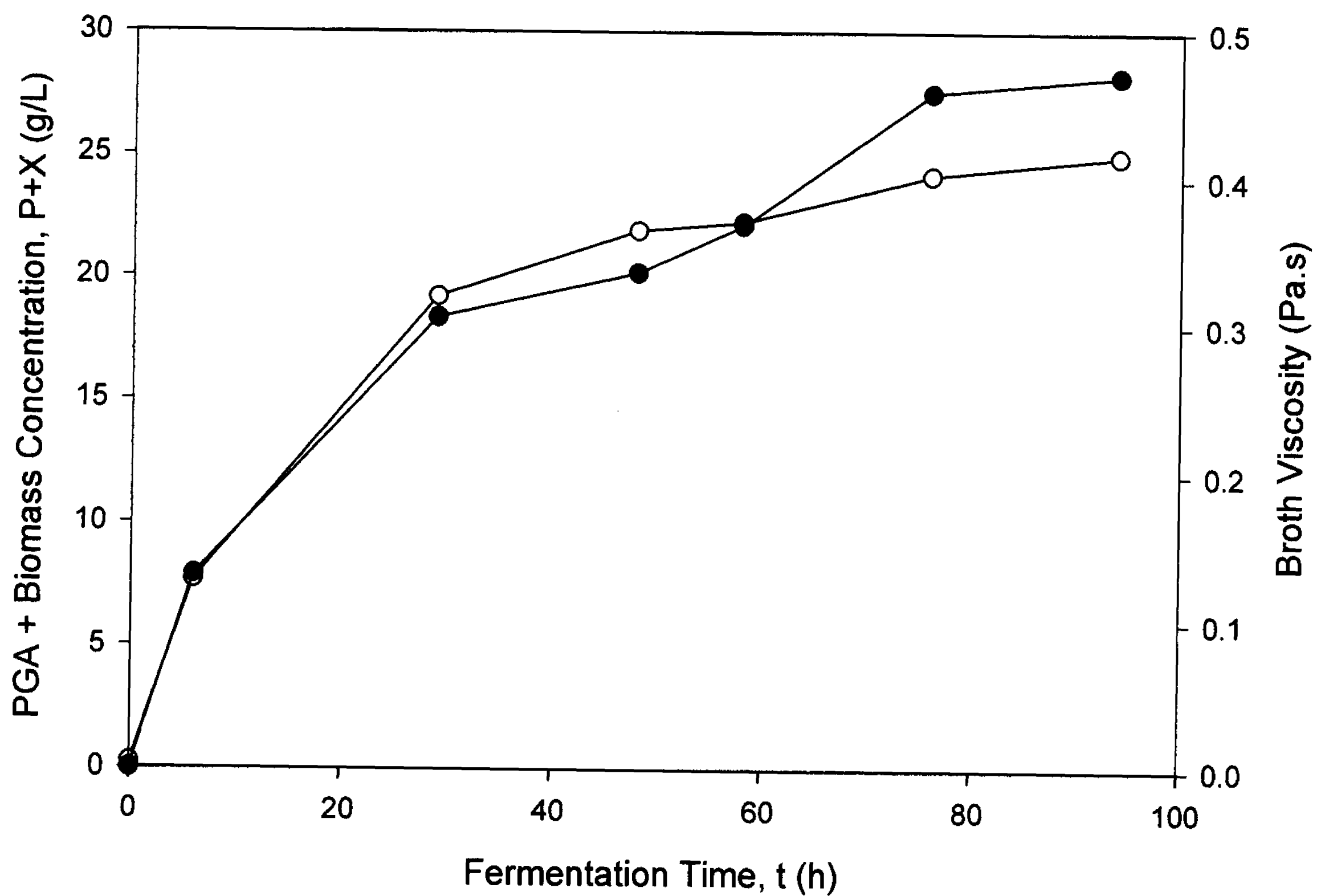


Figure 4-6 Broth Viscosity (○) and the Combined (PGA+Biomass) Concentration (●) as a function of Batch fermentation time (Table A-1 and Table A-5)

To the author's knowledge, the oxygen uptake rate (OUR), the specific oxygen uptake rate (Q_{O_2}) and the volumetric mass transfer coefficient ($k_L a$) have not been investigated in previous works for *B. licheniformis* ATCC 9945a. The only reference to this type of data is for *B. subtilis* IFO 3335 (Richard and Margaritis, 2003).

The oxygen uptake rate ($Q_{O_2 X}$) was plotted as a function of time and can be found in Figure 4-7. The oxygen uptake rate generally decreased as fermentation time increased, but peaked at 48 hours. The reason for this peak is unclear, but Richard and Margaritis (2003) observed a similar peak during the batch fermentation of *B. subtilis*. The oxygen uptake rate ranged from 2.5 mmol of $O_2/L/h$ at 6 hours to 1.6 mmol of $O_2/L/h$ at 94 hours (peaking at 4.7 mmol of $O_2/L/h$ after 48 hours). Although the OUR trend is similar to that found by Richard and Margaritis (2004) during their investigation of *B. subtilis*, these values are lower than those reported by Richard and Margaritis (2004). They found that the OUR peaked at 20 mmol $O_2/L/h$, during the early exponential phase.

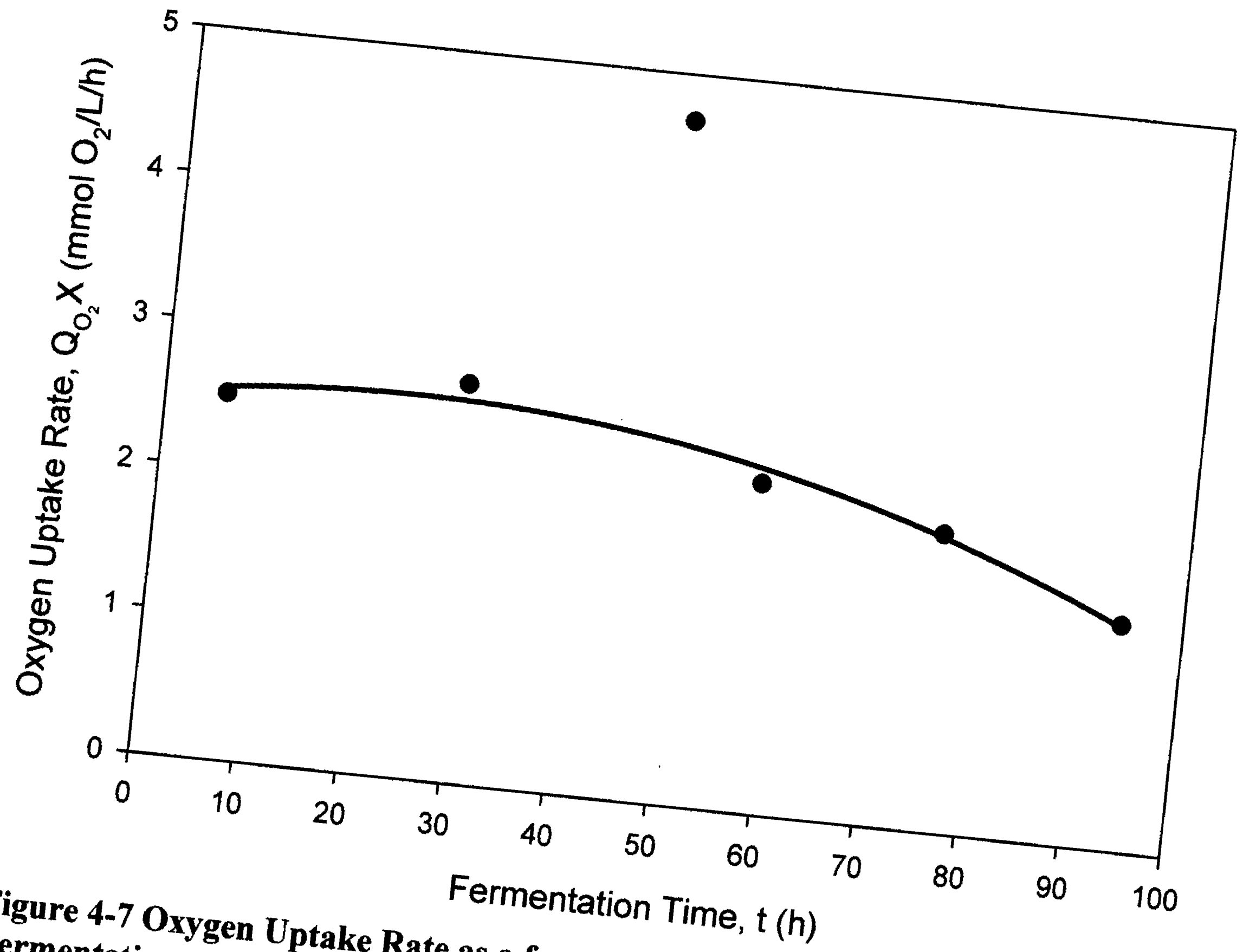


Figure 4-7 Oxygen Uptake Rate as a function of Fermentation Time for the Batch Fermentation of *B. licheniformis* ATCC 9945a (Table A-5)

The specific oxygen uptake rate (Q_{O_2}) was also plotted as a function of fermentation time and can be found in Figure 4-8. The specific oxygen uptake rate was initially very high during the lag phase, where the specific oxygen uptake rate reached over 30 mmol O_2 /g DW/h. After the lag phase, the specific growth rate decreased rapidly. At 29 hours, the specific oxygen uptake rate was reduced to 1.1 mmol O_2 /g DW/h, and after 94 hours was 0.38 mmol O_2 /g DW/h. Compared with the work done by Richard and Margaritis (2003), the Q_{O_2} found in *B. licheniformis* reached a lower peak level than that of *B. subtilis* (which peaked at over 100 mmol O_2 /g DW/h). At later fermentation times, both *B. licheniformis* and *B. subtilis* exhibited a significant reduction in Q_{O_2} . The lower OUR and Q_{O_2} compared to those found with *B. subtilis* may be caused by the lower specific growth rate seen in *B. licheniformis* cultures.

The volumetric mass transfer coefficient (k_La) for oxygen was plotted in Figure 4-9. The k_La value increased as fermentation time increased, and reached a maximum value of 207 h^{-1} at 76 hours. Interestingly, the k_La value was not decreased as fermentation broth viscosity increased.

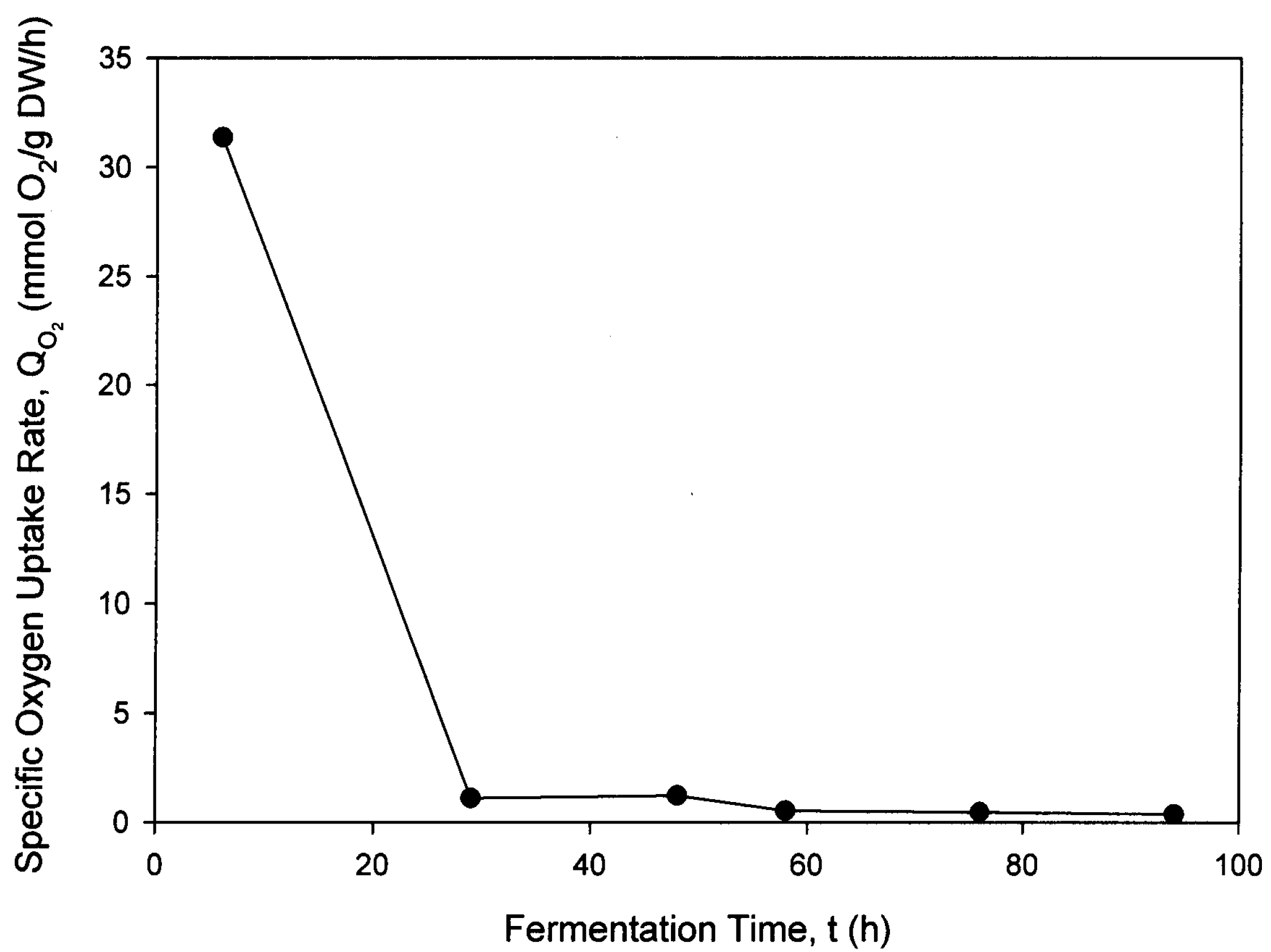


Figure 4-8 Specific Oxygen Uptake Rate as a function of Fermentation Time for *B. licheniformis* ATCC 9945a (Table A-5)

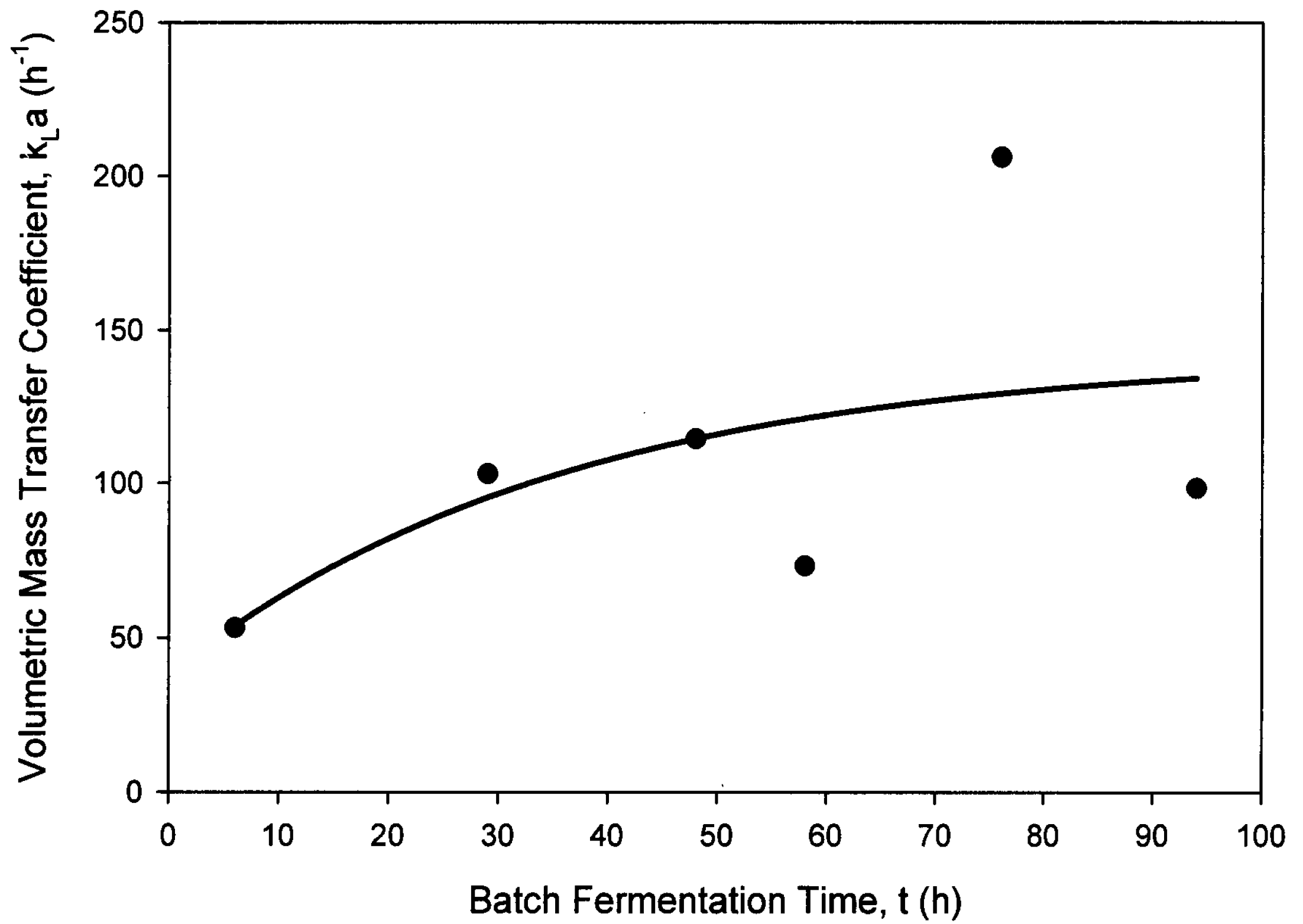


Figure 4-9 Volumetric Mass Transfer Coefficient of Oxygen as a function of Fermentation Time for *B. licheniformis* ATCC 9945a (Table A-5)

4.1.3 Molecular Weight Characteristics of the Biopolymer

The number average molecular weight (M_n) as a function of fermentation time is found in Figure 4-10. The number average molecular weight (M_n) was initially quite high, having a value of 157,000 Da after 6 hours. After this time, the number average only gradually increased with time, reaching a maximum value of 229,000 Da after 71 hours. It then decreased to 192,000 Da at 94 hours. This decrease may be attributed to the release of the degradation enzymes by *B. licheniformis*, suggested in previous works (Tanaka et al. 1993)

The weight average molecular weight (M_w) (Figure 4-11) increased more gradually than the number average molecular weight, and reached a peak of 635,000 Da at 71 hours. After this time the PGA polymer was reduced to 470,000 Da by 94 hours.

The polydispersity (M_w/M_n) is a value indicating how varied in size the polymer is. It can be seen from Figure 4-12 that as fermentation time increased, the size variations of the polymer also increased, to a maximum value of 3.1 at 57 hours of fermentation.

Both the weight average molecular weight and the polydispersity fall within the molecular ranges reported in previous studies. It is generally thought that *B. licheniformis* will produce PGA with a weight average molecular weight in the range of 100,000 – 2,000,000 (Shih and Van, 2001).

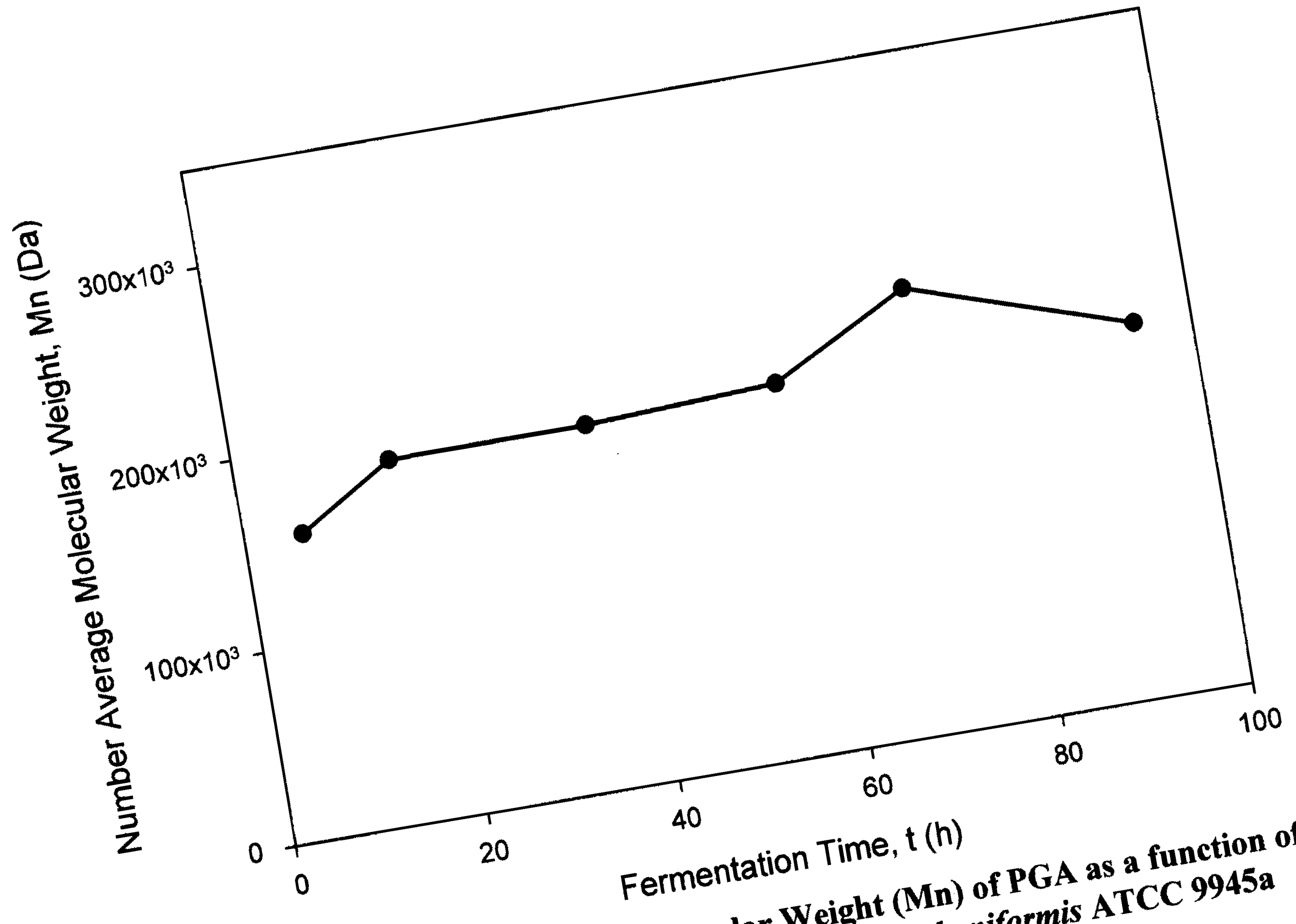


Figure 4-10 The Number Average Molecular Weight (Mn) of PGA as a function of Fermentation Time for the Batch Fermentation of *B. licheniformis* ATCC 9945a (Table A-7)

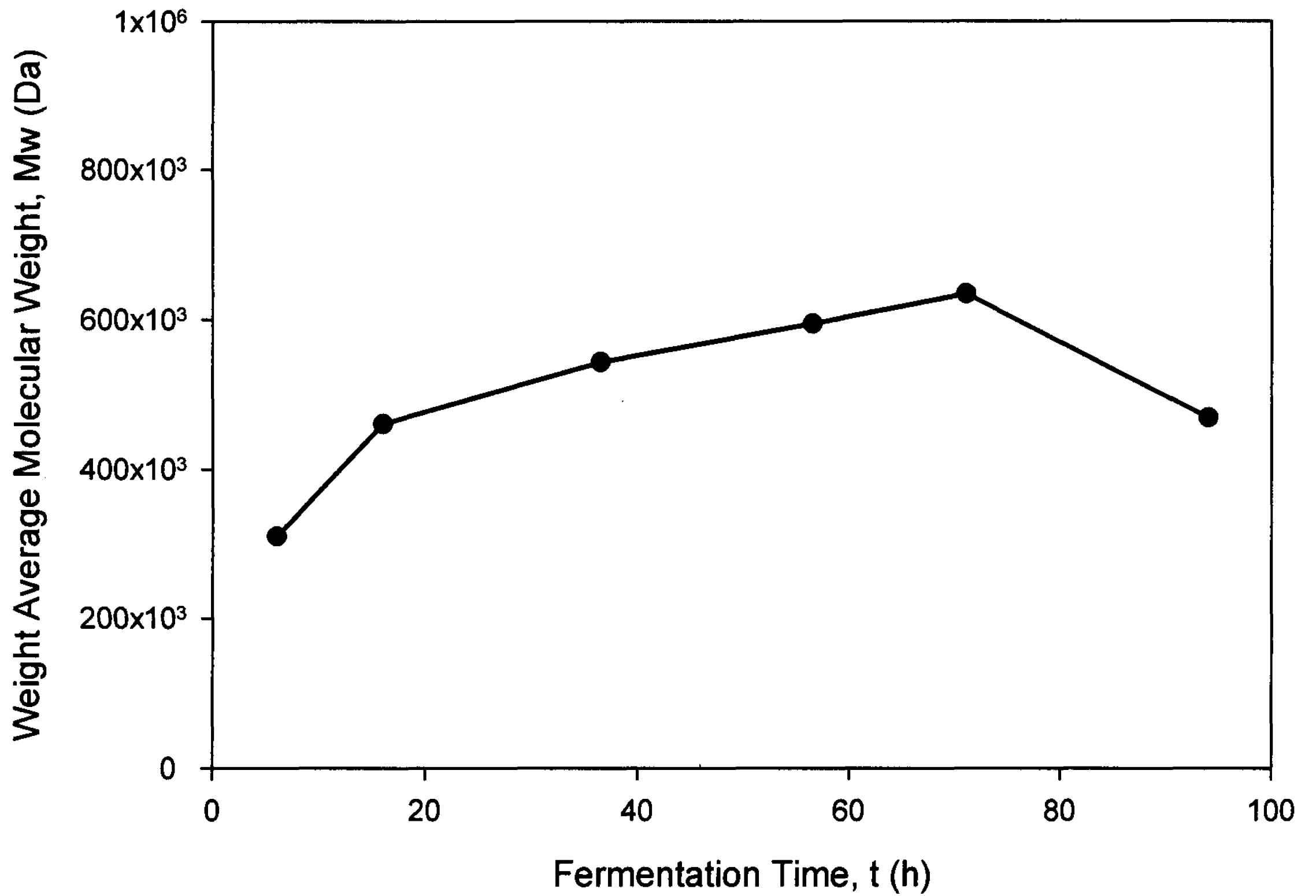


Figure 4-11 The Weight Average Molecular Weight (Mw) of PGA as a function of Fermentation Time for the Batch Fermentation of *B. licheniformis* ATCC 9945a (Table A-7)

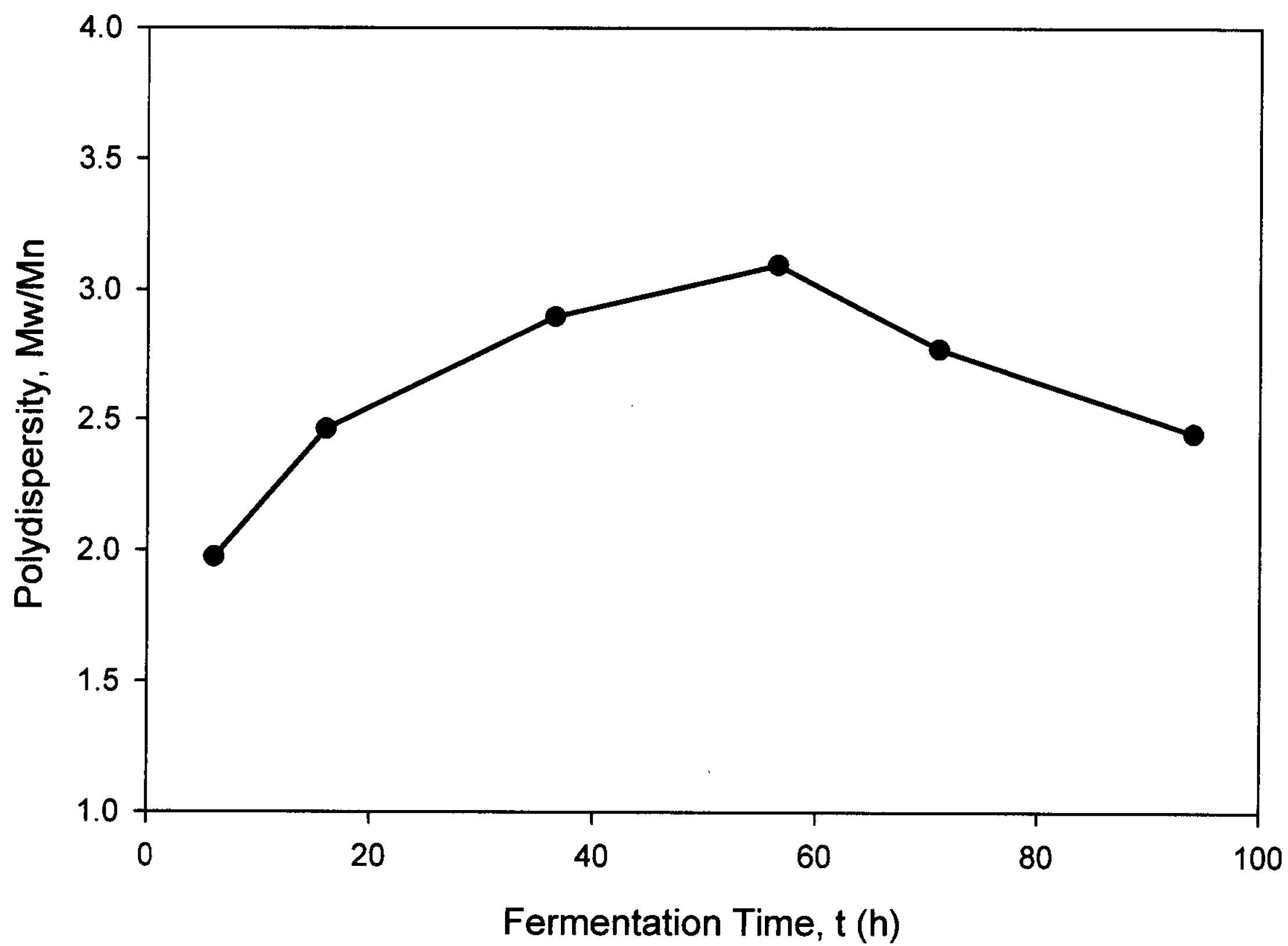


Figure 4-12 The Polydispersity (Mw/Mn) of PGA as a function of Fermentation Time for the Batch Fermentation of *B. licheniformis* ATCC 9945a (Table A-7)

4.2 Continuous Fermentation of *Bacillus licheniformis*

Although there has been extensive investigation into the batch fermentation of polyglutamic acid by several *Bacillus* species, to the author's knowledge there has not been any investigation into the continuous fermentation to produce PGA.

4.2.1 Washout Data and the Maximum Specific Growth Rate

The washout experimental data, namely the biomass concentration and the natural log of the biomass as a function of the washout time are shown in Figures 4-13 and 4-14 respectively. From the washout plots, the maximum specific growth rate (μ_{\max}) was determined by analyzing the slope of the natural log of the biomass as a function of washout time.

Two experiments were performed to determine the maximum specific growth rate. The first experiment used a washout dilution rate of 0.290 h^{-1} and the second experiment had a washout dilution rate of 0.372 h^{-1} (well above the maximum specific growth rate of 0.113 h^{-1} found in the batch experiment). To determine the maximum specific growth rate, the slope of the line of $\ln(X)$ vs washout time ($t - t_0$) is used in the following equation:

$$\ln(X) = \ln(X_0) - (D - \mu_{\max})(t - t_0) \quad (2.16)$$

Where the slope is equal to $-(D - \mu_{\max})$

For the first experiment ($D = 0.290 \text{ h}^{-1}$) the maximum specific growth rate was found to be 0.117 h^{-1} . The second experiment ($D = 0.372 \text{ h}^{-1}$) gave a maximum specific growth rate of 0.130 h^{-1} . This yielded an average maximum specific growth rate of 0.123 h^{-1} .

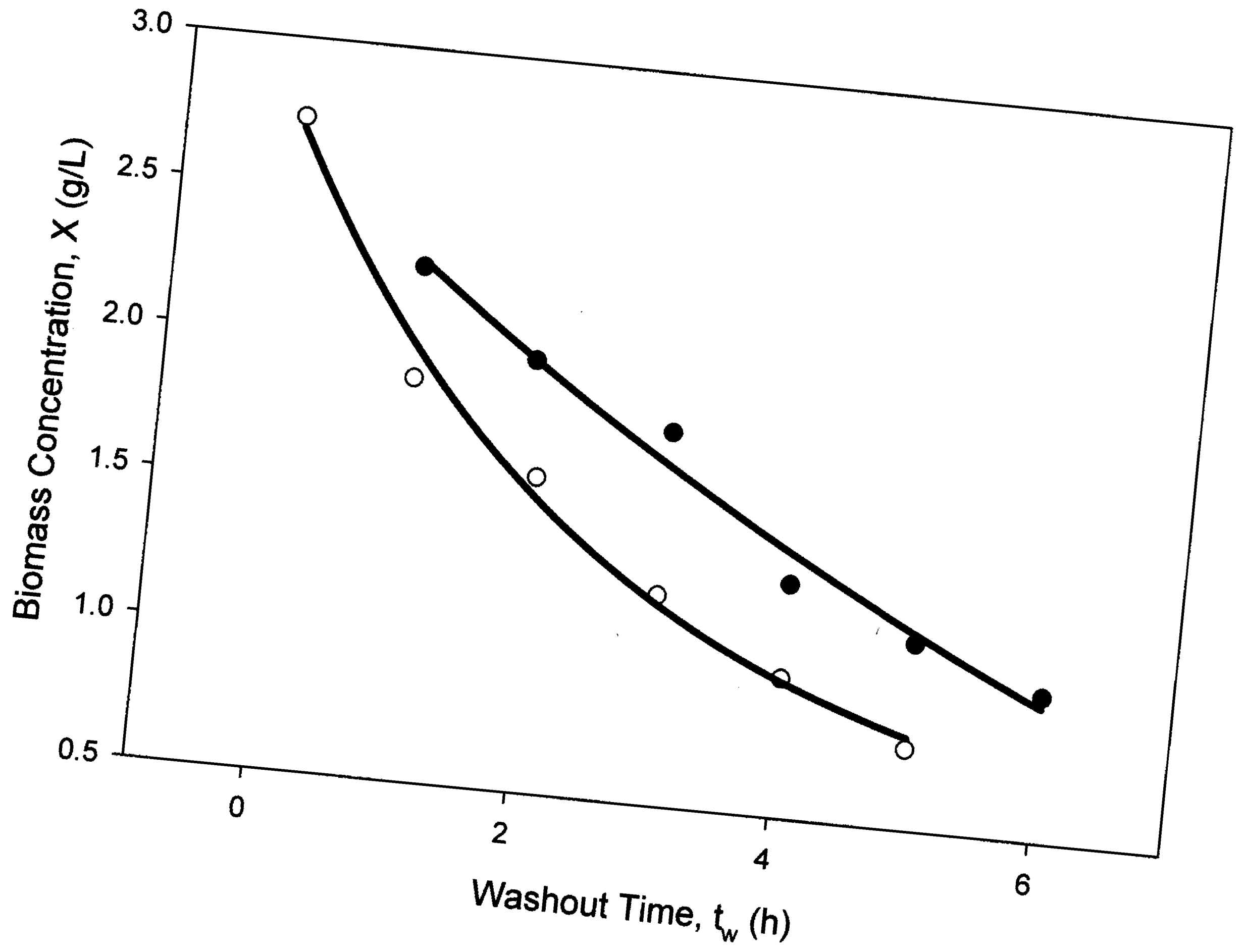


Figure 4-13 Biomass Concentration as a function of Washout Time for washout experiment 1 (●) and washout experiment 2 (○) (Table D-1 and Table D-2)

- Washout dilution rate = 0.290 h^{-1}
- Washout dilution rate = 0.372 h^{-1}

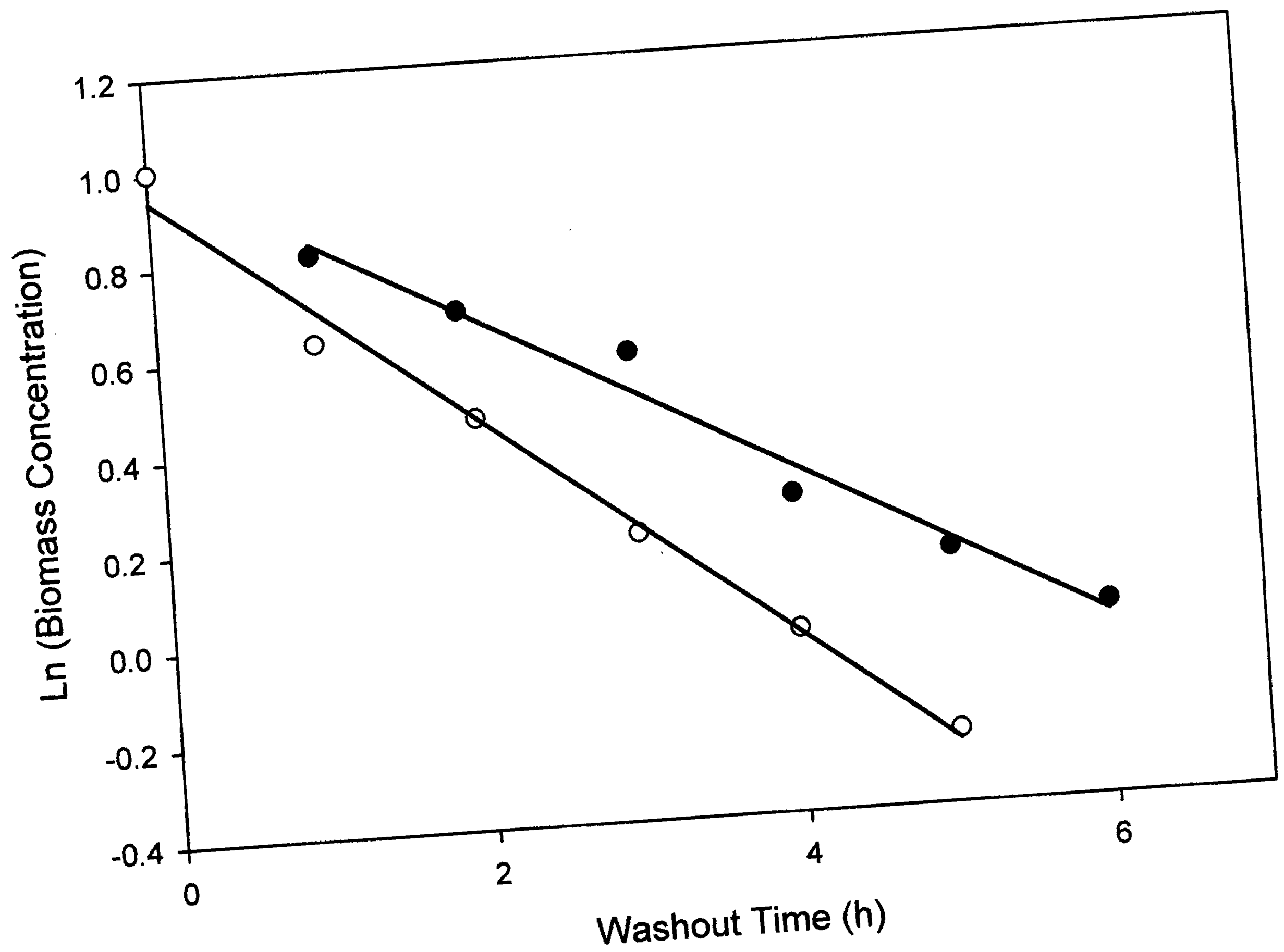


Figure 4-14 Natural Log of the Biomass Concentration from washout experiment #1 (●) and #2 (○) as a function of Washout Time for the washout experiments (Table D-1 and Table D-2)

● Washout dilution rate = 0.290 h^{-1}
 $\text{Ln}(X) = -0.1727(t) + 1.0159$
 $R^2 = 0.977$

○ Washout dilution rate = 0.372 h^{-1}
 $\text{Ln}(X) = -0.242(t) + 0.942$
 $R^2 = 0.991$

4.2.2 Transient Time and Steady State Equilibrium

During the course of the continuous fermentation of *B. licheniformis*, an important aspect is determining when steady state has been achieved. For this thesis, steady state is defined as occurring when the biomass concentration does not vary substantially for 10 – 20 hrs of fermentation time. It is assumed that when biomass reaches a constant concentration, then the rest of the system is also in equilibrium. This assumption was observed by sampling both substrates and PGA during the course of several of the continuous fermentations. Appendix B contains the values of the biomass concentration as a function of real fermentation time for each dilution rate.

Turnover volume can be used to describe how long the system took to reach steady state. Turnover volume can be defined as the volume of fresh medium added into the system divided by the bioreactor volume.

To reach steady state, it took from 2.5 turnover volumes (for $D = 0.035 \text{ h}^{-1}$) to 5 turnover volumes (for $D = 0.063 \text{ h}^{-1}$). The most important factor in determining the number of turnover volumes seemed to be the concentration of biomass at the beginning of the continuous fermentation. For the $D = 0.035 \text{ h}^{-1}$ run, the initial biomass concentration was 3.2 g/L and the steady state concentration was 2.9 g/L. Since these values were quite close, the system took less turnover time to equilibrate. In comparison, for $D = 0.063 \text{ h}^{-1}$ the initial biomass concentration was 1.2 g/L and the steady state was 2.5 g/L. This larger difference may have attributed to the increase in turnover time to reach equilibrium.

Several runs were performed in a sequential fashion. An example appears in Figure 4-15. In this run the system initially functioned in a batch fermentation, and at 36

hours, a dilution rate of 0.063 h^{-1} was initiated. After steady state was achieved (between 100 – 140 hours), a dilution rate of 0.082 h^{-1} was begun. Steady state was achieved for a dilution rate of 0.082 h^{-1} between 200 – 220 hours.

4.2.3 Repeatability of the Continuous Fermentation of *B. licheniformis*

The repeatability of this system was examined by performing the 0.082 h^{-1} dilution rate twice. The tables in Appendix B and C includes both sets of, and are referred to as $D = 0.082a \text{ h}^{-1}$ and $0.082b \text{ h}^{-1}$. The graphs include the average value for $D = 0.082 \text{ h}^{-1}$, as well as a bar indicating the values of each run.

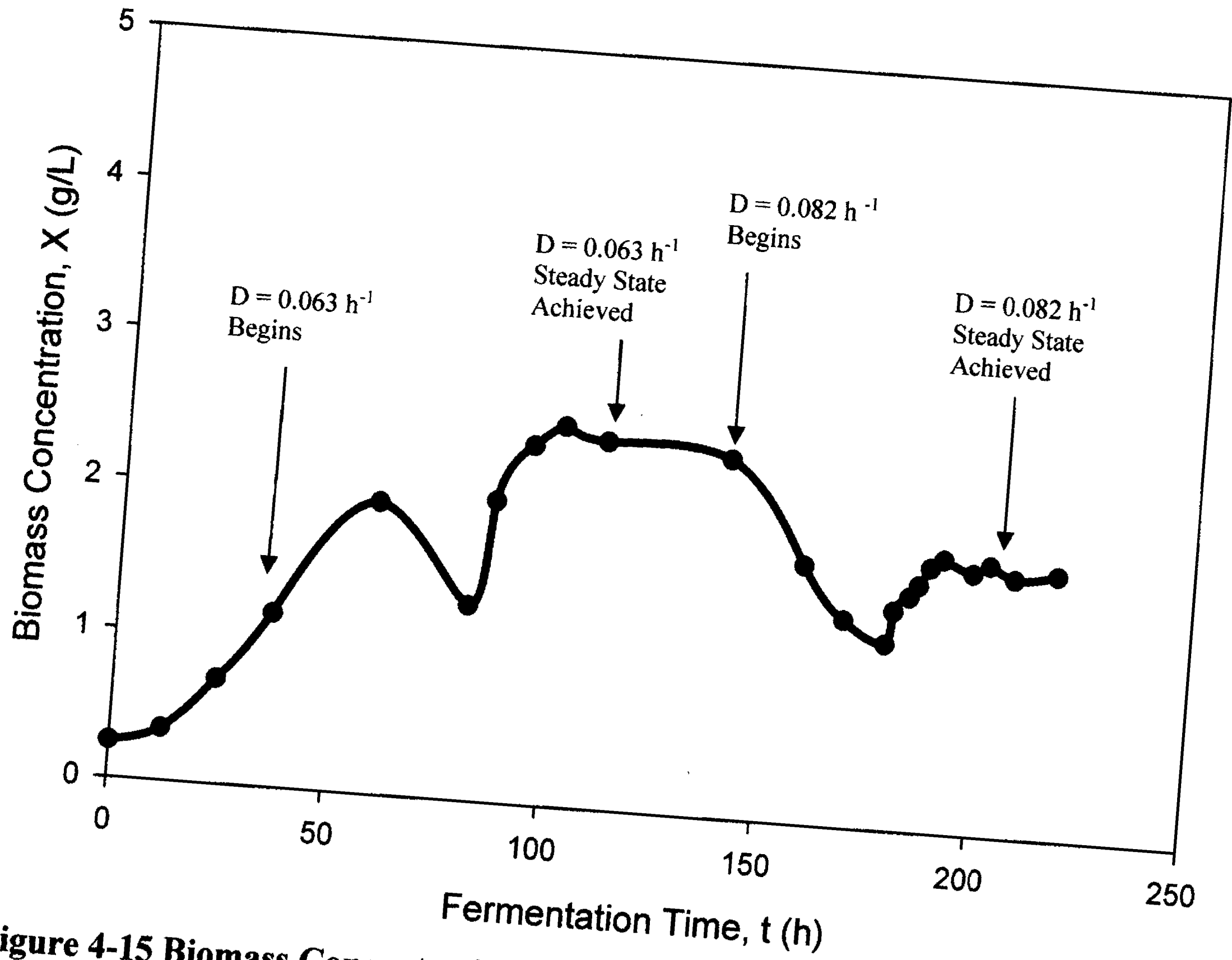


Figure 4-15 Biomass Concentration as a function of Real Fermentation Time for $D = 0.063 \text{ h}^{-1}$ and $D = 0.082 \text{ h}^{-1}$ (Table B-8)

4.2.4 Biomass, Substrates and Polyglutamic Acid Concentration

The graphs produced from the continuous fermentation of *B. licheniformis* include the washout situation. Washout occurs at dilution rates greater than the maximum dilution rate (determined in section 4.2.8), and results in a biomass and product concentration of zero, and substrate concentrations equal to those found in the fresh medium.

The biomass concentration as a function of dilution rate can be found in Figure 4-16. The biomass increased steadily from a dilution rate of 0.097 h^{-1} (with a concentration of 1.1 g/L) to a dilution rate of 0.051 h^{-1} (with a concentration of 2.8 g/L), at which point, decreasing dilution rate only had a slight effect on the biomass concentration. The biomass concentration reached 3.2 g/L at the lowest observed dilution rate, 0.023 h^{-1} . This value is approximately 75% that of the biomass observed during the stationary phase of the batch fermentation (4.4 g/L).

The polyglutamic acid concentration at the various dilution rates can be found in Figure 4-17. The polyglutamic acid concentration increased as the dilution rate was reduced from the washout dilution rate. In fact, at a dilution rate of 0.097 h^{-1} , the PGA concentration was 7.9 g/L and by a dilution rate of 0.082 h^{-1} the PGA concentration had reached 14 g/L . After this point, the decrease in dilution rate only slightly increased the PGA concentration (up to 17.5 g/L). The PGA concentration reached close to 75% of that observed in the stationary phase of the batch fermentation (24.1 g/L).

The citric acid, glutamic acid and glycerol concentrations at the various dilution rates can be found in Figures 4-18, 4-19 and 4-20. Both the citric acid and glycerol concentrations exhibited the same trend as dilution rate was decreased from the washout

levels. In both cases, there was a substantial decrease in the substrate concentrations at a dilution rate of 0.097 h^{-1} . Glycerol concentration was 49 g/L (from a concentration of 80 g/L in the fresh medium) and the citric acid concentration was 7.9 g/L (from an initial concentration of 12 g/L in the fresh medium). This represents a 39% reduction from fresh medium for glycerol and 35% reduction for citric acid. Glutamic acid on the contrary was only slightly utilized at $D = 0.097 \text{ h}^{-1}$. Glutamic acid concentration was 19 g/L , from an initial concentration of 20 g/L , which represents a 5% decrease from fresh medium.

Changing the dilution rate at lower dilution rates did not seem to have the same effect on the substrate concentrations. In fact, from a dilution rate of 0.063 h^{-1} to 0.023 h^{-1} , the glycerol concentration decreased from 41 g/L to 32 g/L . The citric acid concentration decreased from 4.7 g/L to 2.6 g/L and the glutamic acid concentration from 13 g/L to 11 g/L . This corresponds to only a modest increase in both biomass concentration (from 2.5 g/L to 3.2 g/L) and PGA concentration (17.2 g/L to 17.5 g/L).

At the lowest dilution rate observed, $D = 0.023 \text{ h}^{-1}$, the glycerol concentration was reduced 60% from that of the fresh medium, the citric acid concentration was reduced 80% and the glutamic acid concentration was reduced 50% from the fresh medium concentrations.

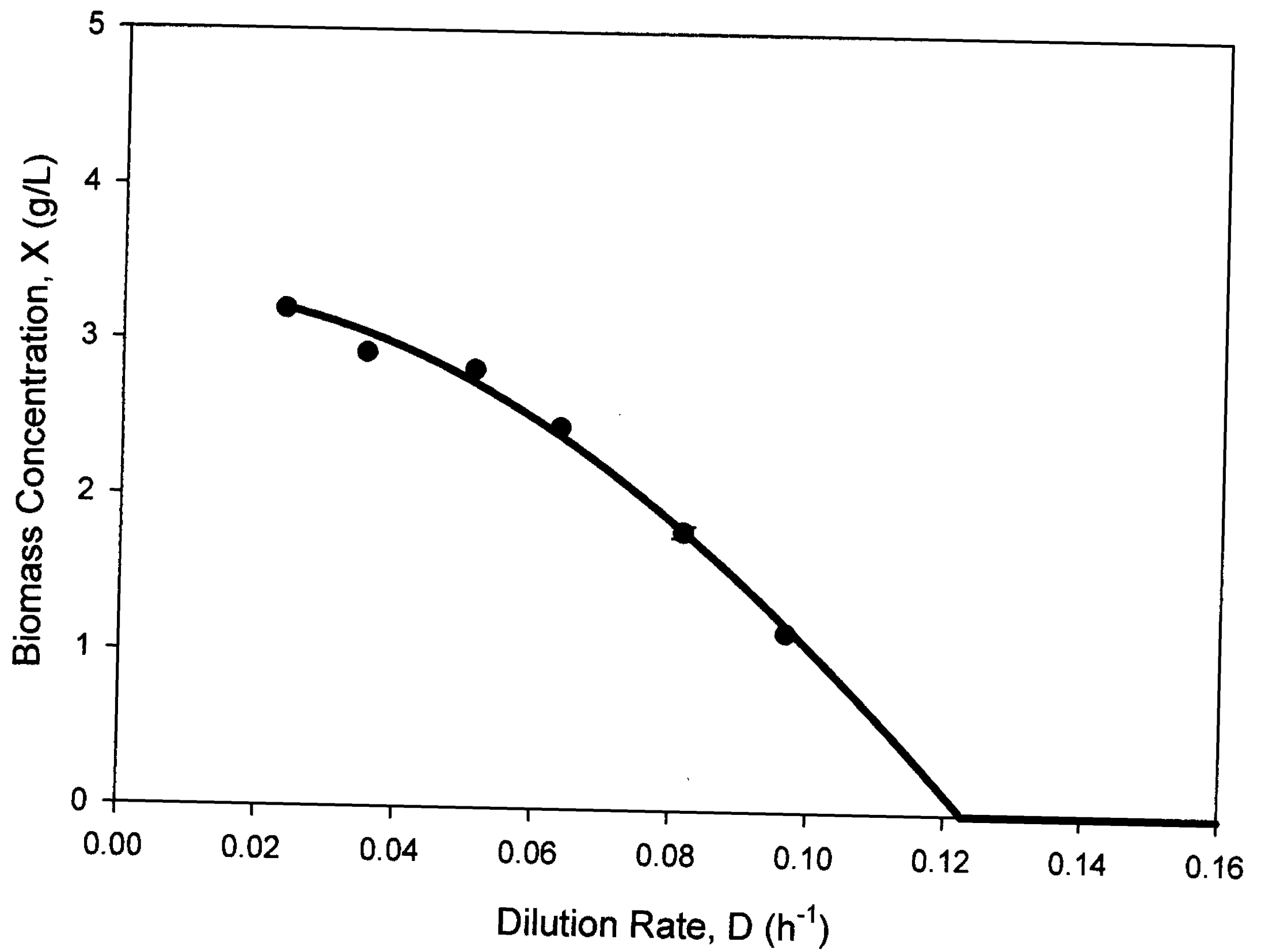


Figure 4-16 The Biomass Concentration as a function of Dilution Rate for the Continuous Fermentation of *B. licheniformis* ATCC 9945a (Table C-1)

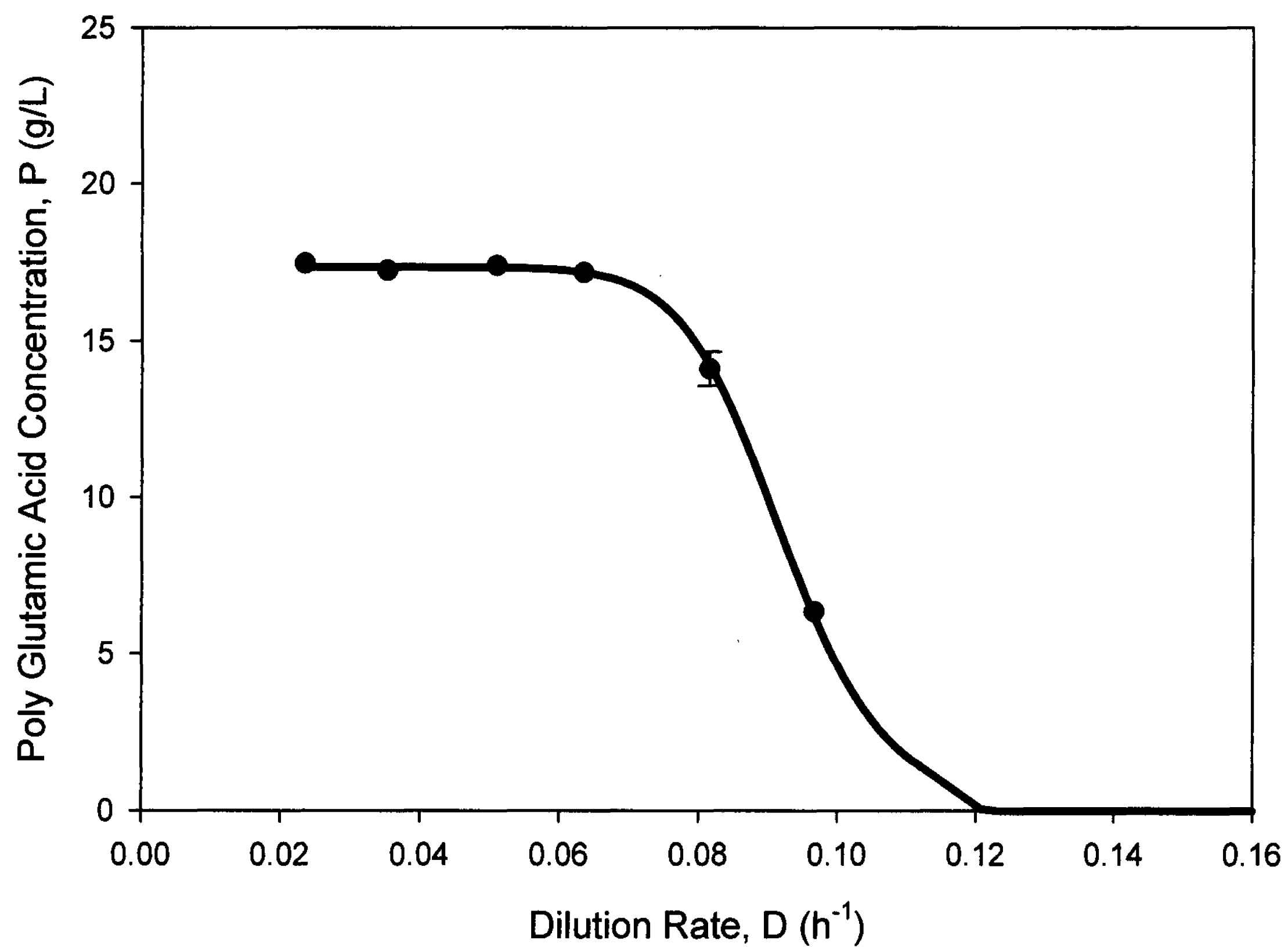


Figure 4-17 The Polyglutamic Acid Concentration as a function of Dilution Rate for the Continuous Fermentation of *B. licheniformis* ATCC 9945a (Table C-1)

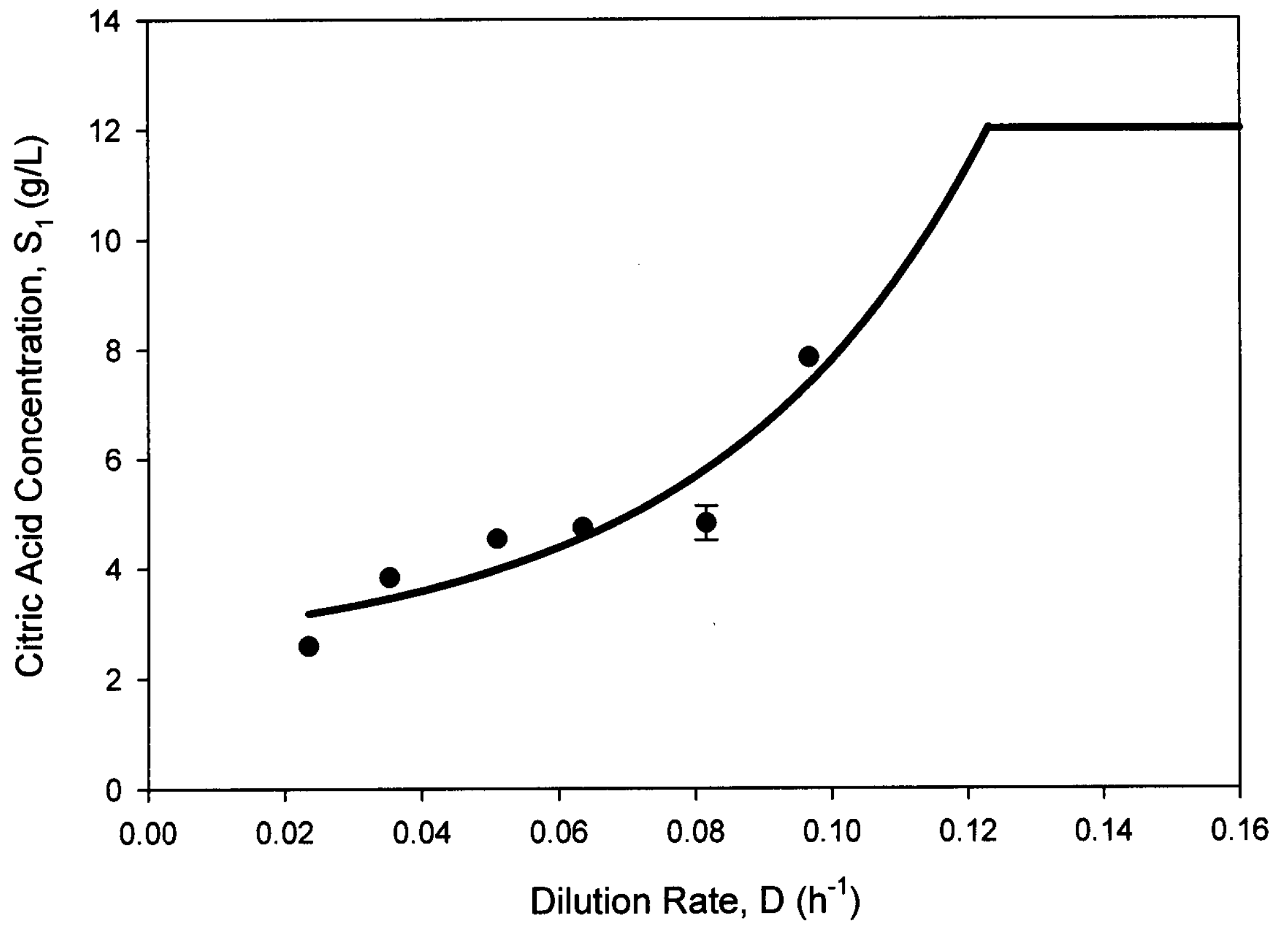


Figure 4-18 The Citric Acid Concentration as a function of Dilution Rate for the Continuous Fermentation of *B. licheniformis* ATCC 9945a (Table C-1)

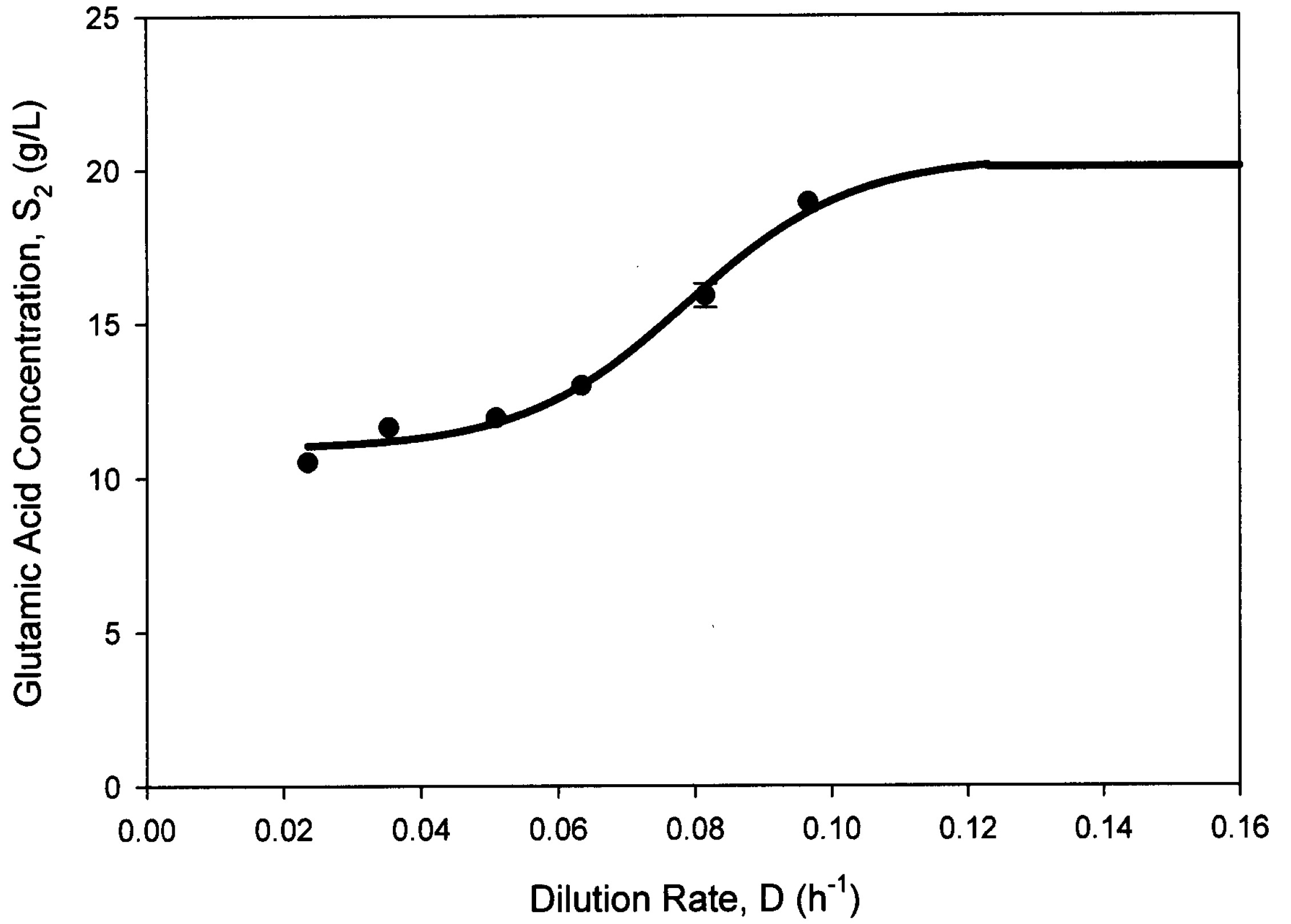


Figure 4-19 The Glutamic Acid Concentration as a function of Dilution Rate for the Continuous Fermentation of *B. licheniformis* ATCC 9945a (Table C-1)

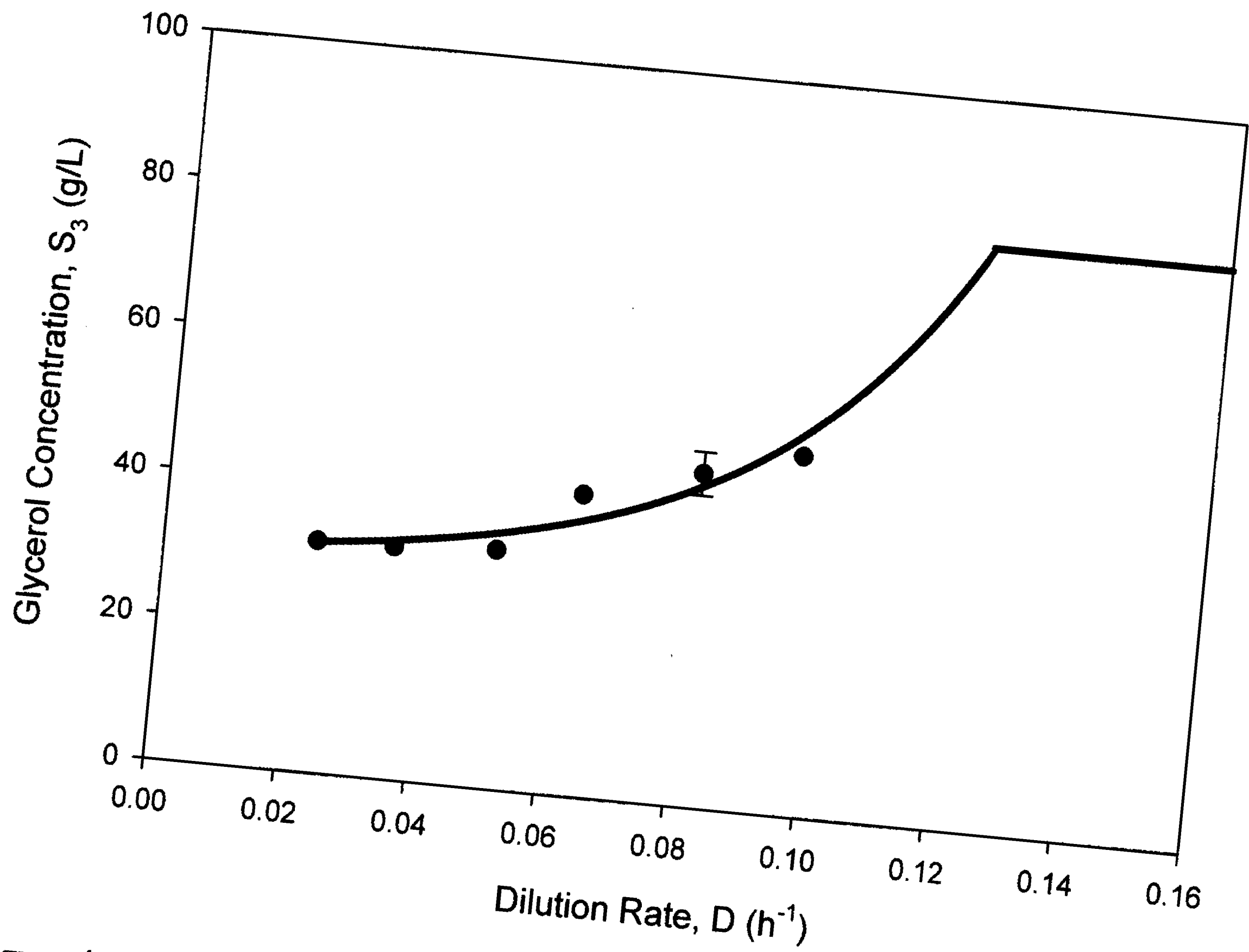


Figure 4-20 The Glycerol Concentration as a function of Dilution Rate for the Continuous Fermentation of *B. licheniformis* ATCC 9945a (Table C-1)

4.2.5 Biomass and Polyglutamic Acid Productivity

The biomass productivity (Figure 4-21) had a maximum value of 0.16 g/L/h at a dilution rate of 0.063 h⁻¹. The biomass productivity in the continuous fermentation was almost a two fold increase over that found in the controlled batch fermentation. The batch fermentation productivity had a maximum reported value of 0.092 g/L/h (this study).

The polyglutamic acid productivity (Figure 4-22) peaked at a dilution rate of 0.082 h⁻¹ and reached 1.2 g/L/h. The continuous system displayed an increase in the PGA productivity over the controlled batch fermentation productivity. In fact the continuous PGA productivity is almost a four fold increase in productivity over the highest batch productivity (0.34 g/L/h) reported in the literature (Cromwick et al., 1996), and one and half times that of the fed batch productivity of 0.83 g/L/h reported by Yoon et al. (2000).

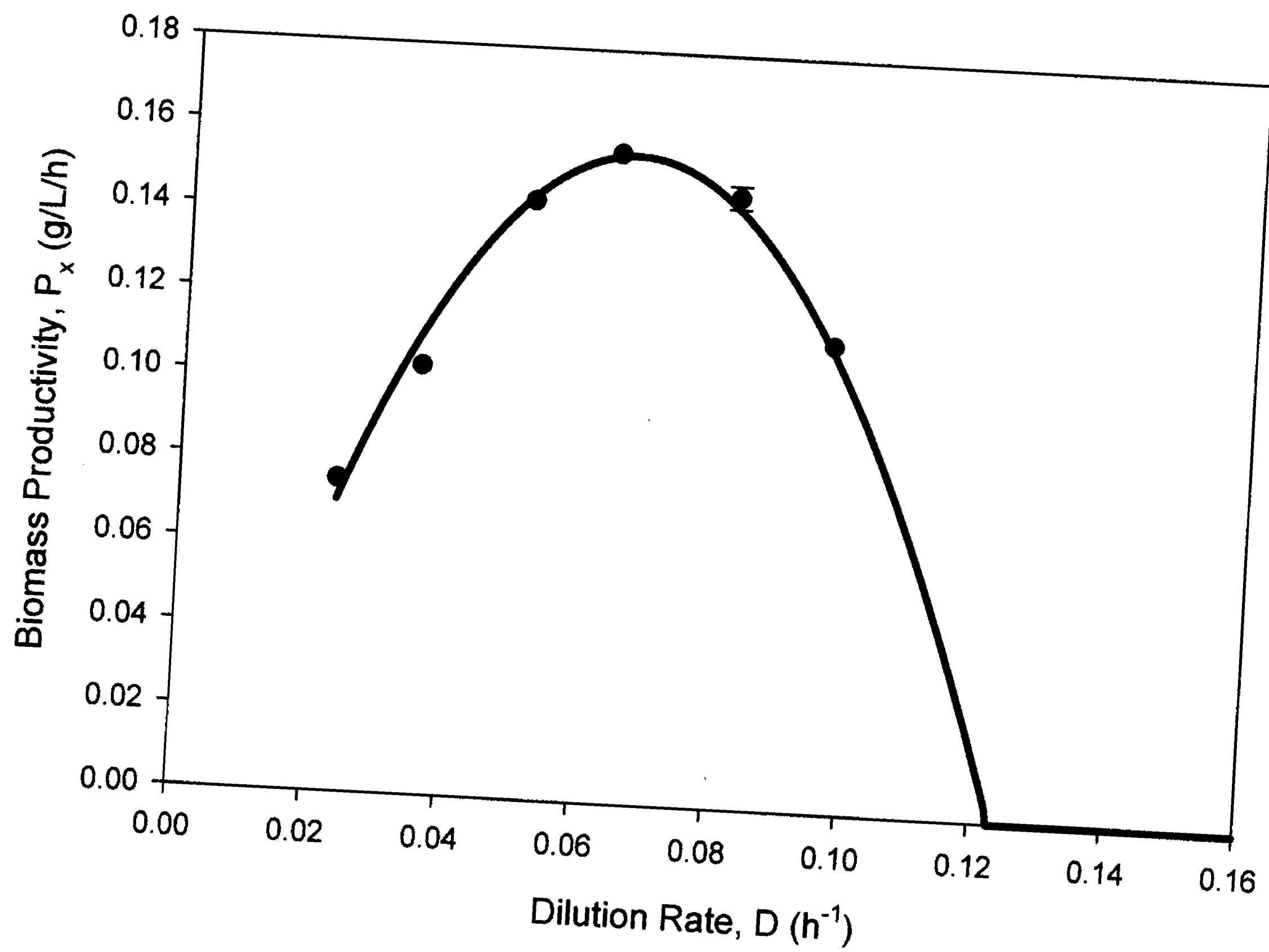


Figure 4-21 Biomass Productivity as a function of Dilution Rate for the Continuous Fermentation of *B. licheniformis* ATCC 9945a (Table C-2)

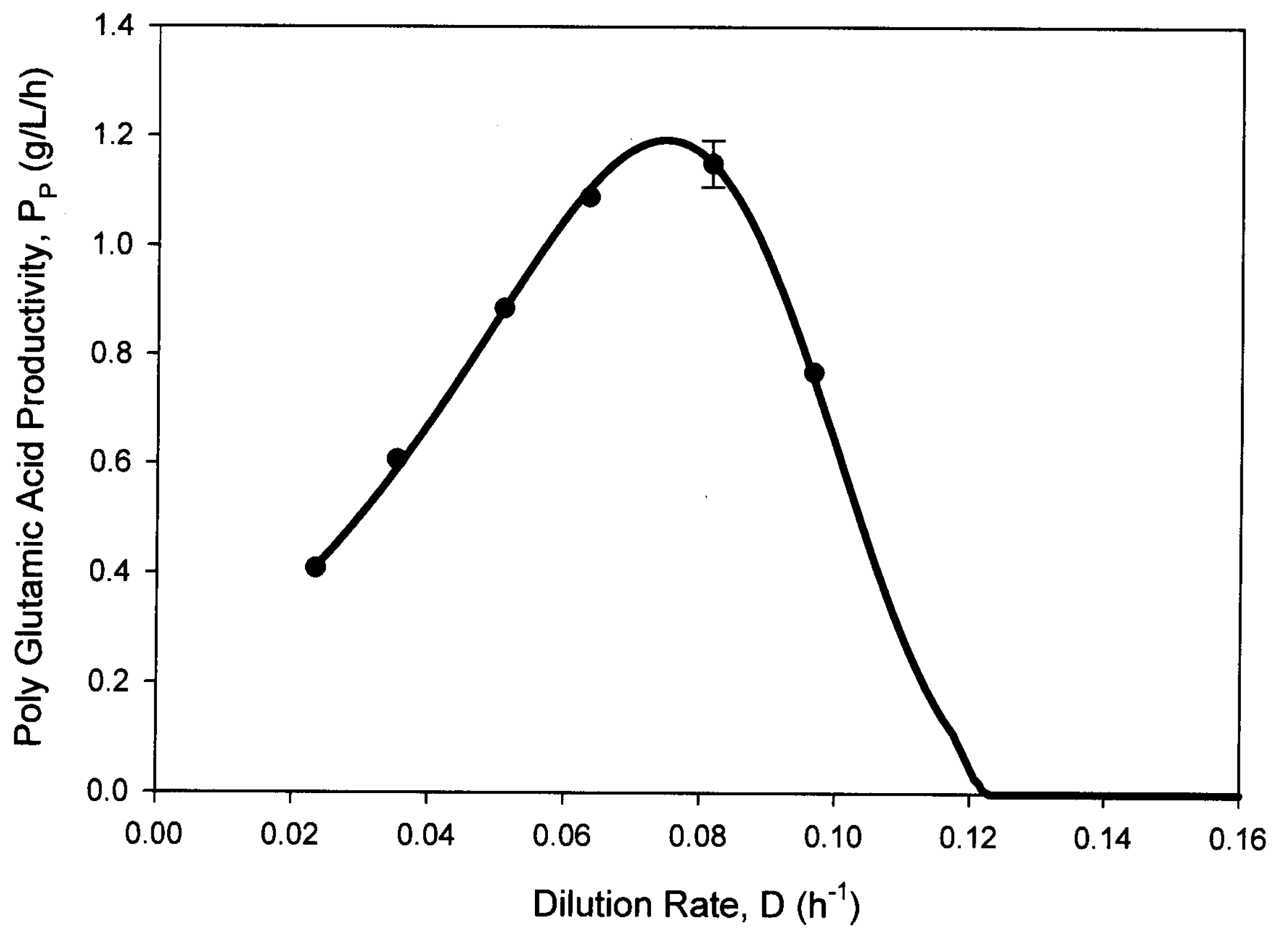


Figure 4-22 Polyglutamic Acid Productivity as a function of Dilution Rate for the Continuous Fermentation of *B. licheniformis* ATCC 9945a (Table C-2)

4.2.6 Biomass and Polyglutamic Acid Yield

The biomass yield from citric acid (Figure 4-23) peaked slightly at a dilution rate of 0.051 h^{-1} and had a value of 0.38 g/g . Between a dilution rate of 0.023 h^{-1} and 0.063 h^{-1} there was not a great change in biomass yield from citric acid. The biomass yield from glutamic acid (Figure 4-23) remained somewhat constant from $D = 0.023 \text{ h}^{-1}$ to $D = 0.063 \text{ h}^{-1}$. At dilution rates greater than this, there was a sharp increase in biomass yield from glutamic acid to 1.1 g/g at $D = 0.097 \text{ h}^{-1}$.

The biomass yield from glycerol followed the same trend as the biomass yield from total carbon sources (Figure 4-24). This is because glycerol was the main substrate used throughout all dilution rates. The biomass yield from the total carbon sources generally declined with increasing dilution rates. The yield was between 0.048 g/g (at $D = 0.023 \text{ h}^{-1}$) and 0.032 g/g (at $D = 0.097 \text{ h}^{-1}$). These yields were lower than those found in the controlled batch fermentation (0.053 g/g).

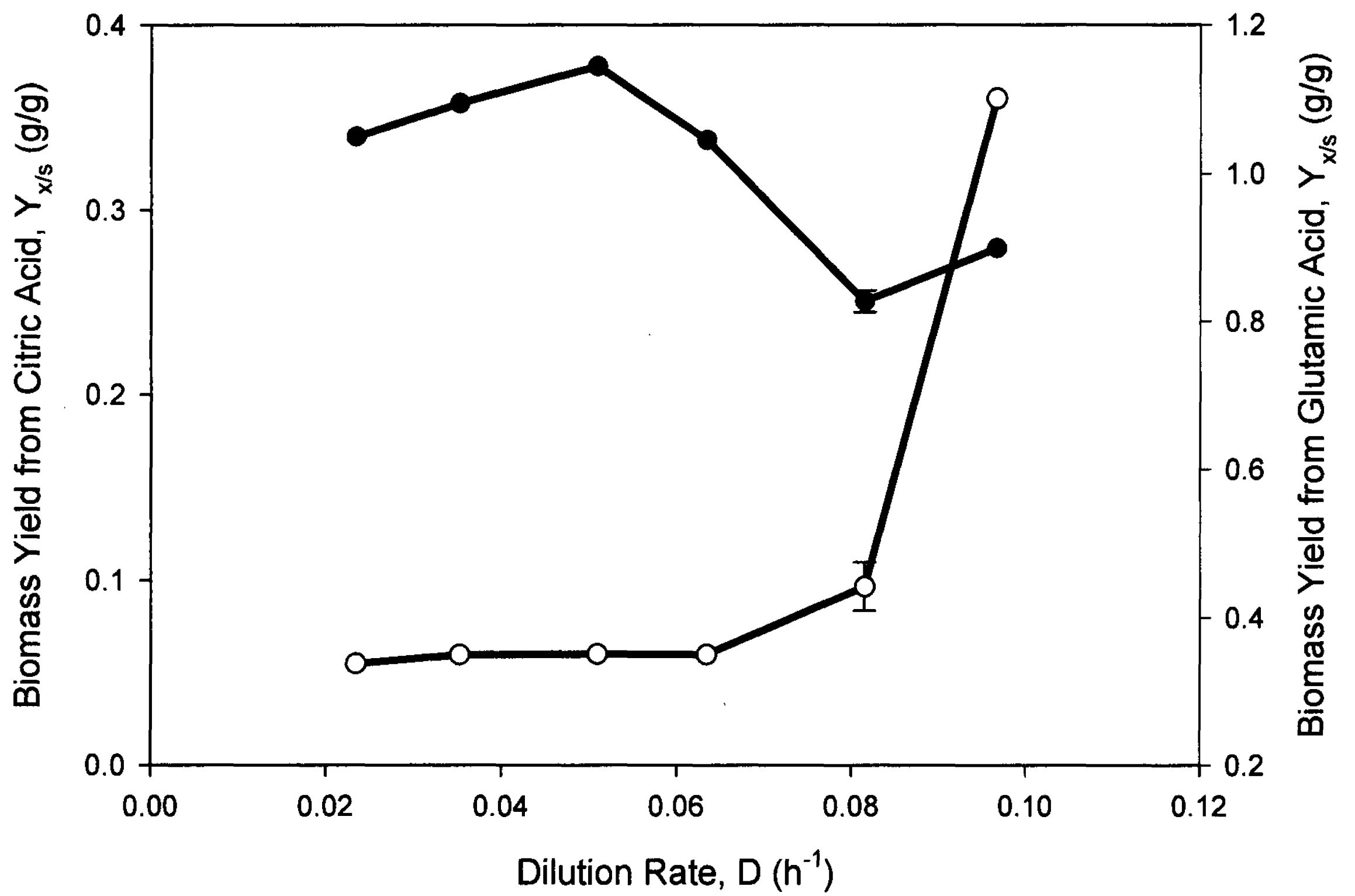


Figure 4-23 Biomass Yield from Citric Acid (●) and Glutamic Acid (○) as a function of Dilution Rate for the Continuous Fermentation of *B. licheniformis* ATCC 9945a (Table C-3)

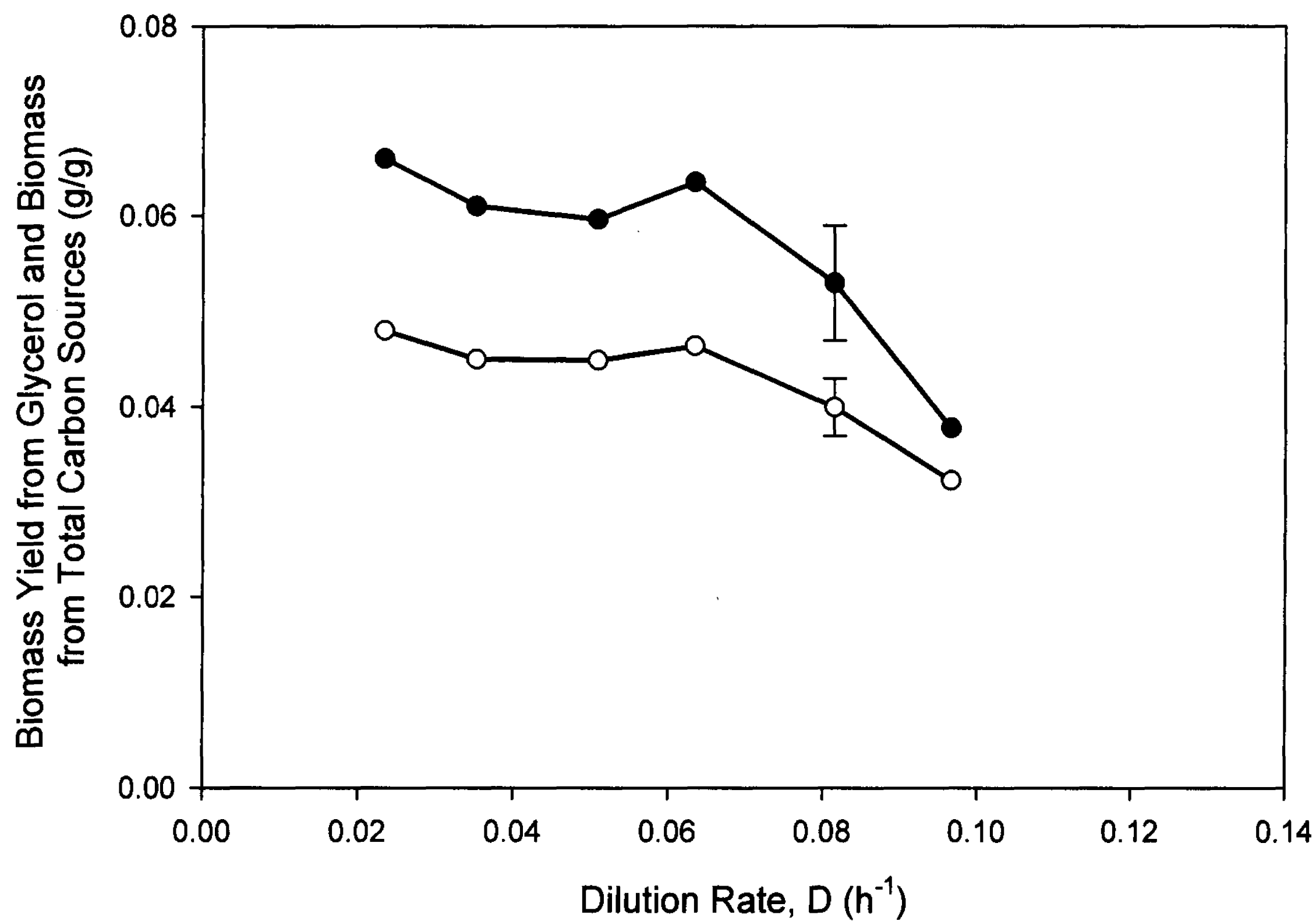


Figure 4-24 Biomass Yield from Glycerol (●) and Total Carbon Sources (○) as a function of Dilution Rate for the Continuous Fermentation of *B. licheniformis* ATCC 9945a (Table C-3)

The PGA yield from biomass (Figure 4-25) increased as the dilution rate was increased from 0.023 h^{-1} to 0.082 h^{-1} . It peaked at a dilution rate of 0.082 h^{-1} , and reached a value of 7.9 g/g . There was a sharp decline in PGA yield from biomass at $D = 0.097 \text{ h}^{-1}$. The continuous fermentation yielded a higher peak PGA yield from biomass than the batch fermentation. The batch fermentation yield from biomass was 5.9 g/g (Table A-4).

The PGA yield from the citric acid (Figure 4-26) peaked at a dilution rate of 0.063 h^{-1} reaching a value of 2.4 g/g . The peak PGA yield from citric acid was lower than that found in the batch fermentation (2.9 g/g). The yield from glutamic acid (Figure 4-26) did not show a peak but continued to increase as dilution rate was increased, reaching 6.0 g/g at a dilution rate of 0.097 h^{-1} . The batch fermentation PGA yield from glutamic acid was 2.3 g/g .

The PGA yield from total carbon sources (Figure 4-27) increased from 0.26 g/g at a dilution rate of 0.023 h^{-1} to 0.33 g/g at a dilution rate of 0.063 h^{-1} . Increasing the dilution rate after this point reduced the PGA yield from the total carbons sources (down to 0.18 g/g at $D = 0.097 \text{ h}^{-1}$). The peak yield of 0.33 g/g is greater than that found in the batch fermentation (0.29 g/g).

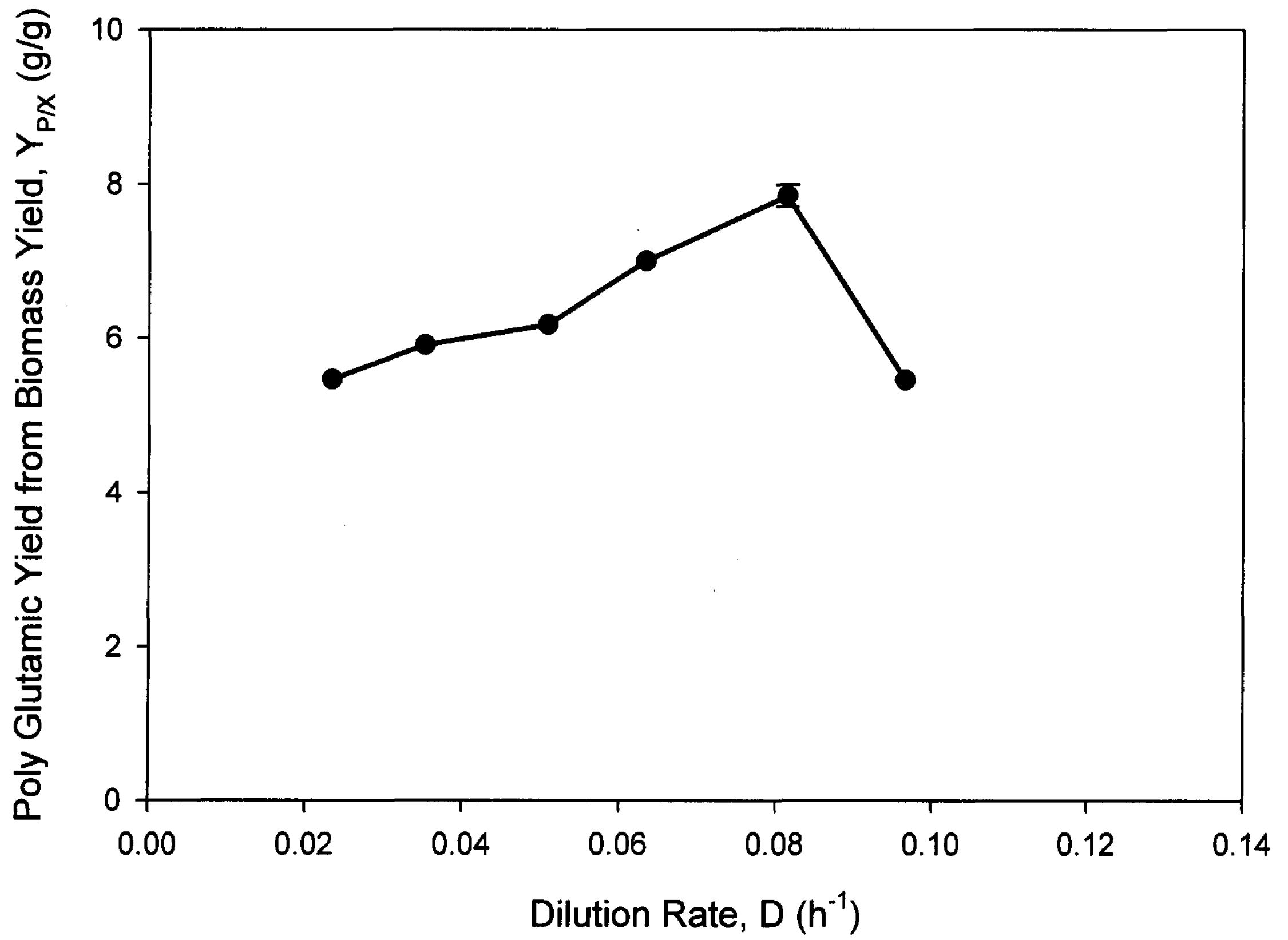


Figure 4-25 Polyglutamic Acid yield from Biomass as a function of Dilution Rate for the Continuous Fermentation of *B. licheniformis* ATCC 9945a (Table C-4)

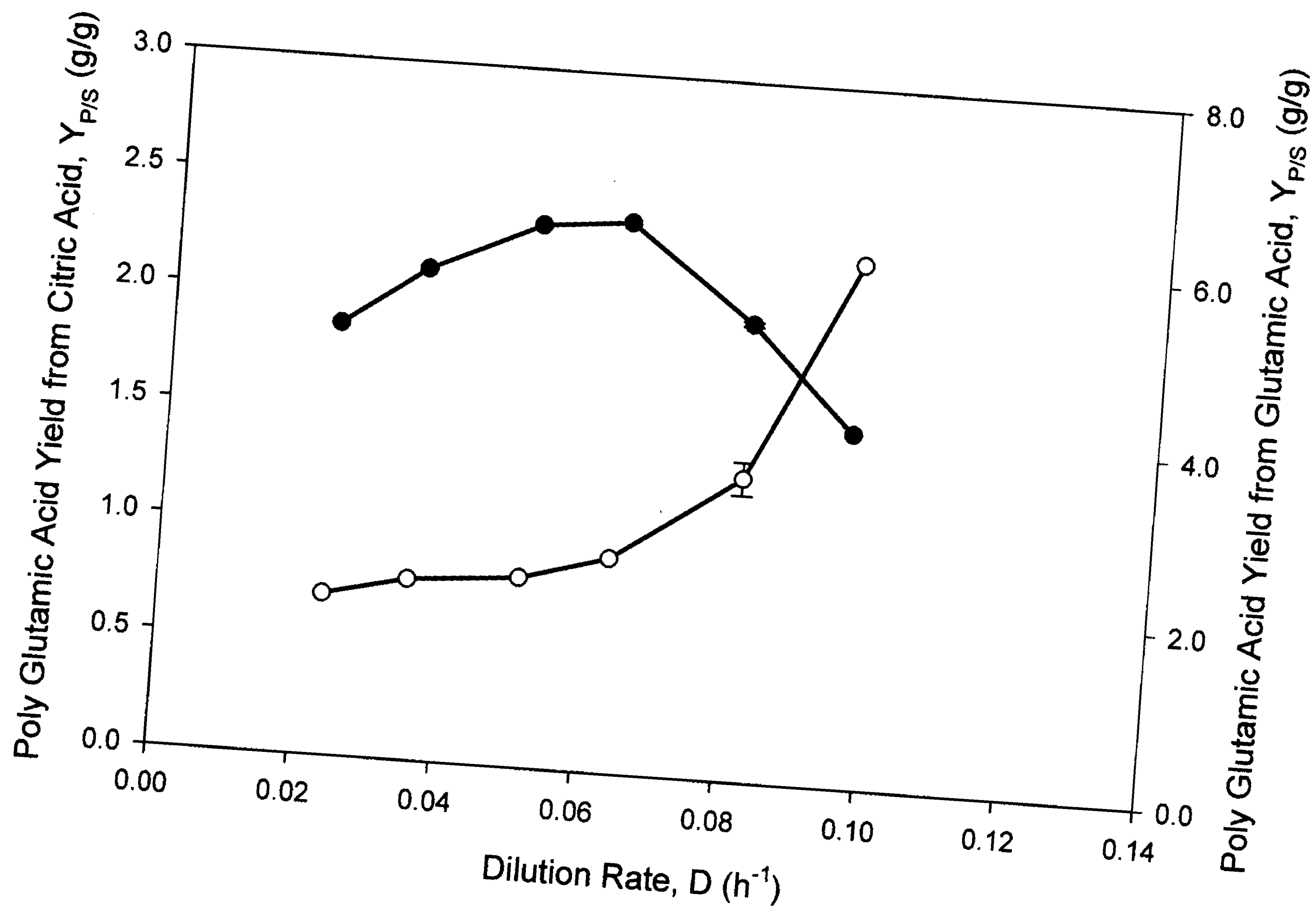


Figure 4-26 Polyglutamic Acid Yield from Citric Acid (●) and Glutamic Acid (○) as a function of Dilution Rate for the Continuous Fermentation of *B. licheniformis* ATCC 9945a (Table C-4)

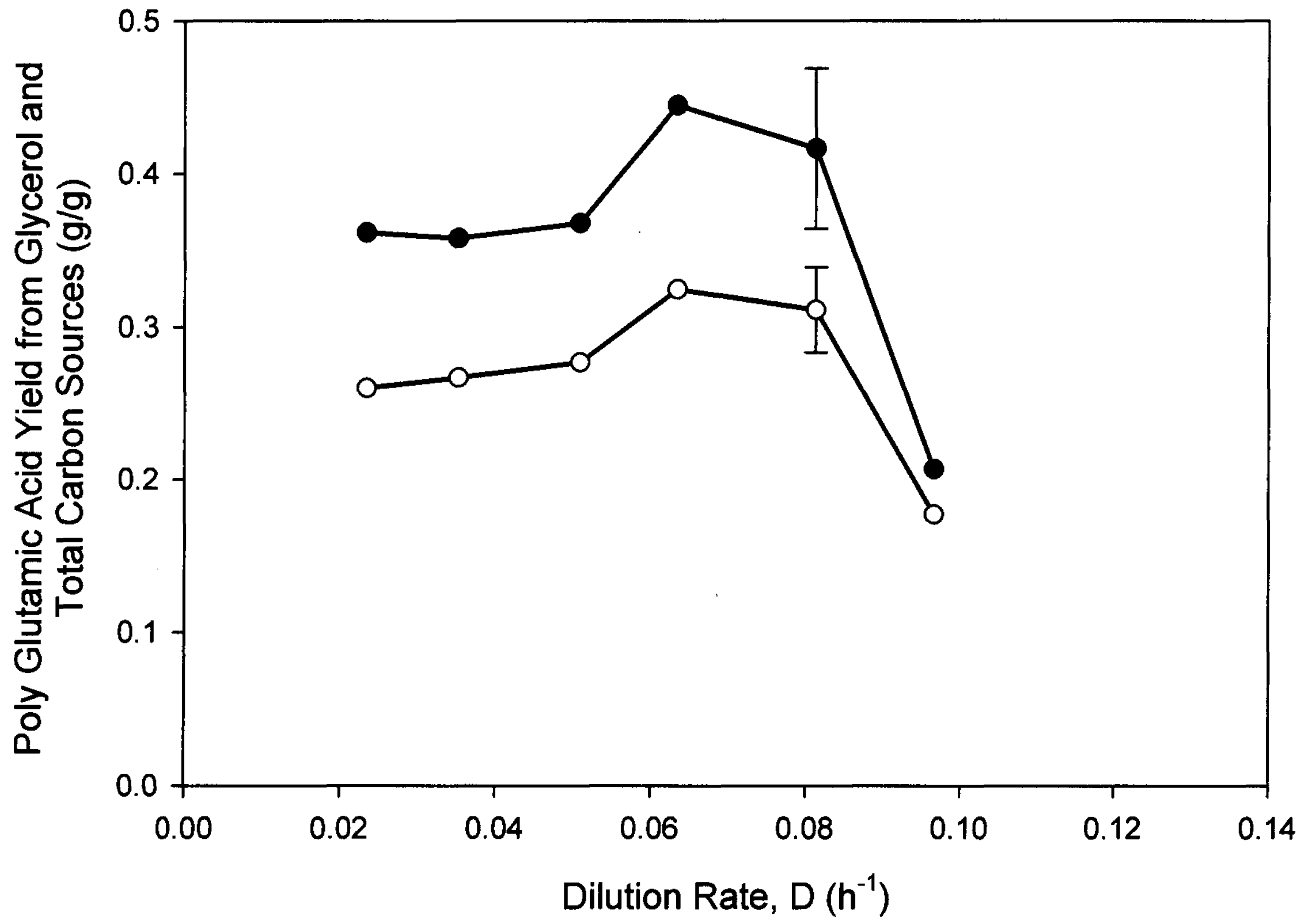


Figure 4-27 Polyglutamic Acid Yield from Glycerol (●) and Total Carbon Sources (○) as a function of Dilution Rate for the Continuous Fermentation of *B. licheniformis* ATCC 9945a (Table C-4)

4.2.7 Molecular Weight Characteristics

The molecular weight characteristics, namely the number average molecular weight (M_n), the weight average molecular weight (M_w) and the polydispersity (M_w/M_n) were calculated for each dilution rate. Figures 4-28, 4-29 and 4-30 display these molecular weight characteristics.

The number average molecular weight was lowest at a dilution rate of 0.023 h^{-1} (149,000 Da) and a dilution rate of 0.097 h^{-1} (144,000 Da). The number average molecular weight did not vary substantially between a dilution rate of 0.035 h^{-1} and 0.082 h^{-1} . The number average ranged from 165,000 Da (at $D = 0.051 \text{ h}^{-1}$) to 196,000 Da (at $D = 0.035 \text{ h}^{-1}$).

The weight average molecular weight was highest at a dilution rate of 0.035 h^{-1} (454,000 Da) and lowest at a dilution rate of 0.097 h^{-1} (311,000 Da). There did not seem to be a definitive trend between dilution rate and number or weight average molecular weight. Although at the highest dilution rate ($D=0.097 \text{ h}^{-1}$) there was the lowest number and weight average molecular weight.

The polydispersity of the PGA polymer was highest at a dilution rate of 0.023 h^{-1} and had a value of 2.8. The polydispersity was as low as 2.1 at a dilution rate of 0.063 h^{-1} , but was fairly consistent throughout the different dilution rates. In fact the polydispersity had an average of 2.4 throughout all the dilution rates observed.

There seemed to be a wider variation between the two repeated runs (at a dilution rate of 0.082 h^{-1}) for the molecular weight distribution characteristics than that seen in the previous sections. This variation was especially apparent in the weight average

molecular weight plot. The Mw value ranged from below 400×10^3 Da to over 500×10^3 Da for a dilution rate of 0.082 h^{-1} .

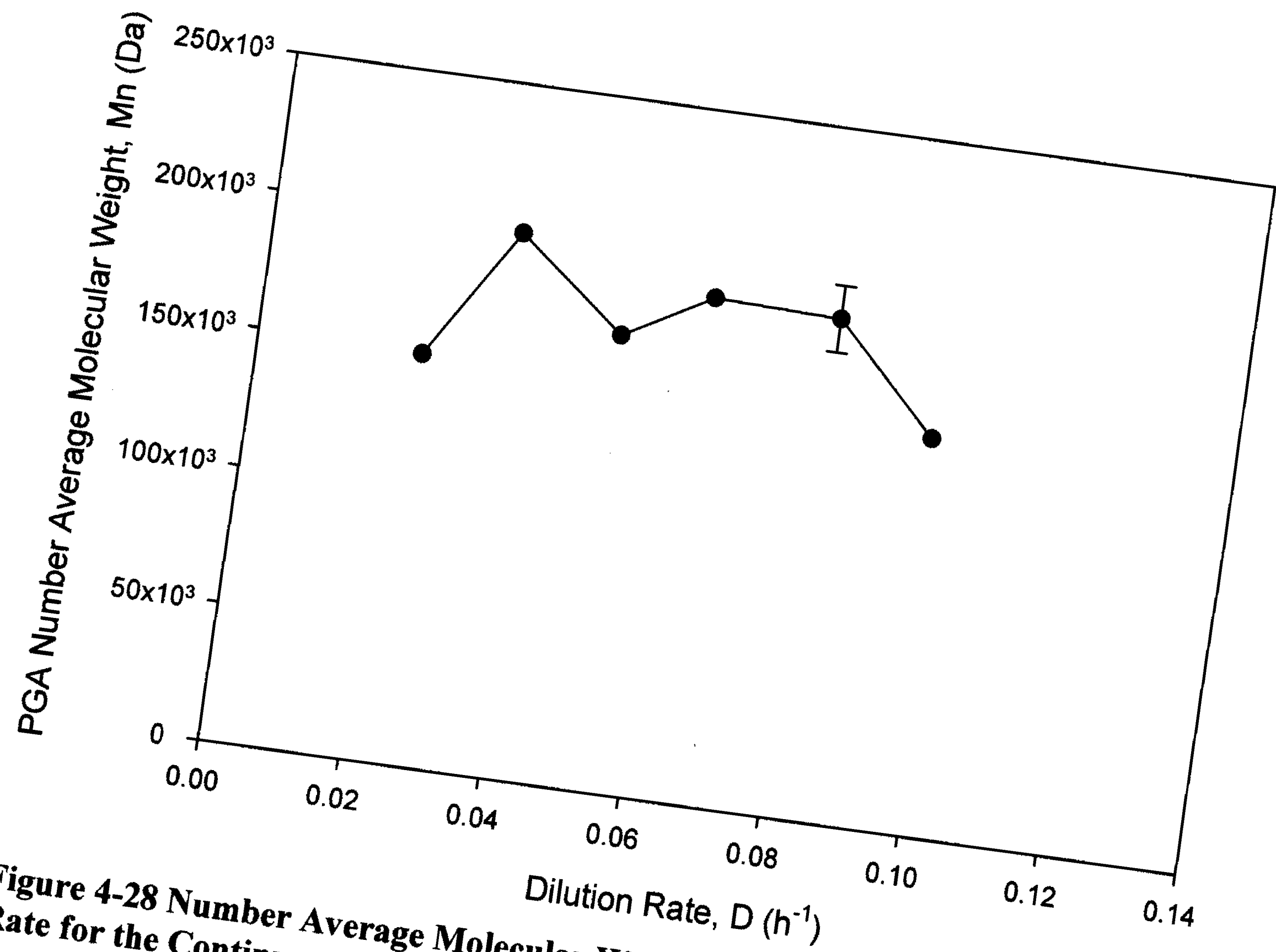


Figure 4-28 Number Average Molecular Weight of PGA as a function of Dilution Rate for the Continuous Fermentation of *B. licheniformis* ATCC 9945a (Table C-5)

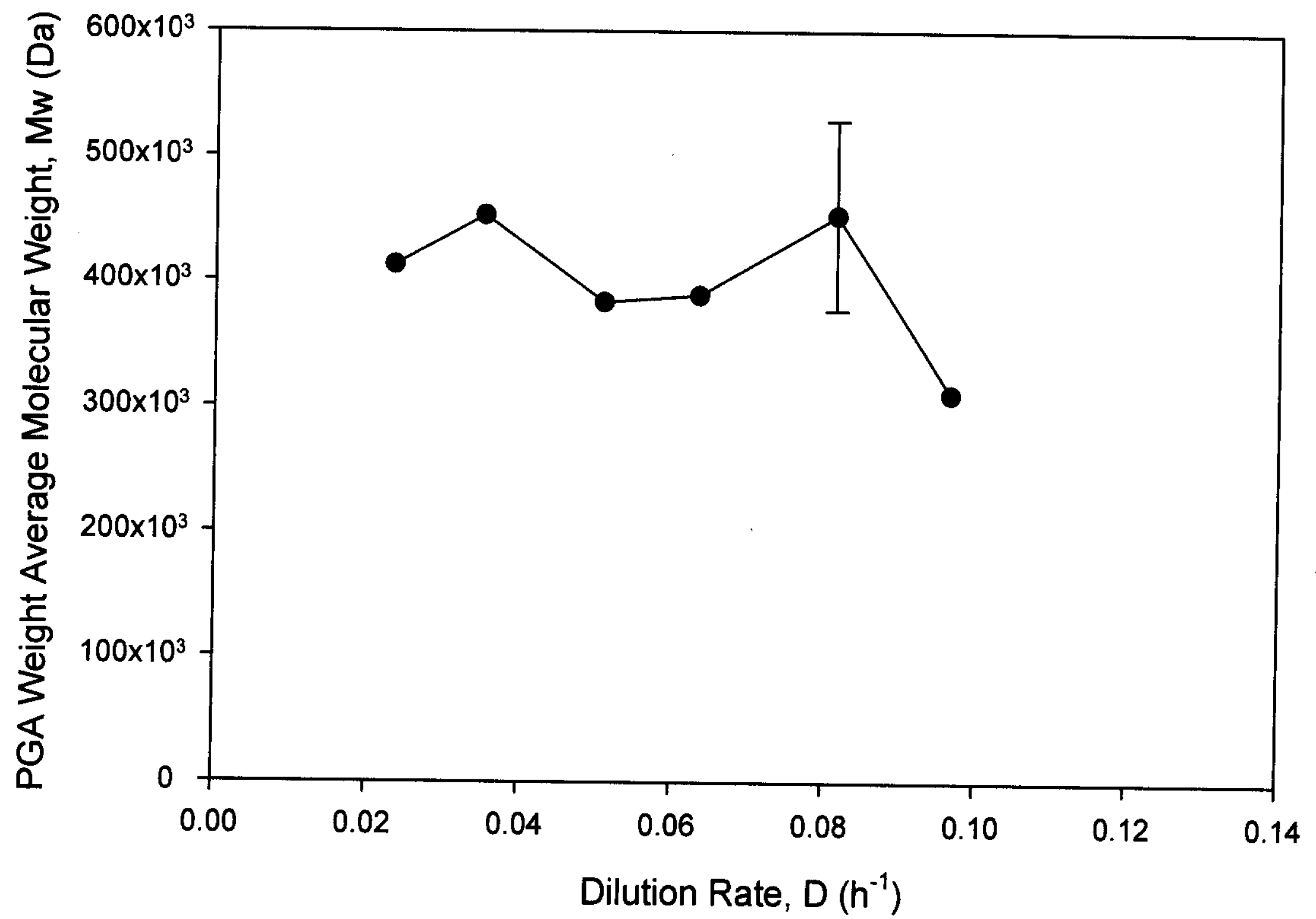


Figure 4-29 Weight Average Molecular Weight as a function of Dilution Rate for the Continuous Fermentation of *B. licheniformis* ATCC 9945a (Table C-5)

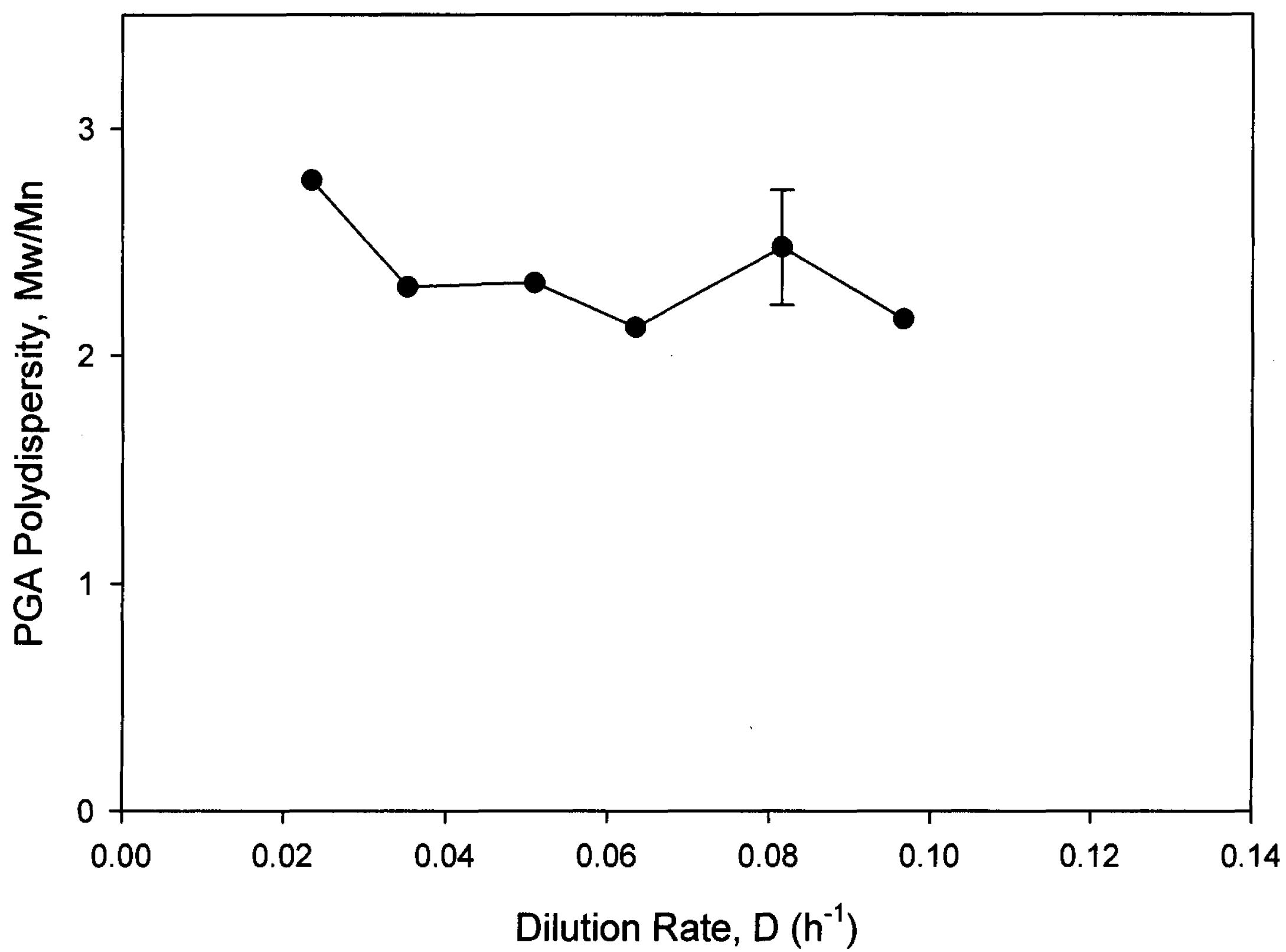


Figure 4-30 Polydispersity as a function of Dilution Rate for the Continuous Fermentation of *B. licheniformis* ATCC 9945a (Table C-5)

4.2.8 Richard – Margaritis Empirical Model

Richard and Margaritis (2004) plotted the specific growth rate as a function of the limiting substrate concentration for several microorganisms producing biopolymers. It was shown that a modified Monod equation was most appropriate in describing the effects of the limiting substrate concentration on the specific growth rate. Kovarova-Kovar and Egli (1998) discussed the possibility of using the total carbon source concentration (as an alternative to the limiting substrate concentration) when modeling systems with multiple carbon sources. For this thesis, the specific growth rate is plotted as a function of the citric acid concentration (Figure 4-31) as well as a function of the total carbon source concentration (Figure 4-32).

From the two plots, it can be seen that the maximum specific growth rate was similar to that found using washout experiments, which was found to be 0.123 h^{-1} . The citric acid plot showed a maximum specific growth rate of 0.132 h^{-1} and the total carbon source plot showed a maximum specific growth rate of 0.130 h^{-1} . The relative coefficient for both plots was greater than one, showing that the biopolymer production was non-growth related. The citric acid plot had a slightly lower relative coefficient than the total carbon source plot, having values of 2.68 and 4.28 respectively.

The calculated maximum dilution rate (which occurs when $S = S_0$) for both the citric acid plot and the total carbon source plot was calculated to be 0.122 h^{-1} .

The two plots fit the Richard – Margaritis model quite closely, but the plot using the total carbon source concentration seemed to be a closer fit, having an R^2 value of 0.978 (compared with 0.932 for the citric acid plot).

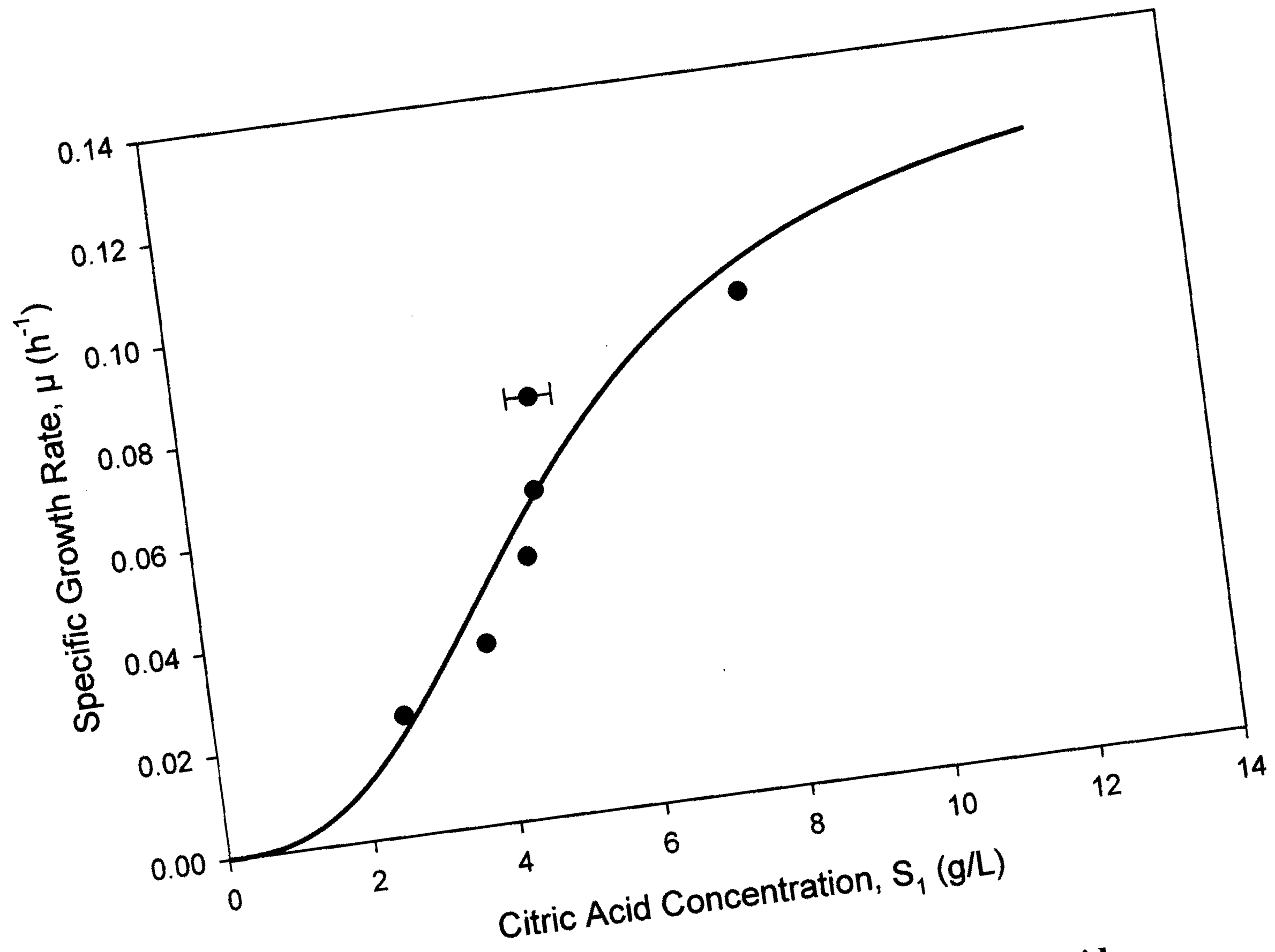


Figure 4-31 The Specific Growth Rate as a function of the Citric Acid Concentration for the Continuous Fermentation of *B. licheniformis* ATCC 9945a (Table C-1)

$$\mu = \frac{\mu_{\max} \times S^r}{K_s^r + S^r} = \frac{0.1318 \times S^{2.68}}{4.617^{2.68} + S^{2.68}}$$

$$R^2 = 0.932$$

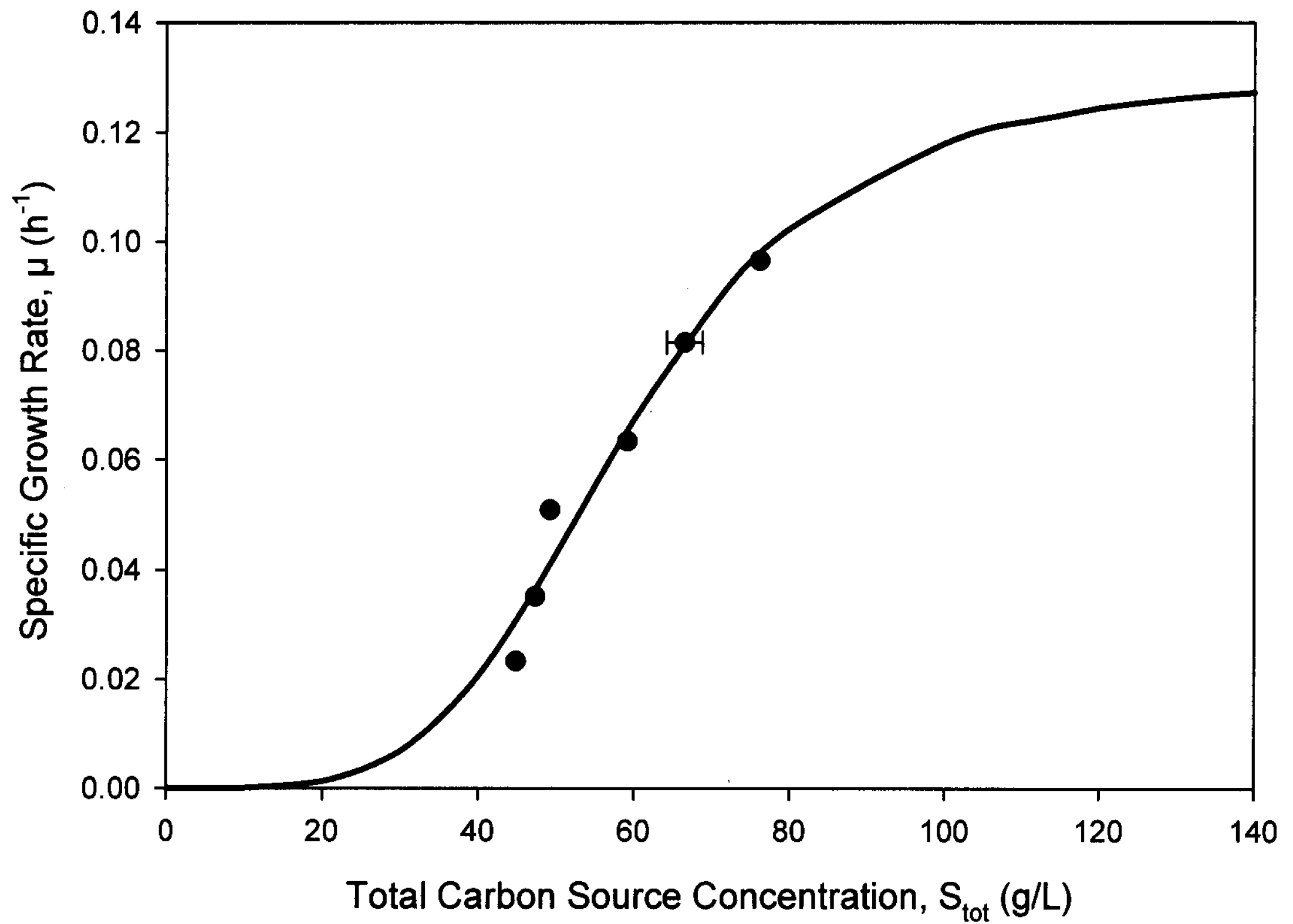


Figure 4-32 The Specific Growth Rate as a function of Total Carbon Source Concentration for the Continuous Fermentation of *B. licheniformis* ATCC 9945a (Table C-1)

$$\mu = \frac{\mu_{\max} \times S^r}{K_s^r + S^r} = \frac{0.1304 \times S^{4.277}}{59.05^{4.277} + S^{4.277}}$$

$$R^2 = 0.978$$

5. CONCLUSIONS AND RECOMMENDATIONS

5.1 Conclusions

Although the batch fermentation of *Bacillus licheniformis* has been extensively studied, to the author's knowledge this is the first time the changes in the oxygen uptake rate (OUR), the specific oxygen uptake rate (Q_{O_2}) and the volumetric mass transfer coefficient (k_{La}) were determined during a batch fermentation. It appeared that the OUR, Q_{O_2} and k_{La} followed similar trends as those reported for *B. subtilis* (Richard and Margaritis, 2003). The OUR reached a maximum of 4.7 mmol O₂/L/h during the early stationary phase. The Q_{O_2} quickly peaked in the early exponential phase and was greatly reduced during the stationary phase. The k_{La} was found to increase during the exponential growth phase, and peaked at a value of 207 h⁻¹.

During the batch run, a biomass concentration of 4.4 g/L was achieved and a polyglutamic acid concentration of 24 g/L was produced. From the early exponential phase, a maximum specific growth rate of 0.113 h⁻¹ was found. The PGA yield from total substrates was 0.29 g/g and was consistent with values reported in the literature.

This work is also the first to be done on the continuous fermentation of *B. licheniformis*. The use of a continuous stirred tank bioreactor has many advantages, including an increase in polymer productivity, an increase in product yield from the substrates and a more accurate determination of the kinetic constants.

Polyglutamic acid was produced at various dilution rates, ranging from 0.023 h⁻¹ to 0.097 h⁻¹. The maximum polyglutamic acid production occurred at a dilution rate of

0.082 h⁻¹ and had a value of 1.2 g/L/h, which was significantly higher than that reported in batch fermentations. The polyglutamic acid yield from substrates also peaked at 0.063 h⁻¹, and was 0.33 g/g, again, significantly higher than the yield found in batch fermentations.

The molecular weight distribution characteristics were observed at the different dilution rates. The number average molecular weight fell between 144,000 Da and 197,000 Da. The weight average molecular weight peaked at a dilution rate of 0.082 h⁻¹ and was above 450,000 Da. It was lowest at a dilution rate of 0.097 h⁻¹ and was just above 300,000 Da. The polydispersity of the polymer remained somewhat consistent throughout the different dilution rates, and had an average of 2.4.

The kinetic constants were found through washout experiments and by fitting the observed data to the Richard – Margaritis empirical model. The two washout experiments showed a maximum specific growth rate of 0.123 h⁻¹. This value was similar to that found by fitting the data to the Richard-Margaritis Model, which gave a value of 0.130 h⁻¹ when the model was fitted using the total carbon source concentration. The relative coefficient was found to be 4.28, which indicates that the polymer is produced in a non-growth related manner. The maximum dilution rate was found to be 0.122 h⁻¹.

5.2 Recommendations

Although this thesis covers a wide range of dilution rates (from 20% to 80% of the maximum specific growth rate), further investigation into other dilution rates is advisable. By increasing the number of dilution rates, and the dilution rate range, a more

accurate picture of the continuous culture characteristics can be found. Also, by investigating the extreme conditions (i.e. dilution rates $>80\%$ of μ_{\max} and $<20\%$ of μ_{\max}) a more complete picture of the molecular weight characteristics of the system can be found.

In addition to a wider range of dilution rates, it may be advisable to investigate the rheology and oxygen transfer characteristics of the continuous system. Lastly, optimization experiments could be implemented to further increase the productivity of the system.

6. REFERENCES

- Akash A, Kelly R, Khan S (1999) Rheology and molecular weight changes during enzymatic degradation of a water-soluble polymer. *Macromolecules* 32:294-300.
- Arbige M-V, Bulthuis B-A, Schultz J, Crabb D (1993) Fermentation of *Bacillus* In *Bacillus subtilis* and other Gram-Positive Bacteria, Biochemistry, Physiology and Molecular Genetics. Soehnshein, A-L, Hoch J-A, Losick R (Eds) American Society for Microbiology, Washington DC
- Ashiuchi M, Tani K, Soda K, Misono H (1998) Properties of glutamate racemase from *Bacillus subtilis* IFO 3336. *J. Biochem.* 123: 1156-1163.
- Ashiuchi M, Tani K, Soda K, Misono H (1999) A poly- γ -glutamate synthetic system of *Bacillus subtilis* IFO 3336: gene cloning and biochemical analysis of poly- γ -glutamate produced by *Escherichia coli* clone cells. *Biochem. Biophys. Res. Commun.* 263: 6-12.
- Bandyopadhyay B and Humphrey A E (1967) Dynamic Measurement of the Volumetric Oxygen Transfer Coefficient in Fermentation Systems. *Biotechnol Bioeng* 9: 533 - 544
- Basedow A, Ebert K, Ederer H (1978) Kinetic studies on the acid hydrolysis of dextran. *Macromolecules* 11:774-781.
- Birrer G-A, Cromwick A-M, Gross R-A (1994) γ -Poly (glutamic acid) formation by *Bacillus licheniformis* 9945a: physiological and biochemical studies. *International J. Biol. Macromol.* 16: 265-275.
- Blanch HW and Clark DS (1996) *Biochemical Engineering*. M. Dekker, New York.
- Borbély M, Nagasaki Y, Borbély J, Fan K, Bhogle A, Sevoian M (1994) Biosynthesis and chemical modification of poly (γ -glutamic acid). *Polymer Bull.* 32:127-132.
- Bovarnick M (1942) The formation of extracellular D (-) glutamic acid polypeptide by *Bacillus subtilis*. *J. Biol. Chem.* 145:415-424.
- Cheng C, Asada Y, Aaida T (1989) Production of γ -polyglutamic acid by *Bacillus subtilis* A35 under denitrifying conditions. *Agric. Biol. Chem.* 53: 2369-2375.
- Cromwick A-M, Gross R-A (1995) Effect of manganese (II) on *Bacillus licheniformis* ATCC9945A physiology and γ -poly(glutamic acid) formation. *Int. J. Biol. Macromol.* 16: 265-275.

- Cromwick A-M, Birrer G, Gross R (1996) Effects of pH and aeration on γ -poly(glutamic acid) formation by *Bacillus licheniformis* in controlled batch fermentor cultures. *Biotechnol. Bioeng.* 50:222-227.
- Gardner J-M, Troy F-A (1979) Chemistry and biosynthesis of the poly (γ -D-glutamyl) capsule in *Bacillus licheniformis*. *J. Biol. Chem.* 254: 6262-6269
- Goto A, Kunioka M (1992) Biosynthesis and hydrolysis of poly(γ -glutamic acid) from *Bacillus subtilis* IFO3335. *Biosci. Biotech. Biochem.* 56: 1031-1035.
- Hara T, Ueda S (1982) Regulation of polyglutamate production in *Bacillus subtilis* (natto): transformation of high PGA productivity. *Agric. Biol. Chem.* 46: 2275-2281.
- Hara T, Fujio T, Ueda S (1982) Polyglutamate production by *Bacillus subtilis* (natto). *J. Appl. Biochem.* 4: 112-120.
- He L-M, Neu M-P, Vanderberg L-A (2000) *Bacillus licheniformis* γ -glutamyl exopolymer: physiochemical characterization and U(VI) interaction. *Environ. Sci. Technol.* 34: 1694-1701.
- Holmes F-A, Kudelka A-P, Kavanagh J-J, Huber M-H, Ajani J-A, Valero V (1995) Current status of clinical trials with Taxol and docetaxel. In: Georg, G-I, Chen T-T, Ojima I, Vyas D-M (Eds) *Taxane Anticancer Agents: Basic Science and Current Status*. American Chemical Society, Washington DC, pp 31-57.
- Hwan Do J, Chang H, Lee S (2001) Efficient recovery of poly(glutamic acid) from highly viscous culture broth. *Biotechnol. Bioeng.* 76:219-223.
- Ito T, Tanaka T, Ohmachi T, Asada Y (1996) Glutamic acid independent production of poly (γ -glutamic acid) by *Bacillus subtilis* TAM-4. *Biosci. Biotechnol. Biochem.* 60:1239-1242.
- Irurzun I, Bou J, Perez-Camero G, Abad, C, Campos, A, Munoz-Guerra S (2000) Mark-Houwink parameters of biosynthetic poly (γ -glutamic acid) in aqueous solution. *Macromol. Chem. Phys.* 202: 3253-3256.
- King E-C, Blacker A-J, Bugg, T-D-M (2000). Enzymatic breakdown of poly- γ -D-polyglutamic acid in *Bacillus licheniformis*: identification of a polyglutamyl- γ -hydrolase enzyme. *Biomacromolecules* 1: 75-83.
- Ko Y-H, Gross R-A, (1998) Effects of glucose and glycerol on γ -poly(glutamic acid) formation by *Bacillus licheniformis* ATCC 9945A. *Biotechnol. Bioeng.* 57: 430-437.
- Kobayashi H, Hyson S-H, Ikada Y, (1991) Water-curable and biodegradable prepolymer. *J. Biomed. Mater. Res.* 25: 1481-1494.

- Kovarova-Kovar K and Egli T (1998) Growth Kinetics of Suspended Microbial Cells: From Single Substrate Controlled Growth to Mixed Substrate Kinetics. *Microbiol. Mol. Biol. Rev.* 62: 646-666.
- Kubota H, Nambu Y, Endo T (1993) Convenient and quantitative esterification of poly(γ -glutamic acid) produced by microorganism. *J. Polym. Sci. Part A: Polym. Chem.* 31: 2877-2878.
- Kubota H, Matsunobu T, Uotani K, Takebe H, Satoh A, Tanaka T, Tanguchi M (1993) Production of poly(γ -glutamic acid) by *Bacillus subtilis* F-2-01. *Biosci. Biotechnol. Biochem.* 57: 1212-1213.
- Kubota H, Nambu Y, Endo T (1996) Alkaline hydrolysis of poly γ -glutamic acid produced by microorganism. *J. Poly. Sci. Chem.* 34: 1347-1351.
- Kunioka M, Goto A, (1994) Biosynthesis of poly(γ -glutamic acid) from L-glutamic acid, citric acid, and ammonium sulfate in *Bacillus subtilis* IFO3335. *Appl. Microbiol. Biotechnol.* 40: 867-872.
- Kunioka M (1995) Biosynthesis of poly(γ -glutamic acid) from L-glutamine, citric acid, and ammonium sulfate in *Bacillus subtilis* IFO3335. *Appl. Microbiol. Biotechnol.* 44: 501-506.
- Kunioka M (1997) Biosynthesis and chemical reactions of poly(amino acid)s from microorganisms. *Appl. Microbiol. Biotechnol.* 47:469-475.
- Kurane R, Takeda K, Suzuki T (1986) Screening for and characteristics of microbial flocculant. *Agric. Biol. Chem.* 50: 2301-2307.
- Leonard C-G, Housewright R-D, Thorne C-B (1958). Effects of some metallic ions on glutamyl polypeptide synthesis by *Bacillus subtilis*. *J. Bacteriol.* 76: 499-503.
- Li C, Yu D-F, Newman A, Cabral P, Stephens C, Hunter N, Milas L, Wallace S, (1998) Complete regression of well-established tumors using novel water-soluble poly(L-glutamic acid)-paclitaxel conjugate. *Cancer Res.* 58: 2404-2409.
- Li C, Price JE, Milas L, Hunter N, Ke S, Tansey W, Charnsagavej C, Wallace S, (1999) Antitumor activity of poly(L-glutamic acid)-paclitaxel on syngeneic and xenografted tumors. *Clin. Cancer Res.* 5: 891-897.
- Li C, Ke S, Wu Q-P, Tansey W, Hunter N, Buchmiller L, Milas L, Chamsangavej C, Wallace S (2000) Experimental therapeutics, preclinical pharmacology – tumor

irradiation enhances the tumor-specific distribution of poly (L-glutamic acid) – conjugated paclitaxel and its anti-tumor efficacy. *Clin. Cancer Res.* 6; 2829-2834.

Liang H-F, Yang T-F, Huang C-T, Chen M-C, Sung H-W (2005) Preparation of nanoparticles composed of poly(γ -glutamic acid)-poly(lactide) block copolymers and evaluation of their uptake by HepG2 cells. *J. Controlled Release* 105: 213-225

Makino S, Uchida I, Terakado N, Sasakawa C, Yoshikawa M, (1989) Molecular characterization and protein analysis of the *cap* region, which is essential for encapsulation in *Bacillus anthracis*. *J. Bacteriol.* 171: 722-730.

McLean R-C, Wolf D-C, Ferris F-G, Beveridge T-J, (1990) Metal-binding characteristics of the gamma-glutamyl capsular polymer of *Bacillus licheniformis* ATCC 9945. *Appl. Environ. Microbiol.* 56: 3671-3677.

Nagai T, Koguchi K, Ito Y (1997) Chemical analysis of poly- γ -glutamic acid produced by plasmid-free *Bacillus subtilis* (natto): evidence that plasmids are not involved in poly- γ -glutamic acid production. *J. Gen. Appl. Microbiol.* 43: 139-143.

Nietri N-J, Marrero R, Hoover T-A, Welkos S-L (1995) Identification and characterization of a trans-activator involved in the regulation of encapsulation by *Bacillus anthracis*. *Gene* 152: 121-129

Noda K, Igata K, Horrikawa Y, Fujii H (1980) Synthesis γ -glutamyi peptides catalyzed by transamidase from *Bacillus natto*. *Agric. Biol. Chem.* 44: 2419-2423.

Ogawa Y, Yamaguchi F, Yuasa K, Tahara Y (1997) Efficient production of γ - polyglutamic acid by *Bacillus subtilis* (natto) in jar fermenters. *Biosci. Biotech. Biochem.* 61: 1684-1687.

Richard A, Margaritis A (2001) Poly (glutamic acid) for biomedical applications. *CRC Crit Rev. Biotechnol.* 21; 219-232.

Richard A, Margaritis A (2002) Production and mass transfer characteristics of non-Newtonian biopolymers for biomedical applications. *CRC Crit. Rev. Biotechnol.* 22; 355-374.

Richard A, Margaritis A (2003) Optimization of cell growth and poly (glutamic acid) production in batch fermentation by *Bacillus subtilis*. *Biotechnol. Lett.* 25; 465-468.

Richard A, Margaritis A (2003) Rheology, Oxygen Transfer, and Molecular Weight Characteristics of Poly (glutamic acid) Fermentation by *Bacillus subtilis*. *Biotech. Bioeng.* 82; 299-305.

- Richard A, Margaritis A (2004) Empirical modeling of batch fermentation kinetics for poly (glutamic acid) production and other microbial biopolymers. *Biotech. Bioeng.* 87; 501-515.
- Skoog D-A, Leary J-J (Eds) (1992) *Principles of Instrumental Analysis* 4th Ed. Harcourt Brace College Publishers. Toronto.
- Shih I-L, Van Y-T, Yeh L-C, Lin H-G, Chang Y-N (2001) Production of a biopolymer flocculant from *Bacillus licheniformis* and its flocculation properties. *Bioresour. Technol.* 78: 267-272.
- Shih I L, Van Y T (2001) The production of poly-(γ - glutamic acid) from microorganisms and its various applications. *Bioresource Technology* 79: 207-225.
- Suh H-H, Kwon G-S, Lee C-H, Kim H-S, Oh H-M, Yoon B-D (1997) Characterization of bioflocculant produced by *Bacillus* sp. DP-152. *J. Ferment. Bioeng.* 84: 108-112.
- Takeda M, Kurane R, Koizumi J, Nakamura I, (1991) A protein bioflocculant produced by *Rhodococcus erythropolis*. *Agric. Biol. Chem.* 55: 2663-2664.
- Takeda M, Koizumi J, Matsuoka H, Hikuma M (1992) Factors affecting the activity of a protein bioflocculant produced by *Nocardia amarae*. *J. Ferment. Bioeng.* 74: 408-409.
- Tanaka T, Yaguchi T, Hiruta O, Futamura T, Uotani K, Satoh A, Taniguchi M, Oi S., (1993) Screening for microorganism having poly(γ -glutamic acid) endohydrolase activity and the enzyme production by *Myrothecium* sp. TM-4222. *Biosci. Biotech. Biochem.* 57: 1809-1810.
- Tanaka T, Hiruta O, Futamura T, Uotani K, Satoh A, Taniguchi M, Oi S (1993) Purification and characterization of poly(γ -glutamic acid) hydrolase from a filamentous fungus, *Myrothecium* sp. TM-4222. *Biosci. Biotech. Biochem.* 57: 2148-2153.
- Tanaka T, Fujita K-I, Takenishi S, Taniguchi M, (1997) Existence of an optically heterogeneous peptide unit in poly(γ -glutamic acid) produced by *Bacillus subtilis*. *J. Ferment. Bioeng.* 84: 361-364.
- Thorne C-B, Gomez C-G, Blind G-R, Housewright R-D (1953) Synthesis of glutamic acid and glutamyl polypeptide by *Bacillus anthracis*. III. Factors affecting peptide production in synthetic liquid media. *J. Bacteriol.* 65: 472-478.
- Thorne C-B, Gomez C-G, Noyes H-E, Housewright R-D, (1954) Production of glutamyl polypeptide by *Bacillus subtilis*. *J. Bacteriol.* 68: 307-315.

Thorne C-B, Gomez C-G, Housewright R-D (1955) Transamination of D-amino acids by *Bacillus subtilis*. J. Bacteriol. 69: 357-362.

Thorne C-B, Molnar D-M (1955) D-amino acid transamination in *Bacillus anthracis*. J. Bacteriol. 70: 420-426.

Troy F-A (1973) Chemistry and biosynthesis of the poly(γ -D-glutamyl) capsule in *Bacillus licheniformis*. 1. Properties of the membrane-mediated biosynthetic reaction. J. Biol. Chem. 248: 305-316.

Uchida I, Makino S, Sasakawa C, Yoshikawa M, Sugimoto C, Terakado M, (1993) Identification of a novel gene, *dep*, associated with depolymerization of the capsular polymer in *Bacillus anthracis*. Mol. Microbiol. 9: 487-496.

Willams W-J, Thorne C-B, (1954) Biosynthesis of glutamyl peptides from glutamine by a transfer reaction. J. Biol. Chem. 210: 203-217.

Wu C-S (Ed) (2004) Handbook of Size Exclusion Chromatography and Related Techniques 2nd Ed. Marcel Dekker Inc. New York.

Yokoi H, Natsuda O, Hirose J, Hayashi S, Takasaki Y (1995) Characteristics of a biopolymer flocculant produced by *Bacillus* sp. PY-90. J. Ferment. Bioeng. 79: 378-380.

Yokoi H, Arima T, Hirose J, Hayashi S, Takasaki Y (1996) Flocculation properties of poly (γ -glutamic acid) produced by *Bacillus subtilis*. J. Ferment. Bioeng. 82: 84-87.

Yoon S-H, Do J-H, Lee S-Y, Chang H-N (2000) Production of poly- γ -glutamic acid by fed-batch culture of *Bacillus licheniformis*. Biotechnol. Lett. 22: 585-588.

A. APPENDIX A Batch Fermentation Data

Fermentation Time, t (h)	Biomass Concentration, X (g/L)	Natural Log of Biomass, Ln(X)	Specific Growth Rate, μ (h ⁻¹)	PGA Concentration, P (g/L)
1	0.05	-3.00	0.00	ND
3	0.02	-3.91	1.71e-3	ND
6	0.08	-2.53	6.25e-3	7.8
8	0.26	-1.35	7.81e-3	ND
16	0.82	-0.20	0.111	13.7
19	1.1	0.10	0.093	ND
22	1.28	0.25	0.084	ND
26	1.78	0.58	0.062	ND
29	2.46	0.90	0.044	15.9
40	2.98	1.09	0.026	ND
44	3.52	1.26	0.018	ND
48	3.80	1.34	0.013	16.4
53.5	3.86	1.35	8.80e-3	ND
58	4.22	1.44	5.60e-3	17.9
64	4.29	1.46	3.02e-3	18.1
72	4.36	1.47	1.24e-3	ND
76	4.36	1.47	7.13e-4	23.2
81.5	4.40	1.48	3.47e-4	ND
94	4.08	1.41	5.49e-5	24.1

Table A-1 Biomass Concentration, Natural Log of the Biomass, Specific Growth Rate and PGA Concentration as a function of Fermentation Time for the Batch Fermentation of *B. licheniformis*

ND = Not Determined

Fermentation Time, t (h)	Citric Acid Concentration, S1 (g/L)	Glutamic Acid Concentration, S2 (g/L)	Glycerol Concentration, S3 (g/L)
1	ND	ND	ND
3	ND	ND	ND
6	13.0	16.5	79.6
8	ND	ND	ND
16	11.7	15.8	78.2
19	ND	ND	ND
22	ND	ND	ND
26	ND	ND	ND
29	10.9	12.5	56.3
40	ND	ND	ND
44	ND	ND	ND
48	10.4	11.3	51.0
53.5	ND	ND	ND
58	10.0	12.2	52.8
64	9.0	12.3	44.3
72	ND	ND	ND
76	6.4	9.9	31.4
81.5	ND	ND	ND
94	3.7	9.6	15.4

Table A-2 Citric Acid, Glutamic Acid and Glycerol Concentration as a function of Fermentation Time for the Batch Fermentation of *B. licheniformis*

Fermentation Time, t (h)	Biomass Yield, Y_{XS} (g/g)			
	From Citric Acid	From Glutamic Acid	From Glycerol	From total Carbon
6	-0.1	0.02	0.18	0.03
16	3.2	0.19	0.44	0.13
29	2.3	0.33	0.10	0.08
48	2.4	0.44	0.13	0.10
58	2.1	0.54	0.16	0.11
64	1.4	0.56	0.12	0.09
76	0.8	0.43	0.09	0.07
94	0.5	0.39	0.06	0.05

Table A-3 Biomass Yield from Citric Acid, Glutamic Acid, Glycerol and Total Substrates as a function of Fermentation time for the Batch Fermentation of *B. licheniformis*

Fermentation Time, t (h)	PGA Yield, Y_{PIS} (g/g)				
	from Biomass	From Citric Acid	From Glutamic Acid	From Glycerol	From total Substrates
6	97.5	-7.7	2.2	17.7	2.6
16	16.7	52.9	3.2	7.4	2.2
29	6.5	14.7	2.1	0.7	0.5
48	4.3	10.3	1.9	0.6	0.4
58	4.2	9.0	2.3	0.7	0.5
64	4.2	6.0	2.4	0.5	0.4
76	5.3	4.1	2.3	0.5	0.4
94	5.9	2.9	2.3	0.4	0.3

Table A-4 PGA yield from Biomass and Substrates as a function of Fermentation Time for the Batch fermentation of *B. licheniformis*

Fermentation Time, t (h)	Oxygen Uptake Rate, $Q_{O_2}X$ (mmol/L/h)	Specific Oxygen Uptake Rate, Q_{O_2} (mmol/g DW/h)	Volumetric Mass Transfer Coefficient, $k_L a$ (h^{-1})	Viscosity (Pa.s)
0				
6	2.51	31.37		0.004
29	2.74	1.11	53.2	0.13
48	4.70	1.23	103	0.32
58	2.26	0.54	114	0.37
76	2.05	0.47	73.3	0.37
94	1.55	0.38	207	0.40
			98.7	0.42

Table A-5 Oxygen Uptake Rate, Specific Oxygen Uptake Rate, Volumetric Mass Transfer Coefficient and Viscosity as a function of Fermentation Time for the Batch Fermentation of *B. licheniformis*

Average Fermentation Time, t (h)	Biomass Productivity, P_x (g/L/h)	Average Fermentation Time, t (h)	PGA Productivity, P_p (g/L/h)
2		11	
4.5	-0.015	22.5	0.588
7	0.020	38.5	0.169
12	0.090	53	0.026
17.5	0.070	61	0.152
20.5	0.093	70	0.032
24	0.060	85	0.423
27.5	0.125		0.054
34.5	0.227		
42	0.047		
46	0.135		
50.75	0.070		
55.75	0.011		
61	0.080		
68	0.011		
74	0.009		
78.75	0.000		
87.75	0.007		
	-0.026		

Table A-6 Biomass and PGA Productivity as a function of Fermentation Time for the Batch Fermentation of *B. licheniformis*

Fermentation Time, t (h)	Number Average Molecular Weight, Mn (Da)	Weight Average Molecular Weight, Mw (Da)	Polydispersity, Mw/Mn (Da/Da)
0	0	0	1
6	157000	310000	1.97
16	187000	461000	2.46
37	188000	543000	2.9
57	192000	595000	3.1
71	229000	635000	2.77
94	192000	470000	2.45

Table A-7 Number and Weight Average Molecular Weight and Polydispersity as a function of Fermentation Time for the Batch Fermentation of *B. licheniformis*

**B. APPENDIX B Continuous and Transient Data as a
Function of Real Fermentation Time**

Fermentation Time, t (h)	Biomass Concentration, X (g/L)	Citric Acid Concentration, S1 (g/L)	Glutamic Acid Concentration, S2 (g/L)	Glycerol Concentration, S3 (g/L)	Polyglutamic Acid Concentration, P (g/L)
0	4.49	ND	ND	ND	ND
18.5	3.24	ND	ND	ND	ND
29.5	2.58	ND	ND	ND	ND
56	2.60	ND	ND	ND	ND
73	3.36	ND	ND	ND	ND
93	3.30	3.46	10.17	ND	ND
115	3.20	2.59	10.52	31.71	17.47
Steady State	3.20	2.59	10.52	31.71	17.47

Table B-1 Biomass, Substrate and Product Concentration as a function of Fermentation Time for $D = 0.023 \text{ h}^{-1}$

ND = Not Determined

Fermentation Time, t (h)	Biomass Concentration, X (g/L)	Citric Acid Concentration, S1 (g/L)	Glutamic Acid Concentration, S2 (g/L)	Glycerol Concentration, S3 (g/L)	Polyglutamic Acid Concentration, P (g/L)
0	3.20	ND	ND	ND	ND
5	2.95	ND	ND	ND	ND
18	2.70	ND	ND	ND	ND
30.5	2.94	ND	ND	ND	ND
42	2.80	ND	ND	ND	ND
54.5	2.9	4.03	12.51	ND	16.24
65	2.94	3.64	10.80	31.82	18.25
Steady State	2.92	3.83	11.65	31.82	17.25

Table B-2 Biomass, Substrate and Product Concentration as a function of Fermentation Time for $D = 0.035 \text{ h}^{-1}$

Fermentation Time, t (h)	Biomass Concentration, X (g/L)	Citric Acid Concentration, S1 (g/L)	Glutamic Acid Concentration, S2 (g/L)	Glycerol Concentration, S3 (g/L)	Polyglutamic Acid Concentration, P (g/L)
0	1.76	ND	ND	ND	ND
19.5	3.18	ND	ND	ND	ND
43	2.88	ND	ND	ND	ND
62	2.88	ND	ND	ND	ND
74	2.91	ND	ND	ND	ND
85	2.73	ND	ND	ND	ND
92	2.82	4.54	11.96	32.7	17.4
Steady State	2.82	4.54	11.96	32.7	17.4

Table B-3 Biomass, Substrate and Product Concentration as a function of Fermentation Time for $D = 0.051 \text{ h}^{-1}$

Fermentation Time, t (h)	Biomass Concentration, X (g/L)	Citric Acid Concentration, S1 (g/L)	Glutamic Acid Concentration, S2 (g/L)	Glycerol Concentration, S3 (g/L)	Polyglutamic Acid Concentration, P (g/L)
0	1.16	ND	ND	ND	ND
23	1.94	5.28	11.93	ND	ND
45	1.30	6.18	13.09	ND	ND
50	2.00	6.05	11.95	ND	ND
58	2.4	5.02	13.17	ND	ND
65	2.52	4.88	13.41	ND	ND
75	2.44	4.62	12.9	41.38	17.17
Steady State	2.45	4.74	13.0	41.38	17.17

Table B-4 Biomass, Substrate and Product Concentration as a function of Fermentation Time for $D = 0.063 \text{ h}^{-1}$

Fermentation Time, t (h)	Biomass Concentration, X (g/L)	Citric Acid Concentration, S1 (g/L)	Glutamic Acid Concentration, S2 (g/L)	Glycerol Concentration, S3 (g/L)	Polyglutamic Acid Concentration, P (g/L)
0	0.67	ND	ND	ND	ND
12	1.1	ND	ND	ND	ND
19	0.95	ND	ND	ND	ND
26.5	1.70	ND	ND	ND	ND
30.5	1.83	ND	ND	ND	ND
43	1.93	ND	ND	ND	ND
45	1.97	ND	ND	ND	ND
47	1.83	5.36	16.00	ND	ND
50	1.83	ND	ND	ND	ND
54	1.85	4.37	15.29	48.57	ND
60	1.82	4.84	15.61	48.91	14.66
Steady State	1.83	4.51	15.52	48.74	14.66

Table B-5 Biomass, Substrate and Product Concentration as a function of Fermentation Time for $D = 0.082\text{a h}^{-1}$

Fermentation Time, t (h)	Biomass Concentration, X (g/L)	Citric Acid Concentration, S1 (g/L)	Glutamic Acid Concentration, S2 (g/L)	Glycerol Concentration, S3 (g/L)	Polyglutamic Acid Concentration, P (g/L)
0	2.4	ND	ND	ND	ND
18.5	1.72	ND	ND	ND	ND
28.5	1.38	ND	ND	ND	ND
38.5	1.24	ND	ND	ND	ND
40	1.46	ND	ND	ND	ND
43.5	1.56	ND	ND	ND	ND
45.5	1.64	ND	ND	ND	ND
48	1.76	ND	ND	ND	ND
51	1.82	ND	ND	ND	ND
58	1.74	ND	ND	ND	ND
62	1.8	ND	ND	ND	ND
68	1.72	ND	ND	ND	ND
78	1.76	5.14	16.29	42.76	13.57
Steady State	1.76	5.14	16.29	42.76	13.57

Table B-6 Biomass, Substrate and Product Concentration as a function of Fermentation Time for $D = 0.082 \text{ h}^{-1}$

Fermentation Time, t (h)	Biomass Concentration, X (g/L)	Citric Acid Concentration, S1 (g/L)	Glutamic Acid Concentration, S2 (g/L)	Glycerol Concentration, S3 (g/L)	Polyglutamic Acid Concentration, P (g/L)
0	2.1	ND	ND	ND	ND
18	2.5	3.80	15.17	ND	ND
22	1.05	5.47	17.26	ND	5.17
25	1.05	ND	ND	ND	ND
28	1.6	ND	ND	ND	ND
34	1.35	8.30	19.20	ND	4.35
37.5	1.2	ND	ND	ND	ND
40	1.2	ND	ND	ND	ND
43	1.1	7.91	19.28	48.37	5.95
49	1.16	7.79	18.61	50.32	6.72
Steady State	1.14	7.9	18.95	49.35	6.33

Table B-7 Biomass, Substrate and Product Concentration as a function of Fermentation Time for $D = 0.097 \text{ h}^{-1}$

Fermentation Time, t (h)	Biomass Concentration, X (g/L)	
0	0.25	
12	0.35	
24	0.70	
36	1.16	Flow Started at D = 0.063 h⁻¹
59	1.94	
81	1.30	
86	2.00	
94	2.4	
101	2.52	
111	2.44	
140	2.4	Flow Started at D = 0.082 h⁻¹
158.5	1.72	
168.5	1.38	
178.5	1.24	
180	1.46	
183.5	1.56	
185.5	1.64	
188	1.76	
191	1.82	
198	1.74	
202	1.80	
208	1.72	
218	1.76	

Table B-8 Biomass Concentration as a Function of Fermentation Time for D = 0.063 h⁻¹ and D = 0.082 h⁻¹

Fermentation Time, t (h)	Biomass Concentration, X (g/L)	
24		
36	0.67	
43	1.1	
50.5	0.95	
54.5	1.70	
67	1.83	
69	1.93	
71	1.97	
74	1.83	
78	1.83	
84	1.85	
96	1.82	
115.5	1.76	
139	3.18	
158	2.88	
170	2.88	
181	2.91	
188	2.73	
	2.82	

$D = 0.082 \text{ h}^{-1}$

$D = 0.051 \text{ h}^{-1}$

Table B-9 Biomass Concentration as a Function of Fermentation Time for $D = 0.082 \text{ h}^{-1}$ and $D = 0.051 \text{ h}^{-1}$

C. APPENDIX C Steady State Continuous Bioreactor Data as a Function of Dilution Rate

Dilution Rate, D (h⁻¹)	[Biomass], X (g/L)	[Citric Acid], S₁ (g/L)	[Glutamic Acid], S₂ (g/L)	[Glycerol], S₃ (g/L)	[Total Carbon Source], S_{tot} (g/L)	[PGA], P (g/L)
0.023	3.20	2.59	10.52	31.71	44.82	17.47
0.035	2.92	3.83	11.65	31.82	47.3	17.25
0.051	2.82	4.54	11.96	32.70	49.2	17.40
0.063	2.45	4.74	12.99	41.38	59.11	17.17
0.082a	1.83	4.51	15.52	48.74	68.77	14.66
0.082b	1.76	5.14	16.29	42.76	64.19	13.57
0.097	1.14	7.9	18.95	49.35	76.15	7.97
Washout = 0.122	0.00	12.00	20.00	80.00	112.00	0.00

Table C-1 Biomass, Substrate and Product Concentrations as a function of Dilution Rate for the Continuous Fermentation of *B. licheniformis*

Dilution Rate, D (h⁻¹)	Biomass Productivity, P_x (g/L/h)	Citric Acid Consumption Rate (g/L/h)	Glutamic Acid Consumption Rate (g/L/h)	Glycerol Consumption Rate (g/L/h)	PGA Productivity, P_p (g/L/h)
0.023	0.07	0.22	0.22	1.13	0.41
0.035	0.10	0.29	0.29	1.70	0.61
0.051	0.14	0.38	0.41	2.41	0.89
0.063	0.16	0.46	0.44	2.45	1.09
0.082a	0.15	0.61	0.36	2.54	1.19
0.082b	0.14	0.56	0.30	3.04	1.11
0.097	0.11	0.40	0.10	2.96	0.77
Washout = 0.122	0.00	0.00	0.00	0.00	0.00

Table C-2 Biomass and PGA Productivity and Substrate Consumption Rate as a function of Dilution Rate for the Continuous Fermentation of *B. licheniformis*

Dilution Rate, D (h ⁻¹)	Biomass Yield Y _{x/s} (g/g) from			
	Citric Acid	Glutamic Acid	Glycerol	Total Carbon Sources
0.023	0.340	0.338	0.066	0.048
0.035	0.358	0.350	0.061	0.045
0.051	0.38	0.351	0.060	0.045
0.063	0.338	0.350	0.064	0.046
0.082a	0.245	0.409	0.059	0.042
0.082b	0.257	0.475	0.047	0.037
0.097	0.280	1.11	0.038	0.032

Table C-3 Biomass Yield from Substrates as a function of Dilution Rate for the Continuous Fermentation of *B. licheniformis*

PGA Yield $Y_{P/X}$ or $Y_{P/S}$ (g/g) from

Dilution Rate, D (h^{-1})	Biomass	Citric Acid	Glutamic Acid	Glycerol	Total Substrates
0.023	5.458	1.857	1.843	0.362	0.260
0.035	5.908	2.112	2.066	0.358	0.267
0.051	6.173	2.332	2.165	0.368	0.277
0.063	7.000	2.367	2.451	0.445	0.33
0.082a	7.996	1.957	3.272	0.469	0.339
0.082b	7.709	1.978	3.660	0.364	0.284
0.097	5.457	1.526	6.008	0.207	0.18

Table C-4 PGA yield from Biomass and Substrates as a function of Dilution Rate for the Continuous Fermentation of *B. licheniformis*

Dilution Rate, D (h)	Number Average Molecular Weight, Mn (Da)	Weight Average Molecular Weight, Mw (Da)	Polydispersity, Mw/Mn (Da/Da)
0.023	148,610	412,486	2.78
0.035	197,000	452,535	2.30
0.051	164,820	382,904	2.3
0.063	182,694	388,529	2.13
0.082a	193,493	528,761	2.73
0.082b	169,291	376,735	2.23
0.097	144,000	310,617	2.16
Washout = 0.122	0	0	NA

Table C-5 Number and Weight Average Molecular Weight and Polydispersity as a function of Dilution Rate for the Continuous Fermentation of *B. licheniformis*

D. APPENDIX D Washout Experiment Data

Washout #1		
Washout Time, t_w (h)	Biomass Concentration, X (g/L)	Ln (Biomass Concentration)
0	3.06	1.119
1	2.26	0.815
2	1.98	0.683
3	1.78	0.577
4	1.30	0.262
5	1.14	0.131
6	1.00	0.000

Table D-1 Biomass Concentration and the Natural Log of the biomass concentration as a function of Washout Time for Washout Experiment #1

Washout #2		
Washout Time, t_w (h)	Biomass Concentration, X (g/L)	Ln (Biomass Concentration)
0	2.73	1.004
1	1.88	0.631
2	1.58	0.457
3	1.22	0.199
4	0.98	-0.020
5	0.78	-0.248

Table D-2 Biomass Concentration and the Natural Log of the biomass concentration as a function of Washout Time for Washout Experiment #2

Washout #	Slope of Line of Ln (X) vs t_w	Dilution Rate	Maximum Specific Growth Rate, μ_{max} (h^{-1})
#1	-0.173	0.2896	0.117
#2	-0.242	0.372	0.130
μ_{max} average (h^{-1}) =			0.123

Table D-3 Slope of Ln(X) vs Washout Time, Dilution Rate and the Calculated Maximum Specific Growth Rate for the Washout Experiments

**E. APPENDIX E SAMPLE GPC AND HPLC
CHROMATOGRAMS**

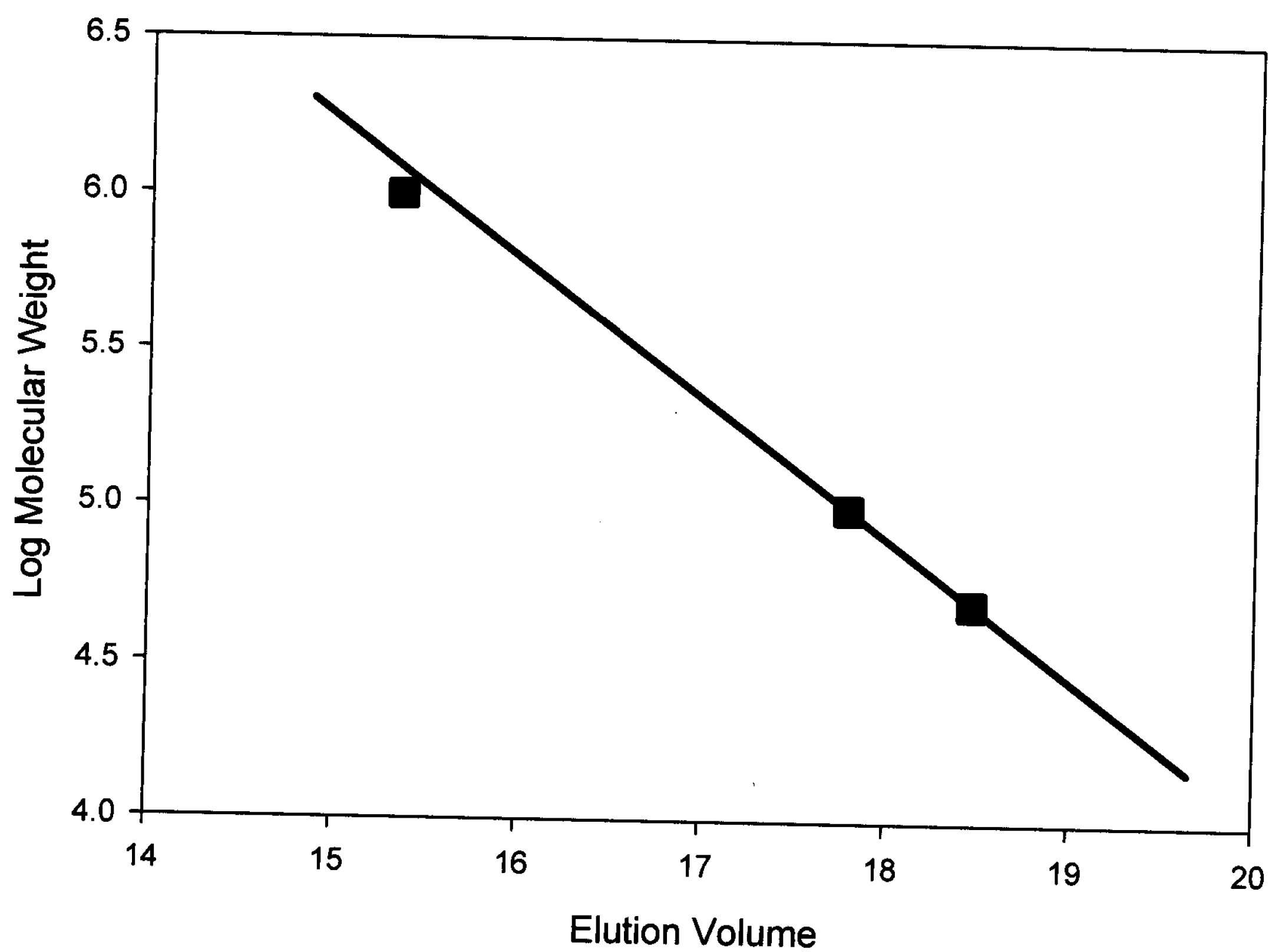


Figure E-1 GPC Calibration Curve for the PGA Polymer using Standards with Mn of 1×10^6 Da, 1×10^5 Da and 5×10^4 Da.

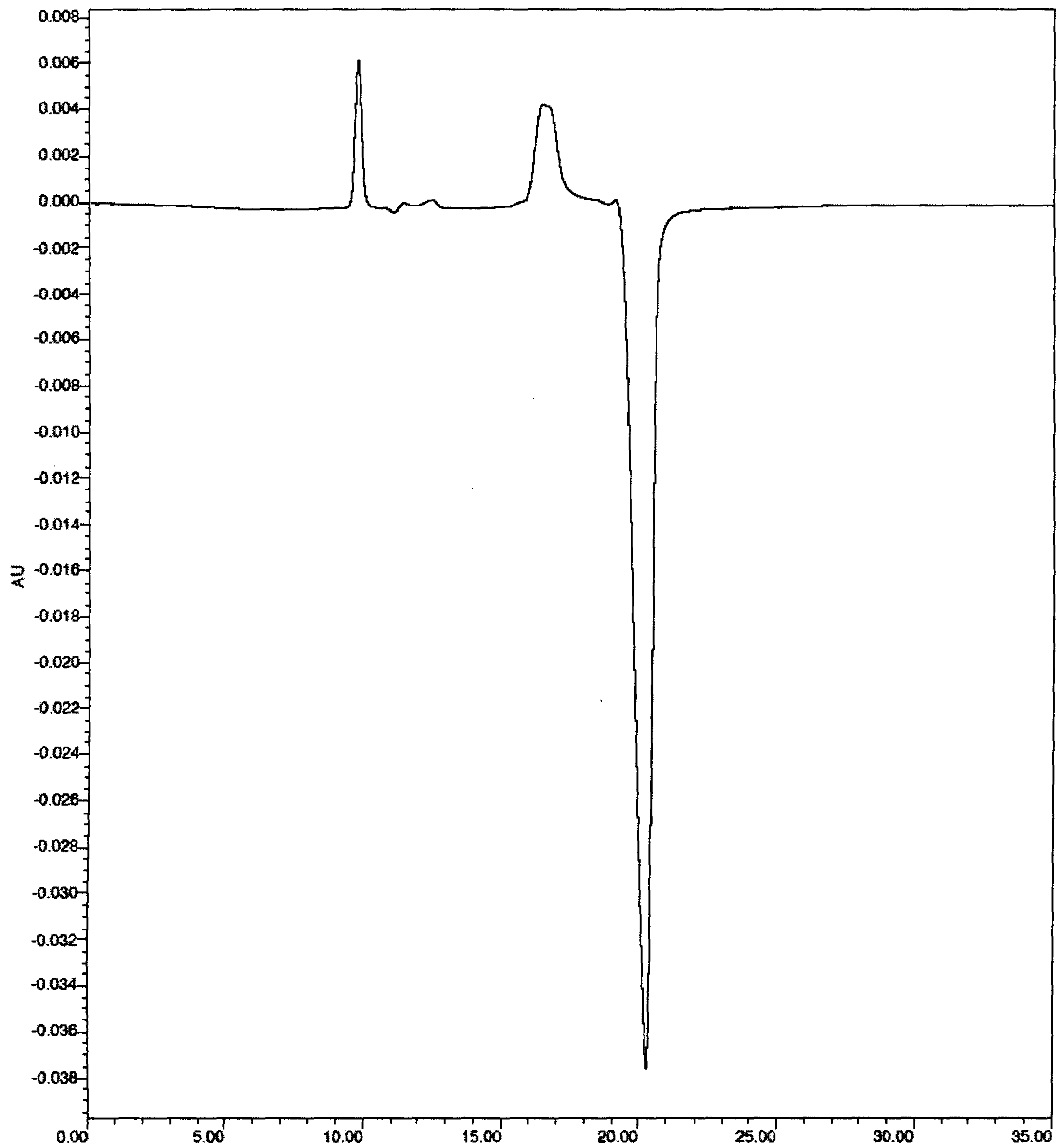


Figure E-2 GPC Chromatogram for the PGA Standard with a Mn of 1×10^5

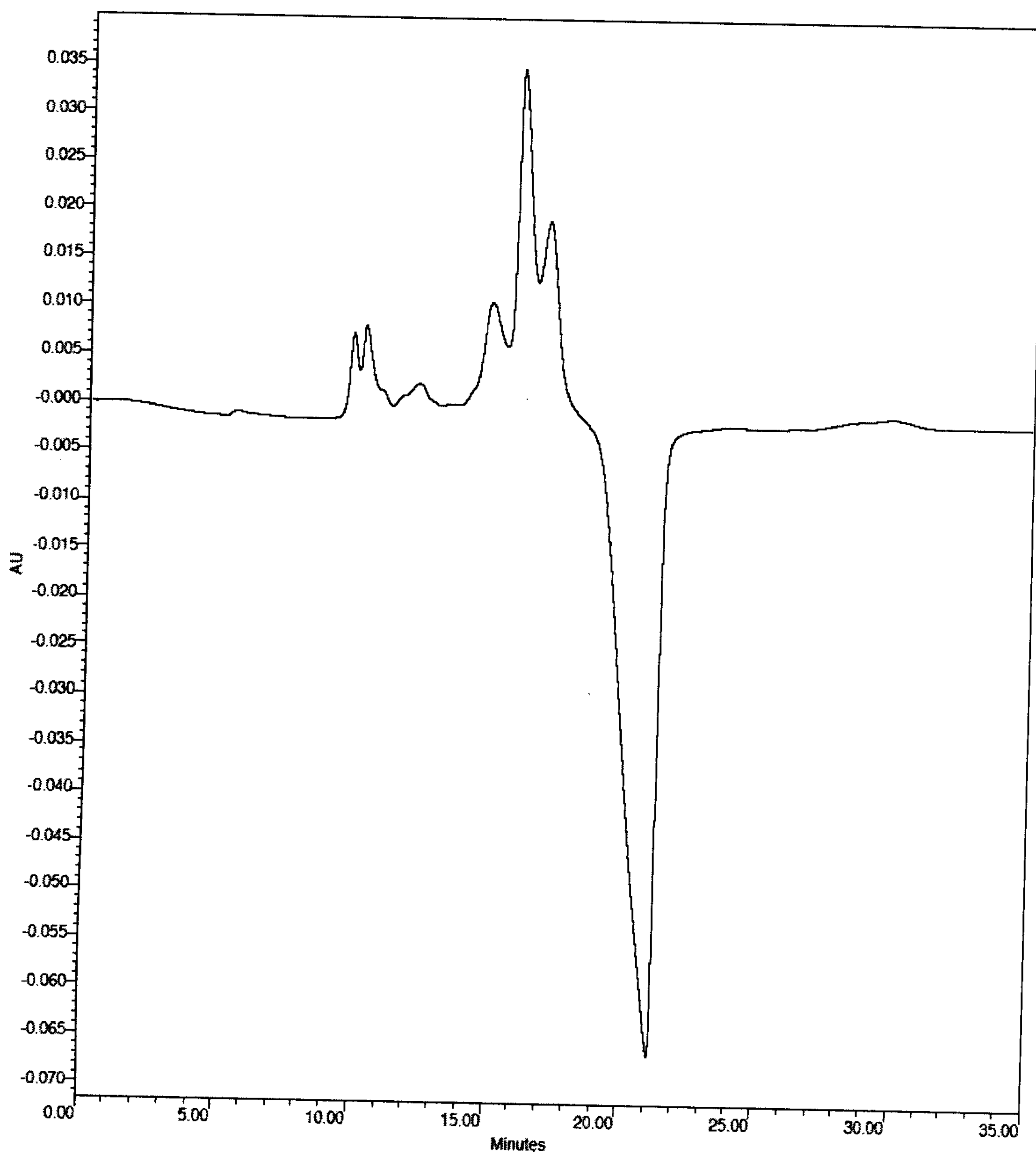


Figure E-3 Sample GPC Chromatogram from Late Batch Run

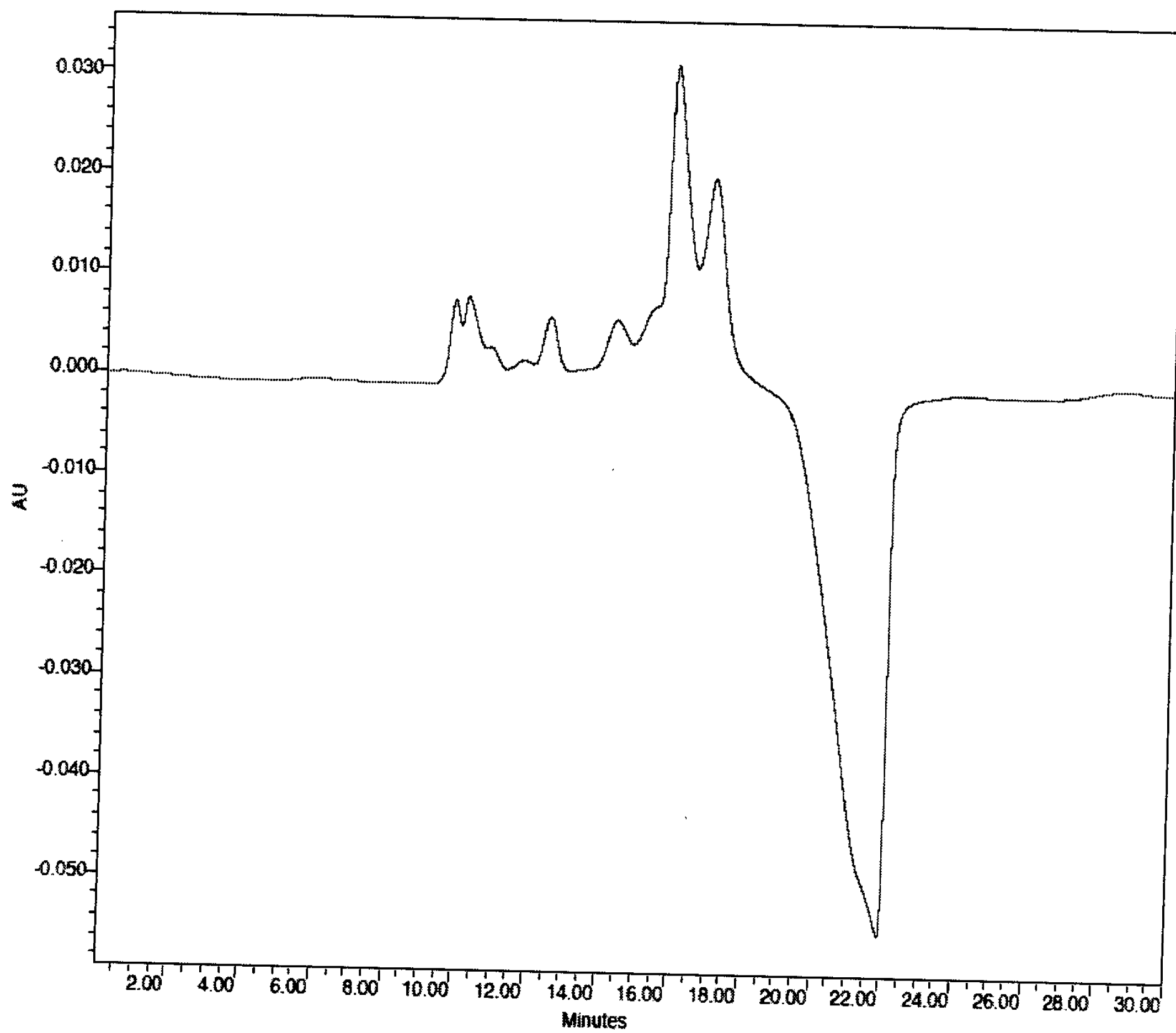


Figure E-4 GPC Chromatogram from D = 0.051

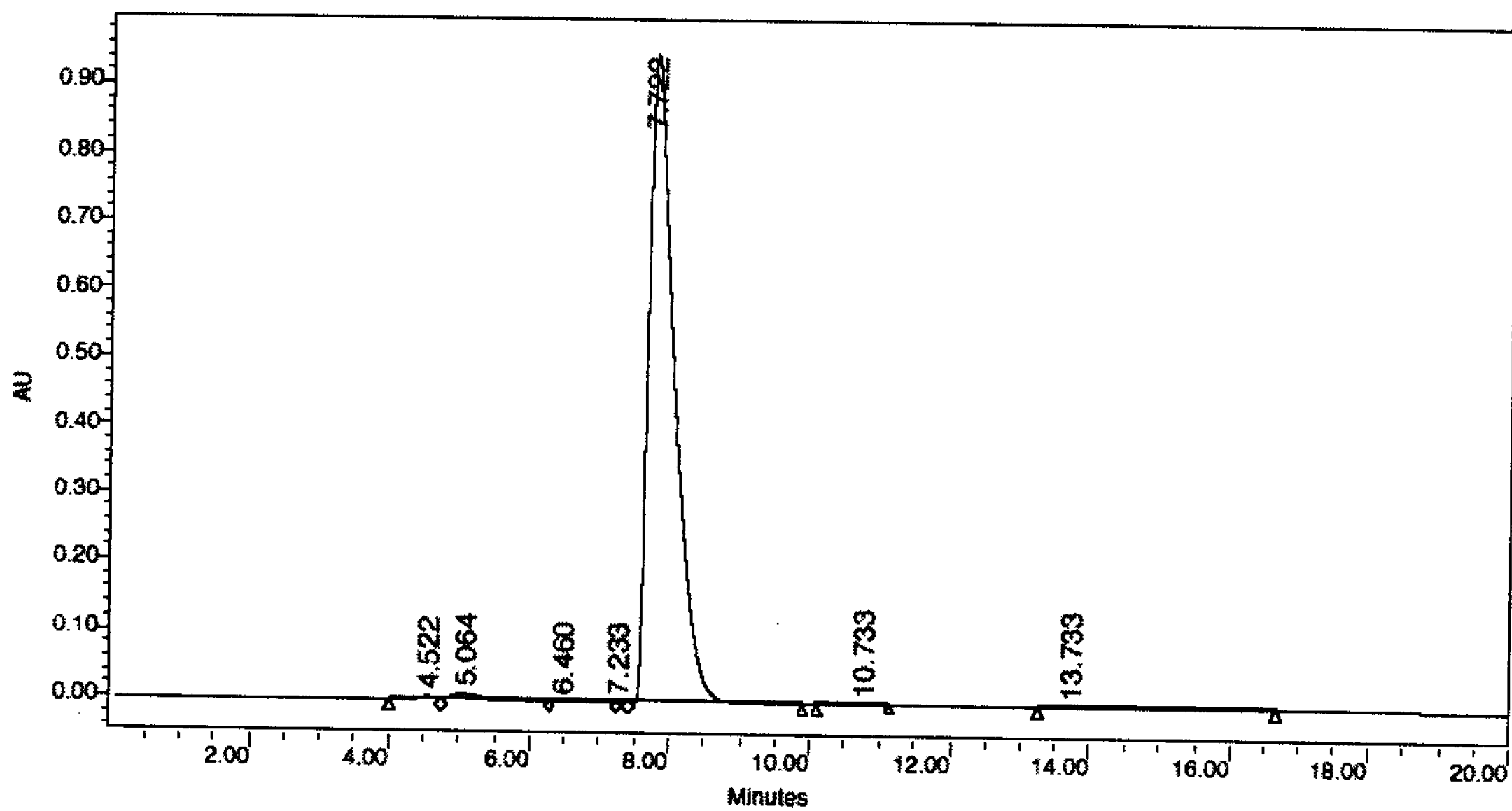


Figure E-5 Standard HPLC Chromatogram for Citric Acid

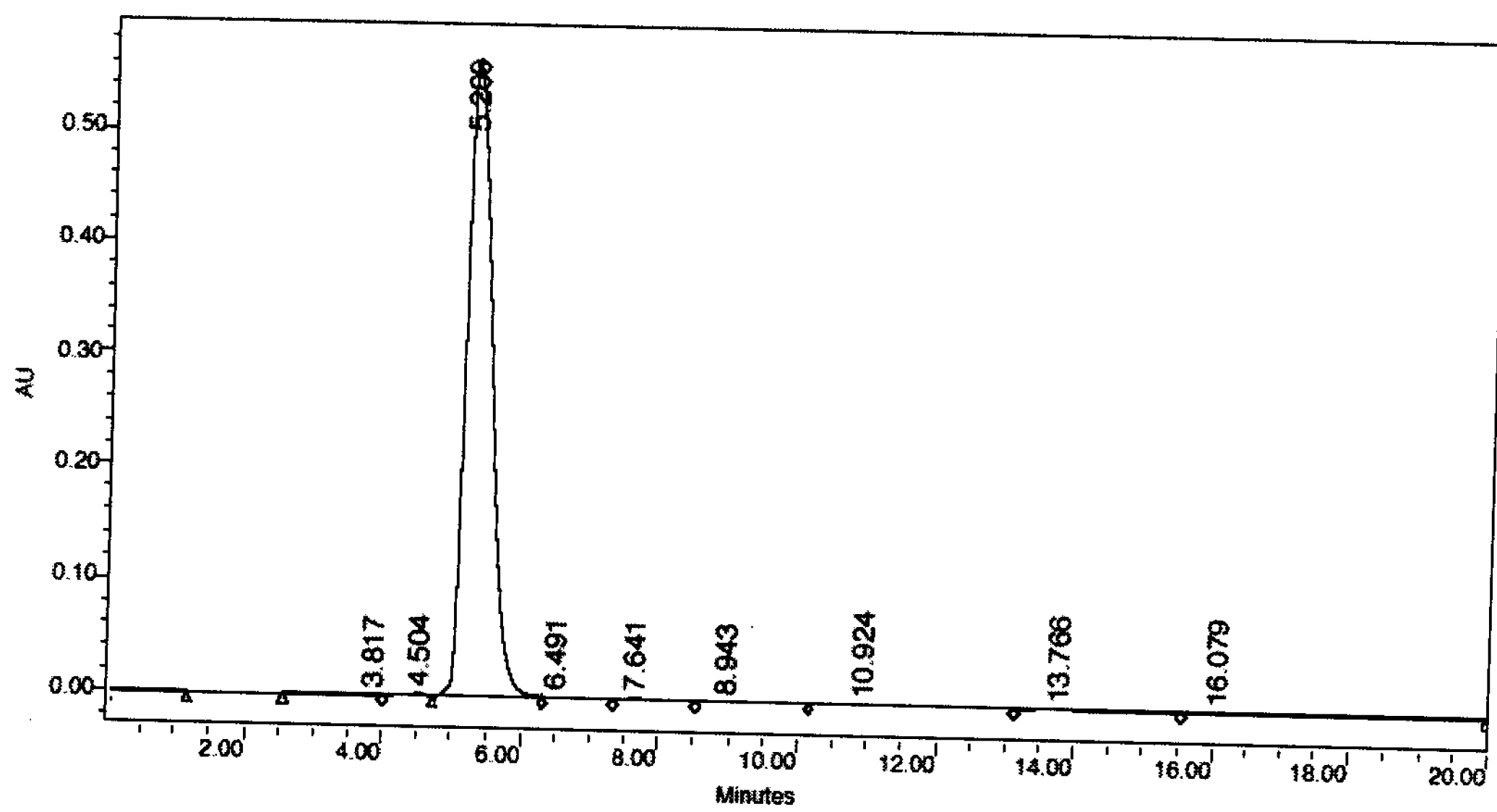


Figure E-6 Standard HPLC Chromatogram Glutamic Acid

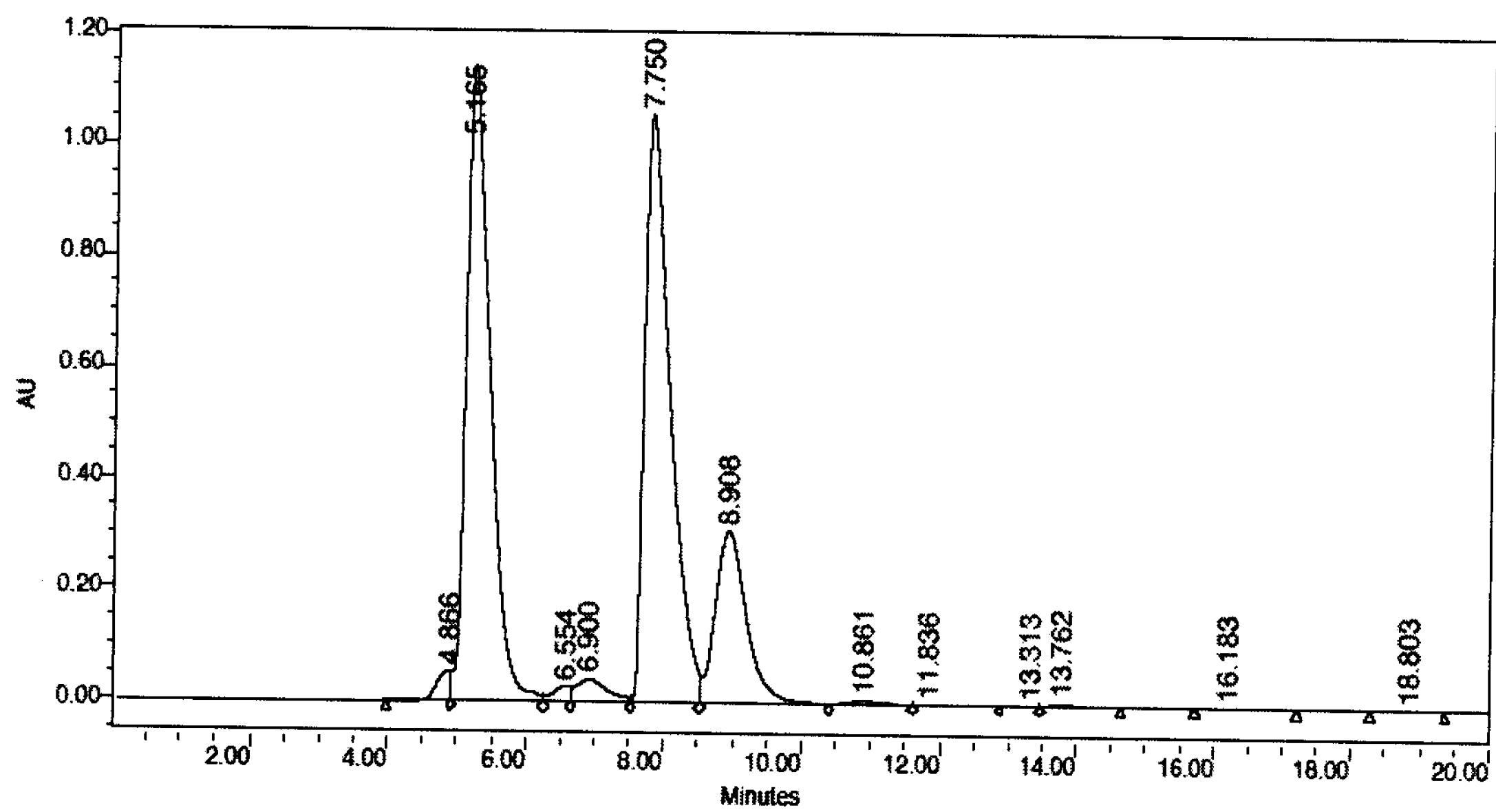


Figure E-7 HPLC Chromatogram of the Fresh Medium

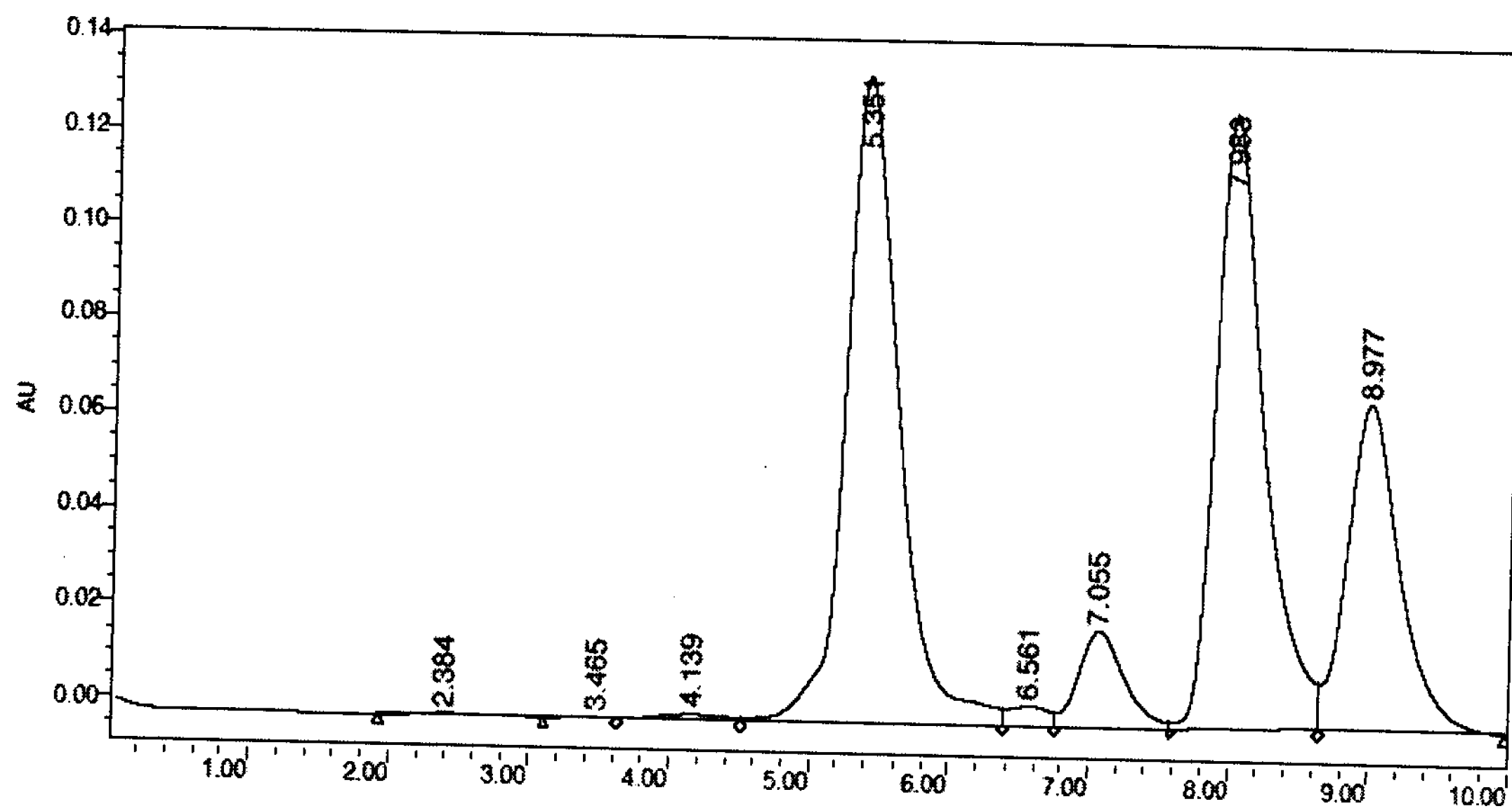


Figure E-8 Sample HPLC Chromatogram from $D = 0.063^{-1}$

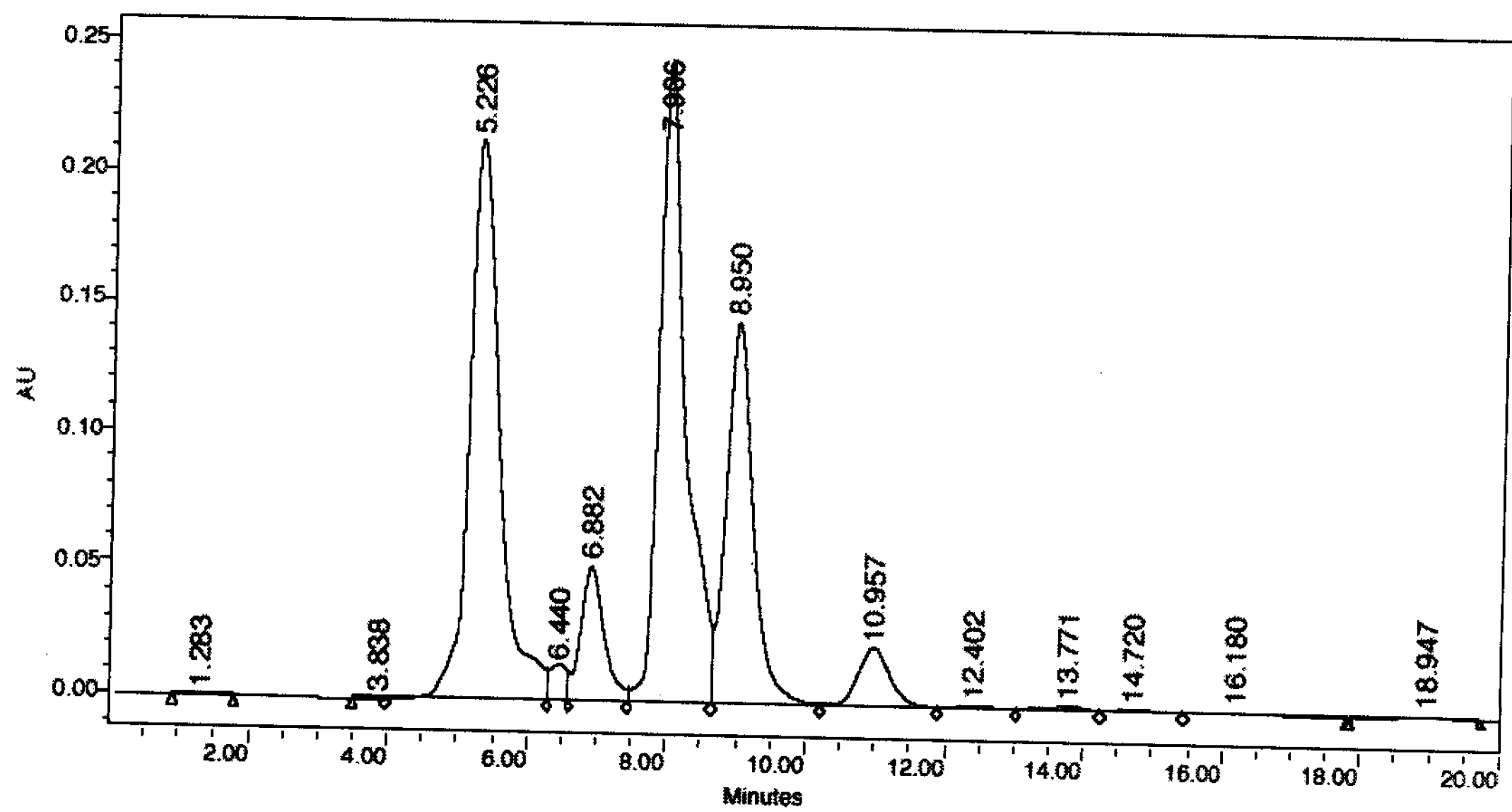


Figure E-9 HPLC Chromatogram from $D = 0.051h^{-1}$